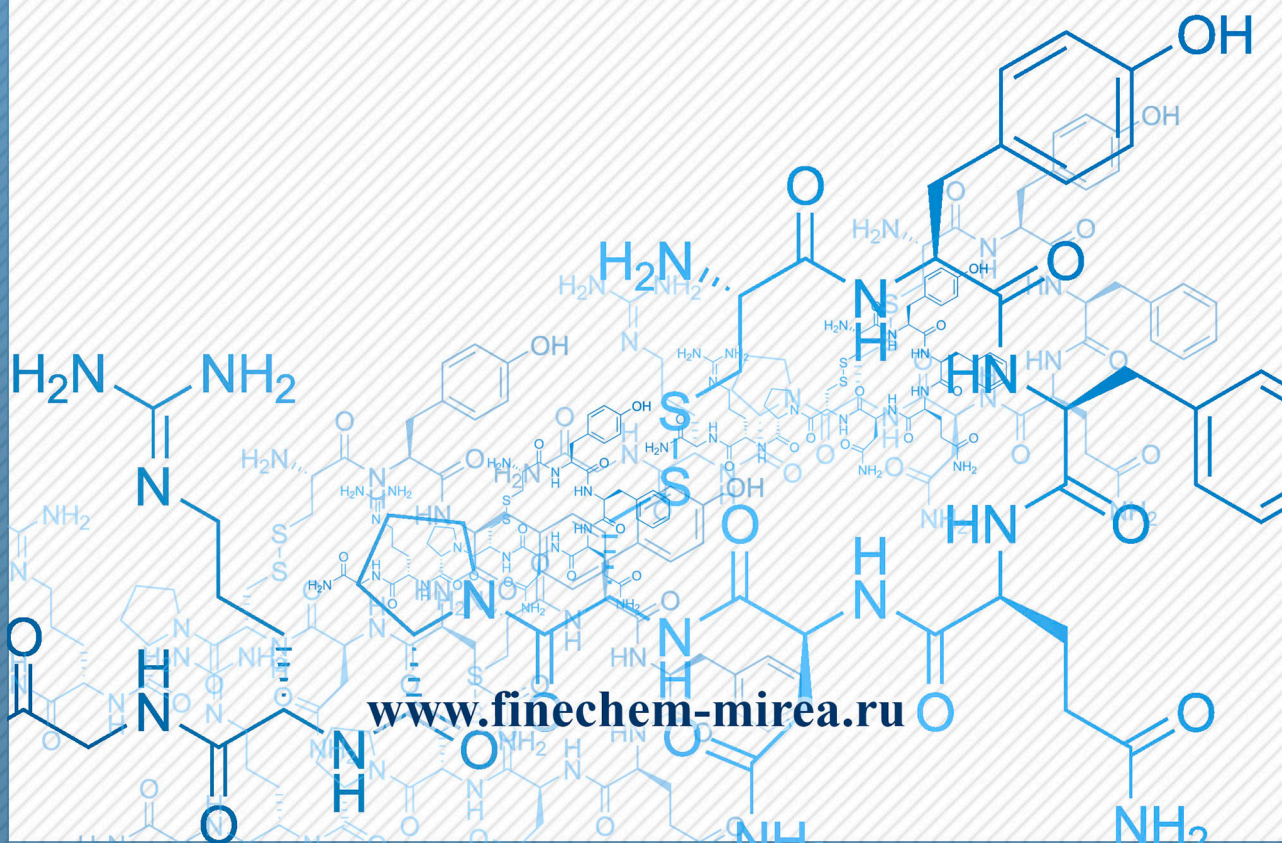


ISSN 2686-7575 (Online)

ТОНКИЕ ХИМИЧЕСКИЕ ТЕХНОЛОГИИ

Fine Chemical Technologies

- | Theoretical Bases of Chemical Technology
- | Chemistry and Technology of Organic Substances
- | Chemistry and Technology of Medicinal Compounds and Biologically Active Substances
- | Biochemistry and Biotechnology
- | Synthesis and Processing of Polymers and Polymeric Composites
- | Chemistry and Technology of Inorganic Materials
- | Analytical Methods in Chemistry and Chemical Technology
- | Mathematical Methods and Information Systems in Chemical Technology



16(6)

2021

www.finechem-mirea.ru



ISSN 2686-7575 (Online)

ТОНКИЕ ХИМИЧЕСКИЕ ТЕХНОЛОГИИ

Fine
Chemical
Technologies

- | Theoretical Bases of Chemical Technology
- | Chemistry and Technology of Organic Substances
- | Chemistry and Technology of Medicinal Compounds and Biologically Active Substances
- | Biochemistry and Biotechnology
- | Synthesis and Processing of Polymers and Polymeric Composites
- | Chemistry and Technology of Inorganic Materials
- | Analytical Methods in Chemistry and Chemical Technology
- | Mathematical Methods and Information Systems in Chemical Technology

Tonkie Khimicheskie Tekhnologii =
Fine Chemical Technologies
Vol. 16, No. 6, 2021

Тонкие химические технологии =
Fine Chemical Technologies
Том 16, № 6, 2021

<https://doi.org/10.32362/2410-6593-2021-16-6>
www.finechem-mirea.ru

**Tonkie Khimicheskie Tekhnologii =
Fine Chemical Technologies
2021, vol. 16, no. 6**

The peer-reviewed scientific and technical journal Fine Chemical Technologies highlights the modern achievements of fundamental and applied research in the field of fine chemical technologies, including theoretical bases of chemical technology, chemistry and technology of medicinal compounds and biologically active substances, organic substances and inorganic materials, synthesis and processing of polymers and polymeric composites, analytical and mathematical methods and information systems in chemistry and chemical technology.

Founder and Publisher

Federal State Budget
Educational Institution of Higher Education
“MIREA – Russian Technological University”
78, Vernadskogo pr., Moscow, 119454, Russian Federation.
Publication frequency: bimonthly.
The journal was founded in 2006. The name was Vestnik MITHT until 2015 (ISSN 1819-1487).

The journal is included into the List of peer-reviewed science press of the State Commission for Academic Degrees and Titles of the Russian Federation.

**The journal is indexed:
SCOPUS, DOAJ, Chemical Abstracts, Science Index, RSCI,
Ulrich’s International Periodicals Directory**

Editor-in-Chief:

Alla K. Frolkova – Dr. Sci. (Eng.), Professor, MIREA – Russian Technological University, Moscow, Russian Federation. Scopus Author ID 35617659200, ResearcherID G-7001-2018, <http://orcid.org/0000-0002-9763-4717>, frolkova_a@mirea.ru

Deputy Editor-in-Chief:

Valery V. Fomichev – Dr. Sci. (Chem.), Professor, MIREA – Russian Technological University, Moscow, Russian Federation. Scopus Author ID 57196028937, <http://orcid.org/0000-0003-4840-0655>, fomichev@mirea.ru

Executive Editor:

Sergey A. Durakov – Cand. Sci. (Chem.), Associate Professor, MIREA – Russian Technological University, Moscow, Russian Federation, Scopus Author ID 57194217518, ResearcherID AAS-6578-2020, <http://orcid.org/0000-0003-4842-3283>, durakov@mirea.ru

Editorial staff:

Managing Editor Cand. Sci. (Eng.) Galina D. Seredina
Science editors Dr. Sci. (Chem.), Prof. Tatyana M. Buslaeva
Dr. Sci. (Chem.), Prof. Anatolii A. Ischenko
Dr. Sci. (Eng.), Prof. Valery F. Kornushko
Dr. Sci. (Eng.), Prof. Anatolii V. Markov
Dr. Sci. (Chem.), Prof. Yuri P. Miroshnikov
Dr. Sci. (Chem.), Prof. Vladimir A. Tverskoy
Desktop publishing Larisa G. Semernya

86, Vernadskogo pr., Moscow, 119571, Russian Federation.
Phone: +7(495) 246-05-55 (#2-88)
E-mail: seredina@mirea.ru

Registration Certificate ПИ № ФС 77–74580, issued on December 14, 2018 by the Federal Service for Supervision of Communications, Information Technology, and Mass Media of Russia

The subscription index of *Pressa Rossii*: **36924**

**Тонкие химические технологии =
Fine Chemical Technologies
2021, том 16, № 6**

Научно-технический рецензируемый журнал «Тонкие химические технологии» освещает современные достижения фундаментальных и прикладных исследований в области тонких химических технологий, включая теоретические основы химической технологии, химию и технологию лекарственных препаратов и биологически активных соединений, органических веществ и неорганических материалов, синтез и переработку полимеров и композитов на их основе, аналитические и математические методы и информационные системы в химии и химической технологии.

Учредитель и издатель

федеральное государственное бюджетное
образовательное учреждение высшего образования
«МИРЭА – Российский технологический университет»
119454, РФ, Москва, пр-кт Вернадского, д. 78.
Периодичность: один раз в два месяца.
Журнал основан в 2006 году. До 2015 года издавался под названием «Вестник МИТХТ» (ISSN 1819-1487).

Журнал входит в Перечень ведущих рецензируемых научных журналов ВАК РФ.

**Индексируется:
SCOPUS, DOAJ, Chemical Abstracts,
РИНЦ (Science Index), RSCI,
Ulrich’s International Periodicals Directory**

Главный редактор:

Фролкова Алла Константиновна – д.т.н., профессор, МИРЭА – Российский технологический университет, Москва, Российская Федерация. Scopus Author ID 35617659200, ResearcherID G-7001-2018, <http://orcid.org/0000-0002-9763-4717>, frolkova_a@mirea.ru

Заместитель главного редактора:

Фомичёв Валерий Вячеславович – д.х.н., профессор, МИРЭА – Российский технологический университет, Москва, Российская Федерация. Scopus Author ID 57196028937, <http://orcid.org/0000-0003-4840-0655>, fomichev@mirea.ru

Выпускающий редактор:

Дураков Сергей Алексеевич – к.х.н., доцент, МИРЭА – Российский технологический университет, Москва, Российская Федерация, Scopus Author ID 57194217518, ResearcherID AAS-6578-2020, <http://orcid.org/0000-0003-4842-3283>, durakov@mirea.ru

Редакция:

Зав. редакцией к.т.н. Г.Д. Середина
Научные редакторы д.х.н., проф. Т.М. Буслеева
д.х.н., проф. А.А. Ищенко
д.т.н., проф. В.Ф. Корнюшко
д.т.н., проф. А.В. Марков
д.х.н., проф. Ю.П. Мирошников
д.х.н., проф. В.А. Тверской
Компьютерная верстка Л.Г. Семерня

119571, Москва, пр. Вернадского, 86, оф. Л-119.
Тел.: +7(495) 246-05-55 (#2-88)
E-mail: seredina@mirea.ru

Свидетельство о регистрации СМИ: ПИ № ФС 77-74580 от 14.12.2018 г. выдано Федеральной службой по надзору в сфере связи, информационных технологий и массовых коммуникаций (Роскомнадзор)
Индекс по Объединенному каталогу «Пресса России»: **36924**

Editorial Board

Andrey V. Blokhin – Dr. Sci. (Chem.), Professor, Belarusian State University, Minsk, Belarus. Scopus Author ID 7101971167, ResearcherID AAF-8122-2019 <https://orcid.org/0000-0003-4778-5872> blokhin@bsu.by

Sergey P. Verevkin – Dr. Sci. (Eng.), Professor, University of Rostock, Rostock, Germany. Scopus Author ID 7006607848, ResearcherID G-3243-2011, <https://orcid.org/0000-0002-0957-5594>, Sergey.verevkin@uni-rostock.de.

Konstantin Yu. Zhizhin – Corresponding Member of the Russian Academy of Sciences (RAS), Dr. Sci. (Chem.), Professor, N.S. Kurnakov Institute of General and Inorganic Chemistry of the RAS, Moscow, Russian Federation. Scopus Author ID 6701495620, ResearcherID C-5681-2013, <http://orcid.org/0000-0002-4475-124X>, kyuzhizhin@igic.ras.ru.

Igor V. Ivanov – Dr. Sci. (Chem.), Professor, MIREA – Russian Technological University, Moscow, Russian Federation. Scopus Author ID 34770109800, ResearcherID I-5606-2016, <http://orcid.org/0000-0003-0543-2067>, ivanov_i@mirea.ru.

Carlos A. Cardona – PhD (Eng.), Professor, National University of Columbia, Manizales, Colombia. Scopus Author ID 7004278560, <http://orcid.org/0000-0002-0237-2313>, ccardonaal@unal.edu.co.

Oskar I. Koifman – Corresponding Member of the RAS, Dr. Sci. (Chem.), Professor, President of the Ivanovo State University of Chemistry and Technology, Ivanovo, Russian Federation. Scopus Author ID 6602070468, ResearcherID R-1020-2016, <http://orcid.org/0000-0002-1764-0819>, president@isuct.ru.

Elvira T. Krut'ko – Dr. Sci. (Eng.), Professor, Belarusian State Technological University, Minsk, Belarus. Scopus Author ID 6602297257, ela_krutko@mail.ru.

Anatolii I. Miroshnikov – Academician at the RAS, Dr. Sci. (Chem.), Professor, M.M. Shemyakin and Yu.A. Ovchinnikov Institute of Bioorganic Chemistry of the RAS, Member of the Presidium of the RAS, Chairman of the Presidium of the RAS Pushchino Research Center, Moscow, Russian Federation. Scopus Author ID 7006592304, ResearcherID G-5017-2017, aiv@ibch.ru.

Aziz M. Muzafarov – Academician at the RAS, Dr. Sci. (Chem.), Professor, A.N. Nesmeyanov Institute of Organoelement Compounds of the RAS, Moscow, Russian Federation. Scopus Author ID 7004472780, ResearcherID G-1644-2011, <https://orcid.org/0000-0002-3050-3253>, aziz@ineos.ac.ru.

Редакционная коллегия

Блохин Андрей Викторович – д.х.н., профессор Белорусского государственного университета, Минск, Беларусь. Scopus Author ID 7101971167, ResearcherID AAF-8122-2019 <https://orcid.org/0000-0003-4778-5872> blokhin@bsu.by

Верёвкин Сергей Петрович – д.т.н., профессор Университета г. Росток, Росток, Германия. Scopus Author ID 7006607848, ResearcherID G-3243-2011, <https://orcid.org/0000-0002-0957-5594>, Sergey.verevkin@uni-rostock.de.

Жижин Константин Юрьевич – член-корр. Российской академии наук (РАН), д.х.н., профессор, Институт общей и неорганической химии им. Н.С. Курнакова РАН, Москва, Российская Федерация. Scopus Author ID 6701495620, ResearcherID C-5681-2013, <http://orcid.org/0000-0002-4475-124X>, kyuzhizhin@igic.ras.ru.

Иванов Игорь Владимирович – д.х.н., профессор, МИРЭА – Российский технологический университет, Москва, Российская Федерация. Scopus Author ID 34770109800, ResearcherID I-5606-2016, <http://orcid.org/0000-0003-0543-2067>, ivanov_i@mirea.ru.

Кардона Карлос Ариэль – PhD, профессор Национального университета Колумбии, Манизалес, Колумбия. Scopus Author ID 7004278560, <http://orcid.org/0000-0002-0237-2313>, ccardonaal@unal.edu.co.

Койфман Оскар Иосифович – член-корр. РАН, д.х.н., профессор, президент Ивановского государственного химико-технологического университета, Иваново, Российская Федерация. Scopus Author ID 6602070468, ResearcherID R-1020-2016, <http://orcid.org/0000-0002-1764-0819>, president@isuct.ru.

Крутько Эльвира Тихоновна – д.т.н., профессор Белорусского государственного технологического университета, Минск, Беларусь. Scopus Author ID 6602297257, ela_krutko@mail.ru.

Мирошников Анатолий Иванович – академик РАН, д.х.н., профессор, Институт биоорганической химии им. академиков М.М. Шемякина и Ю.А. Овчинникова РАН, член Президиума РАН, председатель Президиума Пушкинского научного центра РАН, Москва, Российская Федерация. Scopus Author ID 7006592304, ResearcherID G-5017-2017, aiv@ibch.ru.

Музафаров Азиз Мансурович – академик РАН, д.х.н., профессор, Институт элементоорганических соединений им. А.Н. Несмеянова РАН, Москва, Российская Федерация. Scopus Author ID 7004472780, ResearcherID G-1644-2011, <https://orcid.org/0000-0002-3050-3253>, aziz@ineos.ac.ru.

Ivan A. Novakov – Academician at the RAS, Dr. Sci. (Chem.), Professor, President of the Volgograd State Technical University, Volgograd, Russian Federation. Scopus Author ID 7003436556, ResearcherID I-4668-2015, <http://orcid.org/0000-0002-0980-6591>, president@vstu.ru.

Alexander N. Ozerin – Corresponding Member of the RAS, Dr. Sci. (Chem.), Professor, Enikolopov Institute of Synthetic Polymeric Materials of the RAS, Moscow, Russian Federation. Scopus Author ID 7006188944, ResearcherID J-1866-2018, <https://orcid.org/0000-0001-7505-6090>, ozerin@ispm.ru.

Tapani A. Pakkanen – PhD, Professor, Department of Chemistry, University of Eastern Finland, Joensuu, Finland. Scopus Author ID 7102310323, tapani.pakkanen@uef.fi.

Armando J.L. Pombeiro – Academician at the Academy of Sciences of Lisbon, PhD, Professor, President of the Center for Structural Chemistry of the Higher Technical Institute of the University of Lisbon, Lisbon, Portugal. Scopus Author ID 7006067269, ResearcherID I-5945-2012, <https://orcid.org/0000-0001-8323-888X>, pombeiro@ist.utl.pt.

Dmitrii V. Pyshnyi – Corresponding Member of the RAS, Dr. Sci. (Chem.), Professor, Institute of Chemical Biology and Fundamental Medicine, Siberian Branch of the RAS, Novosibirsk, Russian Federation. Scopus Author ID 7006677629, ResearcherID F-4729-2013, <https://orcid.org/0000-0002-2587-3719>, pyshnyi@niboch.nsc.ru.

Alexander S. Sigov – Academician at the RAS, Dr. Sci. (Phys. and Math.), Professor, President of MIREA – Russian Technological University, Moscow, Russian Federation. Scopus Author ID 35557510600, ResearcherID L-4103-2017, sigov@mirea.ru.

Alexander M. Toikka – Dr. Sci. (Chem.), Professor, Institute of Chemistry, Saint Petersburg State University, St. Petersburg, Russian Federation. Scopus Author ID 6603464176, ResearcherID A-5698-2010, <http://orcid.org/0000-0002-1863-5528>, a.toikka@spbu.ru.

Andrzej W. Trochimczuk – Dr. Sci. (Chem.), Professor, Faculty of Chemistry, Wrocław University of Science and Technology, Wrocław, Poland. Scopus Author ID 7003604847, andrzej.trochimczuk@pwr.edu.pl.

Aslan Yu. Tsvadze – Academician at the RAS, Dr. Sci. (Chem.), Professor, A.N. Frumkin Institute of Physical Chemistry and Electrochemistry of the RAS, Moscow, Russian Federation. Scopus Author ID 7004245066, ResearcherID G-7422-2014, tsiv@phyche.ac.ru.

Новаков Иван Александрович – академик РАН, д.х.н., профессор, президент Волгоградского государственного технического университета, Волгоград, Российская Федерация. Scopus Author ID 7003436556, ResearcherID I-4668-2015, <http://orcid.org/0000-0002-0980-6591>, president@vstu.ru.

Озерин Александр Никифорович – член-корр. РАН, д.х.н., профессор, Институт синтетических полимерных материалов им. Н.С. Ениколопова РАН, Москва, Российская Федерация. Scopus Author ID 7006188944, ResearcherID J-1866-2018, <https://orcid.org/0000-0001-7505-6090>, ozerin@ispm.ru.

Пакканен Тапани – PhD, профессор, Департамент химии, Университет Восточной Финляндии, Йоенсуу, Финляндия. Scopus Author ID 7102310323, tapani.pakkanen@uef.fi.

Помбейро Армандо – академик Академии наук Лиссабона, PhD, профессор, президент Центра структурной химии Высшего технического института Университета Лиссабона, Португалия. Scopus Author ID 7006067269, ResearcherID I-5945-2012, <https://orcid.org/0000-0001-8323-888X>, pombeiro@ist.utl.pt.

Пышный Дмитрий Владимирович – член-корр. РАН, д.х.н., профессор, Институт химической биологии и фундаментальной медицины Сибирского отделения РАН, Новосибирск, Российская Федерация. Scopus Author ID 7006677629, ResearcherID F-4729-2013, <https://orcid.org/0000-0002-2587-3719>, pyshnyi@niboch.nsc.ru.

Сигов Александр Сергеевич – академик РАН, д.ф.-м.н., профессор, президент МИРЭА – Российского технологического университета, Москва, Российская Федерация. Scopus Author ID 35557510600, ResearcherID L-4103-2017, sigov@mirea.ru.

Тойкка Александр Матвеевич – д.х.н., профессор, Институт химии, Санкт-Петербургский государственный университет, Санкт-Петербург, Российская Федерация. Scopus Author ID 6603464176, ResearcherID A-5698-2010, <http://orcid.org/0000-0002-1863-5528>, a.toikka@spbu.ru.

Трохимчук Анджей – д.х.н., профессор, Химический факультет Вроцлавского политехнического университета, Вроцлав, Польша. Scopus Author ID 7003604847, andrzej.trochimczuk@pwr.edu.pl.

Цивадзе Аслан Юсупович – академик РАН, д.х.н., профессор, Институт физической химии и электрохимии им. А.Н. Фрумкина РАН, Москва, Российская Федерация. Scopus Author ID 7004245066, ResearcherID G-7422-2014, tsiv@phyche.ac.ru.

CONTENTS

СОДЕРЖАНИЕ

**Theoretical Bases of Chemical
Technology**

*Frolkova A.V., Fertikova V.G., Rytova E.V.,
Frolkova A.K.*

Evaluation of the adequacy of phase equilibria
modeling based on various sets
of experimental data

457

**Chemistry and Technology
of Medicinal Compounds
and Biologically Active Substances**

Anh C. Ha

Microfluidic method as a promising technique
for synthesizing antimicrobial compounds

465

Biochemistry and biotechnology

*Pashkov E.A., Faizuloev E.B., Korchevaya E.R.,
Rtishchev A.A., Cherepovich B.S., Sidorov A.V.,
Poddubikov A.V., Bystritskaya E.P., Dronina Yu.E.,
Bykov A.S., Svitich O.A., Zverev V.V.*

Knockdown of *FLT4*, *Nup98*, and *Nup205* cellular
genes as a suppressor for the viral activity of
Influenza A/WSN/33 (H1N1) in A549 cell culture

476

**Теоретические основы
химической технологии**

*Фролкова А.В., Фертикова В.Г., Рытова Е.В.,
Фролкова А.К.*

Оценка адекватности моделирования фазовых
равновесий на основе различных наборов
экспериментальных данных

**Химия и технология лекарственных
препаратов и биологически
активных соединений**

Anh C. Ha

Microfluidic method as a promising technique
for synthesizing antimicrobial compounds

Биохимия и биотехнология

*Пашков Е.А., Файзулоев Е.Б., Корчевая Е.Р.,
Ртищев А.А., Черепович Б.С., Сидоров А.В.,
Поддубиков А.В., Быстрицкая Е.П., Дронина Ю.Е.,
Быков А.С., Свитич О.А., Зверев В.В.*

Нокдаун клеточных генов *FLT4*, *Nup98*
и *Nup205* как супрессор вирусной активности
гриппа А/WSN/33 (H1N1) в культуре клеток А549

Synthesis and Processing of Polymers and Polymeric Composites

Stuzhuk A.N., Shkolnikov A.V., Gorbatov P.S., Gritskova I.A.

Influence of emulgator nature on dispersity and stability of artificial polymer suspensions based on polycarbonate and polymethyl methacrylate

490

Chemistry and Technology of Inorganic Materials

Nikishina E.E.

Heterophase synthesis of cobalt ferrite

502

Analytical Methods in Chemistry and Chemical Technology

Aleksandrova D.A., Melamed T.B., Baberkina E.P., Fenin A.A., Osinova E.S., Kovalenko A.E., Yakushin R.V., Shaltaeva Yu.R., Belyakov V.V., Zykova D.I.

Ion mobility spectrometry of *N*-methylimidazole and possibilities of its determination

512

Mathematical Methods and Information Systems in Chemical Technology

Kartashov E.M.

Thermal destruction of polymeric fibers in the theory of temporary dependence of strength

526

Синтез и переработка полимеров и композитов на их основе

Стужук А.Н., Школьников А.В., Горбатов П.С., Грицкова И.А.

Влияние природы эмульгатора и концентрации полимера на дисперсность и устойчивость искусственных полимерных суспензий на основе поликарбоната и полиметилметакрилата

Химия и технология неорганических материалов

Никишина Е.Е.

Гетерофазный синтез феррита кобальта

Аналитические методы в химии и химической технологии

Александрова Д.А., Меламед Т.Б., Баберкина Е.П., Фенин А.А., Осина Е.С., Коваленко А.Е., Якушин Р.В., Шалтаева Ю.Р., Беляков В.В., Зыкова Д.И.

Спектрометрия ионной подвижности *N*-метилимидазола и возможности его определения

Математические методы и информационные системы в химической технологии

Карташов Э.М.

Тепловое разрушение полимерных волокон в теории временной зависимости прочности

THEORETICAL BASES OF CHEMICAL TECHNOLOGY
ТЕОРЕТИЧЕСКИЕ ОСНОВЫ ХИМИЧЕСКОЙ ТЕХНОЛОГИИ

ISSN 2686-7575 (Online)

<https://doi.org/10.32362/2410-6593-2021-16-6-457-464>



UDC 54-145.561

RESEARCH ARTICLE

Evaluation of the adequacy of phase equilibria modeling based on various sets of experimental data

Anastasiya V. Frolkova, Veronica G. Fertikova, Elena V. Rytova[@], Alla K. Frolkova

MIREA – Russian Technological University (M.V. Lomonosov Institute of Fine Chemical Technologies), Moscow, 119571 Russia

[@]Corresponding author, e-mail: erytova@gmail.com

Abstract

Objectives. *The purpose of the paper is to compare the adequacy of mathematical models of vapor–liquid equilibrium (VLE) and their ability to reproduce the phase behavior of the ternary system benzene–cyclohexane–chlorobenzene using different experimental data sets to evaluate binary interaction parameters.*

Methods. *The research methodologies were mathematical modeling of VLE in the Aspen Plus V.10.0 software package using activity coefficient models (Non-Random Two-Liquid (NRTL), Wilson) and the Universal quasichemical Functional-group Activity Coefficients (UNIFAC) group model, which allows for independent information. For the benzene–cyclohexane–chlorobenzene ternary system, the use of the NRTL equation is warranted because it provides a better description of the VLE experimental data.*

Results. *The diagram construction of the constant volatility of cyclohexane relative to benzene lines revealed three topological structures. Only one of them can be considered reliable because it corresponds to the experimental data and coincides with the UNIFAC model diagram constructed based on independent UNIFAC model data. The results indicate that to study systems containing components with similar properties, it is necessary to improve the description quality of the available data sets (the relative error should not exceed 1.5%).*

Conclusions. *The reproduction of the thermodynamic features of various manifolds in the composition simplex obtained by processing direct VLE data can be used to supplement the adequacy of the model. For the cyclohexane–benzene–chlorobenzene system, the best NRTL equation parameters are those regressed from the extensive experimental VLE data available in the literature for the ternary system as a whole.*

Keywords: mathematical modeling, binary interaction parameters, vapor-liquid equilibrium, experimental data, components relative volatility

For citation: Frolkova A.V., Fertikova V.G., Rytova E.V., Frolkova A.K. Evaluation of the adequacy of phase equilibria modeling based on various sets of experimental data. *Tonk. Khim. Tekhnol. = Fine Chem. Technol.* 2021;16(6):457–464 (Russ., Eng.). <https://doi.org/10.32362/2410-6593-2021-16-6-457-464>

НАУЧНАЯ СТАТЬЯ

Оценка адекватности моделирования фазовых равновесий на основе различных наборов экспериментальных данных

А.В. Фролкова, В.Г. Фертикова, Е.В. Рытова[@], А.К. Фролкова

МИРЭА – Российский технологический университет (Институт тонких химических технологий им. М.В. Ломоносова), Москва, 119571 Россия

[@]Автор для переписки, e-mail: erytova@gmail.com

Аннотация

Цели. Сравнительный анализ адекватности математических моделей парожидкостного равновесия (ПЖР) и их возможности воспроизводить особенности фазового поведения тройной системы бензол–циклогексан–хлорбензол при использовании разных наборов экспериментальных данных для оценки параметров бинарного взаимодействия.

Методы. В качестве методов исследования выбрано математическое моделирование ПЖР в программном комплексе AspenPlus V.10.0. с использованием уравнений локальных составов (NRTL, Wilson) и групповой модели UNIFAC, позволяющей получить независимую информацию. Для системы бензол–циклогексан–хлорбензол обоснован выбор уравнения NRTL, обеспечивающего более высокое качество описания экспериментальных данных ПЖР.

Результаты. Построение диаграммы хода линий постоянной летучести циклогексана относительно бензола выявило три топологических структуры, из которых только одна может считаться достоверной, поскольку соответствует данным натурального эксперимента и совпадает с диаграммой, построенной на основе независимых данных модели UNIFAC. Полученные результаты свидетельствуют о том, что при исследовании систем, содержащих близкие по свойствам компоненты, необходимо повышать качество описания имеющихся массивов данных (относительная ошибка не должна превышать 1.5%).

Выводы. Воспроизведение термодинамических особенностей хода различных многообразий в концентрационном симплексе, полученных обработкой прямых данных ПЖР, может служить дополнительной оценкой адекватности модели. Для системы циклогексан–бензол–хлорбензол наилучшим является набор параметров уравнения NRTL, которые оценены по обширным экспериментальным данным ПЖР, имеющимся в литературе для тройной системы в целом.

Ключевые слова: математическое моделирование, параметры бинарного взаимодействия, парожидкостное равновесие, экспериментальные данные, относительная летучесть компонентов

Для цитирования: Фролкова А.В., Фертикова В.Г., Рытова Е.В., Фролкова А.К. Оценка адекватности моделирования фазовых равновесий на основе различных наборов экспериментальных данных. *Тонкие химические технологии.* 2021;16(6):457–464. <https://doi.org/10.32362/2410-6593-2021-16-6-457-464>

INTRODUCTION

Computational experimentation with software products is currently one of the most accessible, widely used, and fast methods for studying phase equilibria and various phase processes, especially the distillation process. The choice of a mathematical model that allows reproducing the physicochemical properties of the object under study with an acceptable error margin is crucial (usually, this margin of error should not exceed 3–6%, depending on the complexity of the system under consideration).

The creation of an adequate mathematical model and the selection of its parameters should be based on experimental data (ED) that has undergone thermodynamic consistency tests [1–4]. Depending on the phase behavior features of the system and the number of components in it, the researcher may have different information for carrying out the parameter estimation procedure: data on different types of equilibrium (liquid–vapor, liquid–liquid, liquid–liquid–vapor, liquid–solid, etc.); boiling points at fixed pressure and azeotrope compositions; data for its overall system or its constituents. Moreover, the values of the binary interaction parameters of the models can be obtained, depending on the data used, their volume, and quality, reproducing the known properties of the system with varying accuracy. The model has good predictive capabilities if it satisfactorily describes not only direct ED but also the course diagram of various isolines of scalar properties obtained on their bases, such as the distribution coefficients of components between phases or the coefficients of relative volatility. These properties are important in the development of flowsheets for distillation separation of mixtures using sharp distillation [5] or extractive distillation [6–9]. The presence of an adequate mathematical model allows for the planning of a computational experiment with a wide range of device operating parameters to determine the optimal modes for separation with the least amount of energy consumption.

The present work aims at comparing description results of the phase behavior of the benzene (B) – cyclohexane (CH) – chlorobenzene (CB) system using Non-Random Two-Liquid (NRTL) and Wilson equations [10], of which binary interaction parameters are determined from various ED sets, as well as the equation of the Universal quasichemical Functional-group Activity Coefficients (UNIFAC) group model.

RESULTS AND DISCUSSION

The B–CH–CB system is well studied in the literature, including experimental vapor–liquid equilibrium (VLE) data for three binary constituents

[11–13] and extensive data for the ternary system in the entire composition simplex [13]. All data were checked for thermodynamic consistency using the Herington and Van Ness tests [1, 2].

To evaluate the parameters of the binary interaction of the equations of local compositions, three ED sets will be considered: ED (2) for the VLE of binary constituents; ED (3) for the VLE of a ternary system; ED (2 + 3) for the entire volume of available data. For each set, the parameters of the NRTL equation (1) and the Wilson equation (2) [5] are evaluated in the AspenPlus V.10.0 software package:

$$\ln \gamma_i = \frac{\sum_j x_j \tau_{ji} G_{ji}}{\sum_k x_k G_{ki}} + \sum_j \frac{x_j G_{ji}}{\sum_k x_k G_{kj}} \left(\tau_{ij} - \frac{\sum_m x_m \tau_{mj} G_{mj}}{\sum_k x_k G_{kj}} \right), \quad (1)$$

where γ_i is an activity coefficient of the i th component;

$$G_{ij} = \exp(-\alpha_{ij} \tau_{ij}); \quad \tau_{ij} = \alpha_{ij} + \frac{b_{ij}}{T} + e_{ij} \ln T + f_{ij} T;$$

$$\alpha_{ij} = c_{ij} + d_{ij}(T - 273.15); \quad \tau_{ii} = 0; \quad G_{ii} = 1.$$

$$\ln \gamma_i = 1 - \ln \left(\sum_j A_{ij} x_j \right) - \sum_j \frac{A_{ji} x_j G_{ji}}{\sum_k A_{jk} x_k}, \quad (2)$$

$$\text{where } \ln A_{ij} = \alpha_{ij} + \frac{b_{ij}}{T} + c_{ij} \ln T + d_{ij} T + \frac{e_{ij}}{T^2}.$$

Tables 1 and 2 show the average relative errors in describing the VLE (ΔT —by boiling point, ΔY —by vapor phase composition) at a pressure of 101.3 kPa, as well as binary interaction parameters (A_{ij} , A_{ji} , B_{ij} , B_{ji} , C_{ij}). The maximum errors in the description of the phase equilibrium of binary systems do not exceed 3%, and the ternary system is less than 6%.

A comparison of the parameter estimation results shows that both models are capable of accurately describing the VLE of the system under study. However, the NRTL model parameters provide a more accurate description, thus further calculations will be performed using this model.

In the software package, the UNIFAC group model was used to calculate the VLE of the ternary system and its binary constituents at a pressure of 101.3 kPa. The errors in the phase equilibrium description in Table 3 also indicate a high reproduction quality of the VLE ED of the ternary system and its binary constituents.

In most cases, the evaluation of the quality of a mathematical model is complete when the values are absolute and relative errors in the description of direct ED are calculated. However, for systems characterized by small differences in components and mixtures, such as the boiling points of benzene and cyclohexane (80.10 and 80.75°C) and the volatility of benzene relative to cyclohexane [13] (in the composition simplex, the range of variation of these values is 0.8–1.4), additional characteristics must be attracted to confirm the adequacy of the model. The course structure diagram of the constant relative volatility lines of components *i, j* is chosen as such a characteristic. In the AspenPlus software package, the VLE in the B–CH–CB system was calculated using three sets of binary interaction parameters

of the NRTL equation (Table 1). The values of the relative volatility coefficients of the α_{ij} cyclohexane (*i*)–benzene (*j*) pair are determined by the formula:

$$\alpha_{ij} = \frac{y_i x_j}{x_i y_j}, \quad (3)$$

where $y_{i(j)}$ is the concentration of component *i(j)* in the vapor phase, $x_{i(j)}$ is the concentration of component *i(j)* in the liquid phase.

Isolines are constructed in the composition triangle, along which the relative volatility takes constant values (α_{ij} -lines). The resulting diagrams are shown in Fig. 1.

Table 1. Binary interaction parameters of the NRTL equation and description results of various ED

Binary system	A_{ij}	A_{ji}	B_{ij}	B_{ji}	C_{ij}	$\Delta T, \%$	$\Delta Y, \%$
ED (2)							
B–CH	–8.20751	–8.1266	1779.9	4156.59	0.01906	0.16	1.66
B–CB	–10.9556	2.22538	3832.44	–231.437	0.3	0.67	0.49
CH–CB	0.776229	2.52749	–690.951	–564.789	0.028905	1.23	1.21
ED (3)							
B–CH	0.00252441	–8.85555	88.8179	3108.78	3.16605	0.92*	3.15* (4.11)*
B–CB	2.6802	–4.01723	–514.445	1050.66	0.3		
CH–CB	–4.43646	2.34578	–409.339	1641.97	0.0303645		
ED (2 + 3)							
B–CH	–3.67734	–4.80805	1744.96	1426.44	0.3	1.01	2.09
B–CB	0.354308	0.345032	–170.497	–132.059	0.3	0.77	0.86
CH–CB	–4.32852	0.619341	1216.07	537.117	0.3	1.03	1.97
B–CH–CB	The sets of binary interaction parameters are the same					1.41*	5.02* (5.14)*

*Average errors in the description of the boiling point and benzene (B) (cyclohexane (CH)) concentration in the vapor phase of the ternary system. CB – chlorobenzene.

Table 2. Binary interaction parameters of the Wilson equation and description results of various ED

Binary system	A_{ij}	A_{ji}	B_{ij}	B_{ji}	$\Delta T, \%$	$\Delta Y, \%$
ED (2)						
B-CH	2.22465	9.39094	-781.052	-3432.02	0.10	1.43
B-CB	-0.2853	-0.2629	-420.976	421.622	0.65	1.41
CH-CB	-5.21084	8.4696	584.647	-2928.92	1.20	1.49
ED (3)						
B-CH	3.50955	1.8551	-1006.89	-1079.4	1.25*	4.79* (6.14)*
B-CB	0.0317	-0.0239	11.4715	44.8354		
CH-CB	0.701629	2.71709	-1041.94	-696.601		
ED (2 + 3)						
B-CH	2.74451	5.25204	-781.05	-2202.57	1.19	2.29
B-CB	-0.2853	-0.2629	122.157	127.361	0.8	0.89
CH-CB	-0.4298	3.62262	-490.08	-1078.44	1.00	1.99
B-CH-CB	The sets of binary interaction parameters are the same				1.45*	5.06* (5.31)*

*Average errors in the description of the boiling point and benzene (B) (cyclohexane (CH)) concentration in the vapor phase of the ternary system. CB – chlorobenzene.

Table 3. ED description results of the VLE by the UNIFAC equation

Binary system	$\Delta T, \%$	$\Delta Y_{B(CH)}, \%$
B-CH	0.20	3.36
B-CB	0.38	2.35
CH-CB	0.87	1.94
B-CH-CB	3.88	3.56 (0.23)

As seen, the structures of the stroke α_{ij} -line diagram differ. Figure 1a shows two singular points on binary constituents: elliptical type (constituent B-CB) and hyperbolic type (constituent CH-CB); in Fig. 1b, there are also two binary singular points, however, an

elliptical type point belongs to the CH-CB constituent and a hyperbolic one belongs to the B-CB; there are no singular points on the binary constituents in Fig. 1b and 1d (these diagrams are similar not only qualitatively, but also quantitatively).

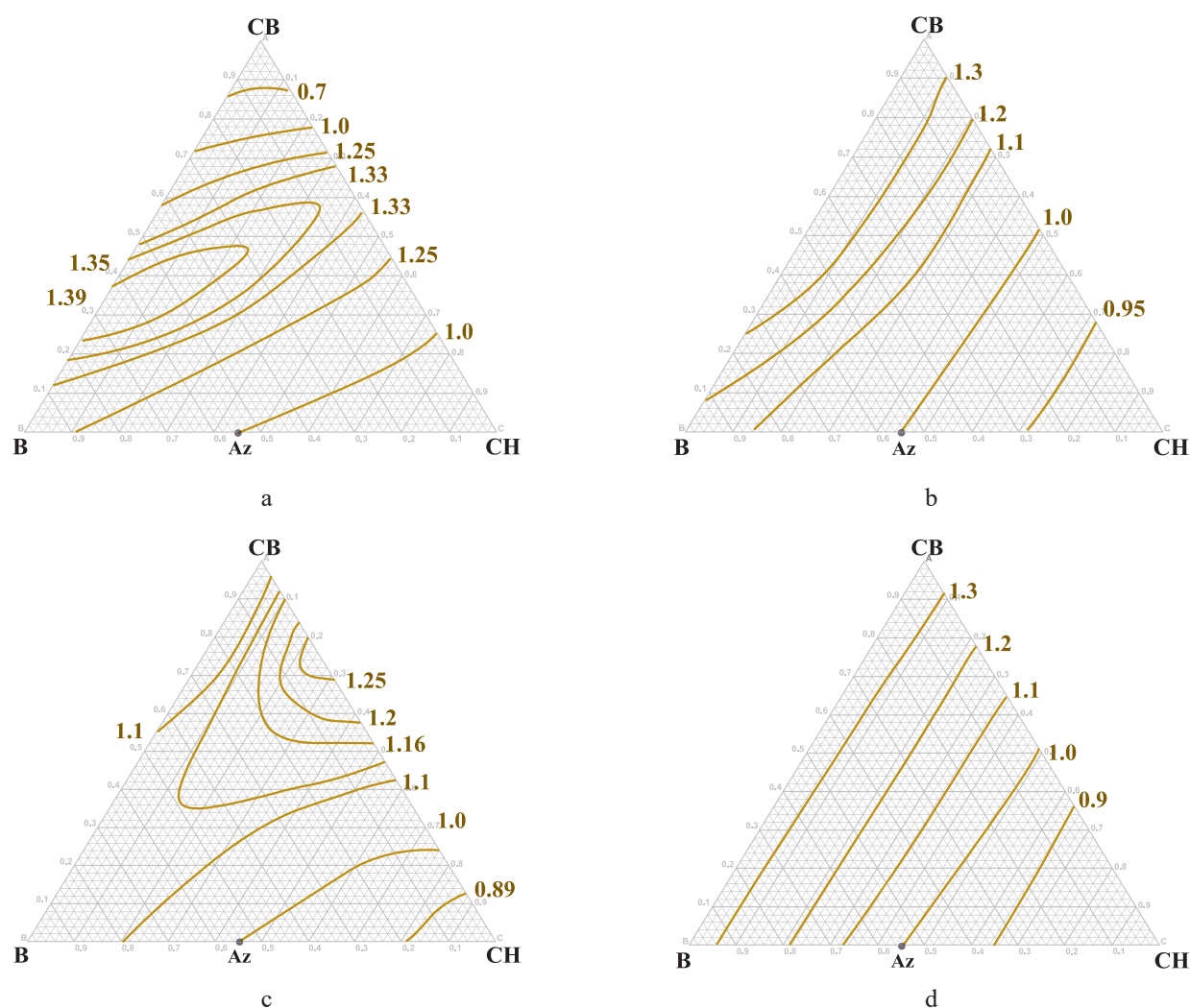


Fig. 1. Diagram of the relative volatility isolines of a cyclohexane (CH)–benzene (B) pair, constructed using the NRTL equation parameters obtained based on ED: (a) ED (2); (b) ED (3); (c) ED (2 + 3), as well as the UNIFAC equation (d).

It is worth noting that the structures of the diagram for the last two systems are topologically equivalent to the structure of the relative volatility contour diagram constructed from ED of the VLE [13].

This fully concerns the recommendations of works [13] on the use of chlorobenzene as a potential separating agent in the extractive distillation process of a binary benzene–cyclohexane mixture and the fact that chlorobenzene has high selectivity. The use of the ED (2) and ED (2 + 3) parameter sets will lead to incorrect column performance and energy consumption values of the extractive distillation complex. Thus, for the B–CH–CB system, the best is a set of NRTL equation parameters determined using extensive ED of the VLE available in the literature for the entire ternary system.

In the absence of the ED, the UNIFAC group model has become widely used in modeling the properties of mixtures. It satisfactorily describes relatively simple objects, as evidenced by practice [14–16]. Simultaneously, with the presence of many

liquid phases in the system [17], an increase in the number of azeotropes and their components, and the emergence of biazeotropic constituents [18–20], the prognostic capabilities of the model decrease rapidly. The use of the UNIFAC model becomes impractical when the system significantly deviates from the ideal behavior.

CONCLUSIONS

It has been demonstrated that different sets of binary interaction parameters of the NRTL equation accurately reproduce the VLE ED, on the basis of which they were obtained. However, the phase equilibrium calculation of the ternary system and the constant relative volatility isoline construction of the cyclohexane–benzene pair revealed the presence of three different topological structures of diagrams α_{ij} -lines, of which only one (Fig. 1b) can be considered reliable because it corresponds to the field experiment data and coincides with the diagram constructed using independent data from the UNIFAC

model. The findings indicate that to study systems with components with similar properties, the description quality of the available data arrays must be improved (the relative error should not exceed 1.5%). It is also crucial to reproduce thermodynamic features of phase behavior. The latter includes the VLE data-processed course structures of various characteristic manifolds. Only in this case can the obtained model parameters be used for further regularities investigation and calculation of the distillation process. Unfortunately, ED for the ternary systems VLE is limited and is not available for most systems. In conditions of limited experimental information, it is necessary to conduct at least a local full-scale experiment to confirm the adequacy of mathematical modeling.

Acknowledgments

The study was supported by the Ministry of Education and Science of the Russian Federation, the State Task No. 0706-2020-0020.

REFERENCES

- Herington E.F.G. Tests for the Consistency of Experimental Isobaric Vapor-Liquid Equilibrium Data. *J. Inst. Pet.* 1951;37:457–470.
- Van Ness H.C., Byer S.M., Gibbs R.E. Vapor-liquid equilibrium: Part I. An appraisal of data reduction methods. *AIChE J.* 1973;19(2):238–244. <https://doi.org/10.1002/aic.690190206>
- Jackson P.L., Wilsak R.A. Thermodynamic consistency tests based on the Gibbs-Duhem equation applied to isothermal, binary vapor-liquid equilibrium data: data evaluation and model testing. *Fluid Phase Equilib.* 1995;10392):155–197. [https://doi.org/10.1016/0378-3812\(94\)02581-K](https://doi.org/10.1016/0378-3812(94)02581-K)
- Wisniak J. The Herington test for thermodynamic consistency. *Ind. Eng. Chem. Res.* 1994;33(1):177–180. <https://doi.org/10.1021/ie00025a025>
- Peshkehontseva M.E., Maevskiy M.A., Gaganov I.S., Frolkova A.V. Areas of energy advantage for flowsheets of separation modes for mixtures containing components with similar volatilities. *Tonk. Khim. Tekhnol. = Fine Chem. Technol.* 2020;15(3):7–20 (in Russ.). <https://doi.org/10.32362/2410-6593-2020-15-3-7-20>
- Gerbaud V., Rodríguez-Donis I., Hegely L., Láng P., Dénes F., et al. Review of Extractive Distillation. Process design, operation optimization and control. *Chemical Engineering Research and Design.* 2019;141:229–271. <https://doi.org/10.1016/j.cherd.2018.09.020>
- Lei Z., Li C., Chen B. Extractive Distillation: A Review. *Separation & Purification Reviews.* 2003;32(2):121–213. <https://doi.org/10.1081/SPM-120026627>
- Hilal N., Yousef G., Langston P. The reduction of extractive agent in extractive distillation and auto-extractive distillation. *Chem. Eng. Process.* 2002;41(8):673–679. [https://doi.org/10.1016/S0255-2701\(01\)00187-8](https://doi.org/10.1016/S0255-2701(01)00187-8)

Authors' contributions

A.V. Frolkova – calculation of vapor-liquid equilibrium, construction and analysis of diagrams, writing the paper;

V.G. Fertikova – estimation of binary interaction parameters, verification of the adequacy of mathematical modeling;

E.V. Rytova – evaluation of binary interaction parameters; verification of the adequacy of mathematical modeling;

A.K. Frolkova – analysis of diagrams, formulation of conclusions, writing the paper.

The authors declare that there is no conflict of interest.

9. Sazonova A.Y., Raeva V.M., Chelyuskina T.V., et al. Choice of extractive agents for separating benzene-perfluorobenzene biazotropic mixture based on thermodynamic criterion. *Theor. Found. Chem. Eng.* 2014;48(2):148–157. <https://doi.org/10.1134/S0040579514020122>

[Original Russian Text: Sazonova A.Y., Raeva V.M., Chelyuskina T.V., et al. Choice of extractive agents for separating benzene-perfluorobenzene biazotropic mixture based on thermodynamic criterion. *Teoreticheskie Osnovy Khimicheskoi Tekhnologii.* 2014;48(2):163–172 (in Russ.). <https://doi.org/10.7868/S0040357114020122>]

10. Renon H.; Prausnitz J.M. Local Compositions in Thermodynamic Excess Functions for Liquid Mixtures. *AIChE J.* 1968;14(1):135–144. <https://doi.org/10.1002/aic.690140124>

11. Rolemberg M.P.; Krahenbuhl M.A. Vapor-Liquid Equilibria of Binary and Ternary Mixtures of Benzene, Cyclohexane, and Chlorobenzene at 40 kPa and 101.3 kPa. *J. Chem. Eng. Data.* 2001;46(2):256–260. <https://doi.org/10.1021/je0000591>

12. Saito S. Separation of hydrocarbons. Asahi Garasu Kogyo Gijutsu Shorekai Kenkyu Hokoku. 1969;15:397–407. <http://www.ddbst.com/en/EED/VLE/VLE%20Hexane%3Bp-Xylene.php>, <http://www.ddbst.com/en/EED/VLE/VLE%20Benzene%3Bp-Xylene.php>

13. Silva L.M.C., Mattedi S., Gonzalez-Olmos R., Iglesias M. Azeotropic behavior of (benzene + cyclohexane + chlorobenzene) ternary mixture using chlorobenzene as entrainer at 101.3 kPa. *J. Chem. Thermodynamics.* 2006;38:1725–1736. URL: <http://www.repositorio.ufba.br/ri/handle/ri/6341>

14. Skjold-Jorgensen S., Kolbe B., Gmehling J., Rasmussen P. Vapor-Liquid Equilibria by UNIFAC Group Contribution. Revision and Extension. *Ind. Eng. Chem. Process Des. Dev.* 1979;18(4):714–722. <https://doi.org/10.1021/i260072a024>

15. Aznar M., Telles A.S. Prediction of electrolyte vapor-liquid equilibrium by UNIFAC-Dortmund. *Braz. J. Chem. Eng.* 2001;18(2):127–137. <https://doi.org/10.1590/S0104-66322001000200001>

16. Luo W., Wang Q., Fu L., Deng W., Zhang X., Guo C. New Group-Interaction Parameters of the UNIFAC Model: Aromatic Carboxyl Binaries. *Ind. Eng. Chem. Res.* 2011;50(7):4099–4105. <https://doi.org/10.1021/ie101934j>

17. Frolkova A.V., Zakharova D.S., Frolkova A.K., Balbenov S.A. Liquid-liquid and liquid-liquid-liquid equilibrium for ternary system water–acetonitrile–cyclohexane at 298.15 K. *Fluid Phase Equilibria.* 2016;408:10–14. <https://doi.org/10.1016/j.fluid.2015.06.039>

18. Frolkova A.V., Ososkova T.E., Frolkova A.K. Thermodynamic and Topological Analysis of Phase Diagrams of Quaternary Systems with Internal Singular Points. *Theor. Found. Chem. Eng.* 2020;54(3):407–419. <https://doi.org/10.1134/S0040579520020049>

19. Myagkova T.O., Chelyuskina T.V., Frolkova A.K. The special features of the phase behavior of multicomponent bizaotropic systems. *Russ. J. Phys. Chem.* 2007;81(6):841–846. <https://doi.org/10.1134/S0036024407060027>

20. Zhuchkov V.I., Frolkova A.K., Nazanskiy S.L. Experimental research and mathematical modeling of vapor-liquid equilibrium in the ternary benzene – hexafluorobenzene – dimethyl sulfoxide system. *Russ. Chem. Bull.* 2018;67(2):200–205. <https://doi.org/10.1007/s11172-018-2059-x>

About the authors:

Anastasiya V. Frolkova, Cand. Sci. (Eng.), Associate Professor, Department of Chemistry and Technology of Basic Organic Synthesis, M.V. Lomonosov Institute of Fine Chemical Technologies, MIREA – Russian Technological University (86, Vernadskogo pr., Moscow, 119571, Russia). E-mail: frolkova_nastya@mail.ru. Scopus Author ID 12782832700, ResearcherID N-4517-2014, <https://orcid.org/0000-0001-5675-5777>

Veronica G. Fertikova, Student, Department of Chemistry and Technology of Basic Organic Synthesis, M.V. Lomonosov Institute of Fine Chemical Technologies, MIREA – Russian Technological University (86, Vernadskogo pr., Moscow, 119571, Russia). E-mail: fertikova1998@yandex.ru. <https://orcid.org/0000-0001-5450-5846>

Elena V. Rytova, Cand. Sci. (Eng.), Head of the Laboratory, Department of Chemistry and Technology of Basic Organic Synthesis, M.V. Lomonosov Institute of Fine Chemical Technologies, MIREA – Russian Technological University (86, Vernadskogo pr., Moscow, 119571, Russia). E-mail: erytova@gmail.com. <https://orcid.org/0000-0002-9244-5319>

Alla K. Frolkova, Dr. Sci. (Eng.), Professor, Head of the Department of Chemistry and Technology of Basic Organic Synthesis, M.V. Lomonosov Institute of Fine Chemical Technologies, MIREA – Russian Technological University (86, Vernadskogo pr., Moscow, 119571, Russia). E-mail: frolkova@gmail.com. Scopus Author ID 35617659200, ResearcherID G-7001-2018, <https://orcid.org/0000-0002-9763-4717>

Об авторах:

Фролкина Анастасия Валериевна, к.т.н., доцент, кафедра химии и технологии основного органического синтеза Института тонких химических технологий им. М.В. Ломоносова ФГБОУ «МИРЭА – Российский технологический университет» (119571, Россия, Москва, пр-т Вернадского, д. 86). E-mail: frolkova_nastya@mail.ru. Scopus Author ID 12782832700, ResearcherID N-4517-2014, <https://orcid.org/0000-0001-5675-5777>

Фертикова Вероника Геннадьевна, студент магистратуры кафедра химии и технологии основного органического синтеза Института тонких химических технологий им. М.В. Ломоносова ФГБОУ «МИРЭА – Российский технологический университет» (119571, Россия, Москва, пр-т Вернадского, д. 86). E-mail: fertikova1998@yandex.ru. <https://orcid.org/0000-0001-5450-5846>

Рытова Елена Вячеславовна, к.т.н., заведующий лабораторией, кафедра химии и технологии основного органического синтеза Института тонких химических технологий им. М.В. Ломоносова ФГБОУ «МИРЭА – Российский технологический университет» (119571, Россия, Москва, пр-т Вернадского, д. 86). E-mail: erytova@gmail.com. <https://orcid.org/0000-0002-9244-5319>

Фролкина Алла Константиновна, д.т.н., профессор, заведующий кафедрой химии и технологии основного органического синтеза Института тонких химических технологий им. М.В. Ломоносова ФГБОУ «МИРЭА – Российский технологический университет» (119571, Россия, Москва, пр-т Вернадского, д. 86). E-mail: frolkova@gmail.com. ResearcherID G-7001-2018, Scopus Author ID 35617659200, <https://orcid.org/0000-0002-9763-4717>

The article was submitted: October 21, 2021; approved after reviewing: November 01, 2021; accepted for publication: November 20, 2021.

Translated from Russian into English by N. Isaeva

Edited for English language and spelling by Enago, an editing brand of Crimson Interactive Inc.

**CHEMISTRY AND TECHNOLOGY OF MEDICINAL COMPOUNDS
AND BIOLOGICALLY ACTIVE SUBSTANCES**

**ХИМИЯ И ТЕХНОЛОГИЯ ЛЕКАРСТВЕННЫХ ПРЕПАРАТОВ
И БИОЛОГИЧЕСКИ АКТИВНЫХ СОЕДИНЕНИЙ**

ISSN 2686-7575 (Online)

<https://doi.org/10.32362/2410-6593-2021-16-6-465-475>



UDC 615.28

REVIEW ARTICLE

**Microfluidic method as a promising technique
for synthesizing antimicrobial compounds**

Anh C. Ha^{1,2,@}

¹Faculty of Chemistry, Ho Chi Minh City University of Technology (HCMUT), 268 Ly Thuong Kiet Street, Ho Chi Minh City, Vietnam

²Vietnam National University Ho Chi Minh City (VNU-HCM), Linh Trung ward, Thu Duc District, Ho Chi Minh City, Vietnam

@Corresponding author, e-mail: hcanh@hcmut.edu.vn

Abstract

Objectives. The study aimed to analyze the current antiseptics and disinfectants, explore the possibility of synthesizing various antiseptics including oligohexamethylene guanidine hydrochloride (OHMG-HC) using microfluidic technology, and investigate the main synthesis parameters affecting the properties of the resulting product.

Methods. This article presented a review of literature sources associated with investigations of antimicrobial resistance, the uses of agents based on polyhexamethylene guanidine hydrochloride, oligohexamethylene guanidine hydrochloride, and other salts, obtained using modern synthesis technologies with microreactors.

Results. The relevance of developing production technologies for the “OHMG-HC branched” substance was determined. The microfluidic method for the synthesis of polymers, and its application prospects for obtaining the target substance were compared with the existing methods. Advantages of the microfluidic method were indicated.

Conclusions. Microreactor technologies allow for more accurate control of the conditions of the polycondensation reaction of the starting monomers and increase the yield and selectivity of the oligomers obtained, leading to an increase in the product purity and process efficiency, in contrast with other known methods. The use of microreactor technologies for the synthesis of branched oligohexamethylene guanidine hydrochloride products is a promising strategy.

Keywords: antiseptic, disinfectant, alkylene guanidines, oligohexamethylene guanidine hydrochloride, microfluidic technologies, microreactor

For citation: Ha A.C. Microfluidic method as a promising technique for synthesizing antimicrobial compounds. *Tonk. Khim. Tekhnol. = Fine Chem. Technol.* 2021;16(6):465–475. <https://doi.org/10.32362/2410-6593-2021-16-6-465-475>

ОБЗОРНАЯ СТАТЬЯ

Микрофлюидный метод как перспективная технология для синтеза антимикробных соединений

А.К. Ха^{1,2,@}

¹Химико-технологический факультет, Технологический университет Хошимина, 268 Ли Тхыонг Кьет ул., г. Хошимин, Вьетнам

²Вьетнамский национальный университет, Район Тхёк, г. Хошимин, Вьетнам

@ Автор для переписки, e-mail: hcanh@hcmut.edu.vn

Аннотация

Цели. Цель исследования – проанализировать применяющиеся антисептики и дезинфектанты, рассмотреть возможность синтеза различных антисептиков и отдельно синтеза олигогексаметиленгуанидина гидрохлорида (ОГМГ-ГХ) с применением микрофлюидной технологии, а также изучить основные параметры синтеза, влияющие на характеристики получаемого продукта.

Методы. Представлен обзор литературных источников, связанных с исследованиями антимикробной резистентности, применением средств на основе полигексаметиленгуанидина гидрохлорида, олигогексаметиленгуанидина гидрохлорида, а также других солей, полученных современными технологиями синтеза с использованием микрореакторов.

Результаты. Определена актуальность разработки технологии получения субстанции «ОГМГ-ГХ разветвленный». Рассмотрены существующие способы получения субстанции и их недостатки. Также рассмотрен микрофлюидный способ синтеза полимеров, его достоинства и перспективы его использования для получения целевой субстанции.

Выводы. Микрореакторные технологии позволяют более точно контролировать условия реакции поликонденсации исходных мономеров и повышать выход и селективность полученных олигомеров, что приводит к повышению чистоты продукта и эффективности процесса, в отличие от других известных способов. Использование микрореакторных технологий для синтеза разветвленных продуктов гидрохлорида олигогексаметиленгуанидина является перспективной стратегией.

Ключевые слова: антисептик, дезинфектант, алкиленгуанидины, олигогексаметиленгуанидина гидрохлорид, микрофлюидные технологии, микрореактор

Для цитирования: Ha A.C. Microfluidic method as a promising technique for synthesizing antimicrobial compounds. *Tonk. Khim. Tekhnol. = Fine Chem. Technol.* 2021;16(6):465–475. <https://doi.org/10.32362/2410-6593-2021-16-6-465-475>

INTRODUCTION

Currently, one of the most important global problems is the progressive resistance of pathogenic microorganisms to applied biocidal drugs, and special measures are being developed to combat this problem [1]. Approximately 50000 people die annually from infectious diseases caused by antimicrobial-resistant microbes in Europe and the United States, with this number reaching hundreds of thousands in developing countries.

The resistance of microorganisms is manifested by the presence of structural polymers in their cell membrane, e.g., peptidoglycan. Peptidoglycan provides mechanical strength and structure to the cell, as well as thickness and shape, which depend on the type of peptidoglycan.¹ To protect their cytoplasmic membrane, gram-positive bacteria possess a thick layer of peptidoglycan, while gram-negative bacteria possess inner and outer membranes surrounding a relatively thin peptidoglycan matrix and periplasmic space. There are components associated with both types of cell walls that limit the ability of antibiotics and antiseptics to penetrate these structures (efflux pumps that remove toxins, protective enzymes (e.g., β -lactamases), and complex carbohydrate networks). In general, the resistance of microorganisms can be divided into two types. The first is antibiotic tolerance, i.e., where a cell under the influence of chemical action reduces its growth and metabolism or inactivates the targets of the antibacterial drug. Antibiotic tolerance is not inherited, but is developed under certain external conditions, where part of the population evolve into persistent forms with multiple tolerance. The second type is antibiotic resistance, in which the targets are modified, destroyed, released from the cell, or rendered inaccessible because of the decrease in the cell membrane permeability. This decrease in cell permeability is the nonspecific resistance mechanism that leads to the development of multidrug resistance. This resistance information is transmitted at the genetic level and is an invariable trait in particular species [2]. Furthermore, this resistance problem is aggravated by the enclosure of most pathogenic bacteria in biofilms, which create an additional barrier for antimicrobial agents [3]. The biofilm contains a cellular component—one or several cultures of bacteria—and an extracellular matrix containing polysaccharides, glycopeptides, nucleic acids, and lipids in its structure [4].

¹ The Review on Antimicrobial Resistance, 2014. Available from URL: https://amr-review.org/sites/default/files/AMR%20Review%20Paper%20-%20Tackling%20a%20crisis%20for%20the%20health%20and%20wealth%20of%20nations_1.pdf (accessed March 27, 2021).

In addition to antibiotic resistance, the resistance of pathogenic microflora to disinfectants is attracting significant concern. According to a study [5], several microorganisms exhibit resistance to the ubiquitous chlorhexidine, as evidenced by the increased value of the minimum inhibitory concentration. Healthcare-associated infections (HAIs) pose a threat to patients in hospitals. The inappropriate use of antibacterial agents by medical institutions has led to the rapid development of multidrug resistance. According to expert forecasts, the mortality rate associated with HAI will increase annually, if effective measures to combat resistance are not developed. There are various/different routes for solving this problem, from reducing the use frequency of antibiotics and replacing them with antiseptics [6–9] to, of course, exploring and implementing new antimicrobial agents that meet modern requirements.

The development of new antibacterial agents is a long and complex process, which is why large companies are wary of investing in this area. The results of screening new compounds against a group of ESKAPE pathogens characterized by significantly high resistance have been reported, and not a single compound was found to be active against gram-negative organisms. Many compounds that exhibit good whole cell activity have been found to be cytotoxic to mammals. In this regard, the development of new and effective antibiotics requires an in-depth study of the mechanisms of cell permeability, point mutations using molecular modeling, and other innovative methods; unfortunately, these require high material costs that may be unjustified [10].

Regarding the above information, it is necessary to review the antiseptics currently in use, considering the advantages and disadvantages of each of the presented classes.

TYPES OF ANTISEPTICS

The current classes of antiseptics can be categorized as follows.

Oxygen-active compounds (hydrogen peroxide, sodium percarbonate, peracetic and performic acids, and others). The biocidal effect is manifested by the released active oxygen. The representatives of this class have several disadvantages, namely toxicity, the ability to cause burns, and high cost².

Chloractive compounds (bleach, chloramines, sodium and lithium hypochlorites, and others). The antimicrobial action is effected by the released

² Policy for the Control of Multi-Resistant gram Negative Bacteria. NHS, The document for the development and management of UHSM-wide policy or procedural documents. Available from URL: <http://mft.nhs.uk> (accessed March 30, 2021).

chlorine. These compounds are economical and effective against many groups of microorganisms; however, they exhibit high toxicity [11, 12].

Aldehydes (glutaraldehyde, succinic aldehyde, formaldehyde, glyoxal, and others). Most representatives of this group are toxic and exert allergenic, carcinogenic, mutagenic effects; further, they cause diseases of the skin, mucous membranes, internal organs [13, 14].

Alcohols (ethanol, 2-propanol, and others). For the manifestation of antiseptic properties, the concentrations of ethanol and isopropanol must be above 70% and 60%, respectively. Alcohols are fire hazardous substances and can have a narcotic effect [15].

Phenol and its derivatives have a film-forming effect, which accounts for their prolonged action. However, the representatives of this group are overly toxic [16].

Iodine compounds. They consist of iodine-carrier complexes, which allow the release of iodine. The main disadvantages of these compounds are their weak sporicidal effect and the ability to cause burns [17].

Alkylamines. Here, the biocides are primary, secondary, and tertiary amines. Although they influence most microorganisms, they do not exert any sporicidal effect. Thus, as a rule, they are used in combined composition [18].

Quaternary ammonium compounds (QACs) are widely used in practice and meet safety requirements. However, they have a narrow spectrum of action, which manifests in the absence of proper action against spores, simple viruses, gram-negative bacteria, and mycobacteria. Additionally, QACs are inactivated by negatively charged surfactants. Therefore, this group can be used in a combined composition with guanidines, amines, and aldehydes. In this combination, they are effective against both non-enveloped and enveloped viruses [19, 20].

Guanidines. An important advantage of guanidine derivatives is their propensity for prolonged action. These compounds have a wide spectrum of activity, including against bacteria from the ESKAPE group [21] and viruses [22], as well as low toxicity to humans and animals [23]. Compared to other compounds, guanidine derivatives are promising and have practically no drawbacks; therefore, their use as alternatives to antibiotics and antiseptics that have lost their relevance due to resistance is recommended.

GUANIDINE DERIVATIVES

Guanidine derivatives are referred to as cationic surfactants. For most guanidines, the main targets are important biogenic compounds and cell biopolymers,

which have a high affinity for nitrogenous bases, such as pyridines and xanthenes. There are two interaction mechanisms for binding with the targets: 1) by metabolite substitution and 2) competitive antagonism with normal metabolites [24]. In general, the action mechanism of guanidine derivatives is initiated by the protonation of guanidine, followed by the formation of a cation (Fig. 1), in which the positive charge is evenly distributed among all nitrogen atoms [25].

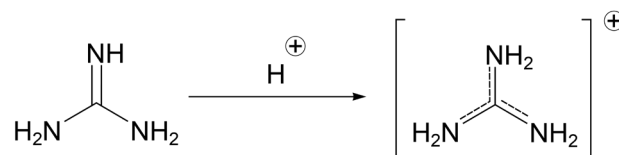


Fig. 1. Guanidinium cation formation.

The subsequent processes are as follows. Upon adsorption on the negatively charged surface of the cell membrane of bacterial cells, guanidine polycations block important vital processes, such as respiration, nutrition, and the transport of metabolites through the bacterial cell wall. Further diffusion of antiseptic macromolecules through the cell wall causes irreversible damage to the cytoplasmic membrane, nucleotide, and cytoplasm. This process depends on many factors, including the magnitude of the surface activity, lipophilicity, water solubility, and the molecular volume of the guanidine derivative molecule. The binding of guanidine derivatives with acid phospholipids, proteins of the cytoplasmic membrane, leads to its rupture. Subsequently, the blockage of the respiratory system, loss of pathogenicity, and collapse of the microbial cell occur [26].

Among the derivatives of guanidine are compounds with polymeric and oligomeric structures, containing fragments of various guanidine derivatives. The advantages of polyguanidines, which are applied in the form of salts of various acids, enable their application as biocidal agents in various fields.

Polyguanidines and their derivatives. The prominent representatives of this class of compounds are polyhexamethylene guanidine hydrochloride (PHMG-HC) and PHMG phosphate (Figs. 2a and 2b). The spectrum of antimicrobial activity of PHMG-HC covers gram-positive and gram-negative bacteria, aerobic and anaerobic bacteria, spore-forming bacteria, mycobacteria, and viruses. Despite its wide spectrum, PHMG-HC is hypoallergenic and has low toxicity [27, 28]; it can also be used in conjunction with other biocidal components, e.g., as a skin antiseptic [29, 30] or in solid dosage form [31]. The antifungal activity of PHMG-HC enables its application for conservation [32] and as an effective sporicidal tool for combating bacterial spores and nosocomial infections [33]. This compound can be applied as a component of composite nanofibers based on chitosan and polyethylene oxide [34].

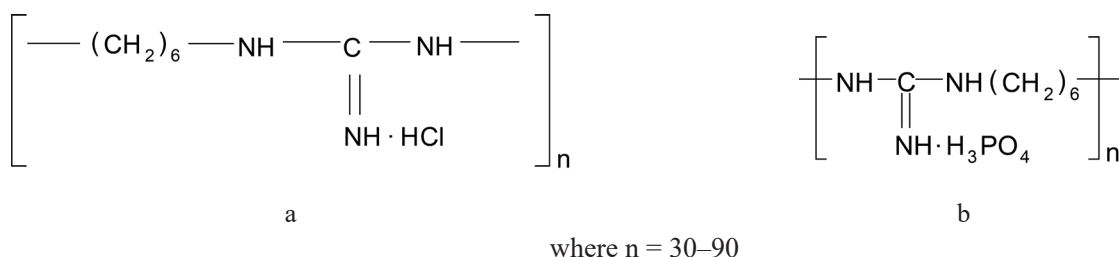


Fig. 2. Structural formulas of polyguanidine derivatives: (a) PHMG-HC and (b) PHMG phosphate.

Phosphate PHMG, similar to PHMG-HC, is synthesized by incorporating an acid anion into the structure of PHMG. In preclinical studies, this salt has exhibited increased antimicrobial activity against gram-positive and gram-negative bacteria, as well as fungi [35]. Fungicides based on PHMG phosphate can be formulated for use in dental practice [36, 37].

In addition to PHMG-HC and PHMG phosphate, other salts of this guanidine derivative can be used in practice. Gluconate and sulfate PHMG are employed for the treatment of infectious diseases of the gastrointestinal tract; hydrosuccinate PHMG, for ophthalmic diseases, particularly conjunctivitis [38]; and stearate and myristate PHMG, for use as biocidal additives [39, 40]. In addition, PHMG can be used in combination with chitosan [41], since this combination has good biocidal activity against gram-positive bacteria.

According to the literature [42, 43], the salts of PHMG can be widely used in medicine and pharmacy. In particular, the oligomeric analogs of PHMG, namely oligoguanidines, are known for their biocidal activity and low toxicity.

Branched oligoguanidines have significantly lower toxicity and pronounced bactericidal and antiviral activities compared with polymer analogs with linear structures [44, 45]. This confirms their application potential as active ingredients in the development of antibacterial drugs. A well-known representative of oligoguanidines is oligohexamethylene guanidine hydrochloride (OHMG-HC), the structural formula of which is shown in Fig. 3.

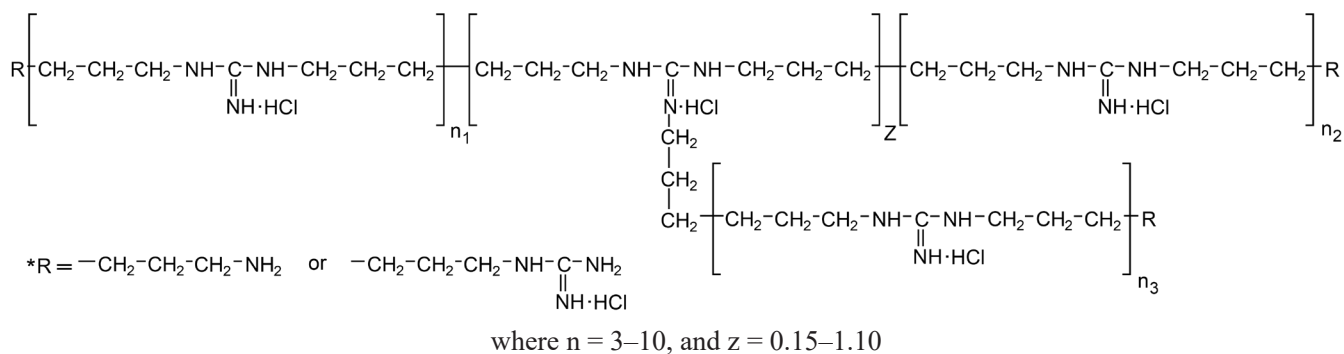


Fig. 3. Structural formula of branched OHMG-HC.

PREPARATION OF POLYGUANIDINES AND THEIR DERIVATIVES

Polyguanidines and their derivatives are obtained mainly in bulk reactors under different conditions, e.g., by the interaction of melts of guanidine hydrochloride (GHC), formed, in turn, from dicyandiamine and ammonium chloride, and hexamethylenediamine (HMDA) at 180°C, followed by heating to 240°C [46]. The disadvantages of this method are the impurities introduced by the initial highly toxic substances and the sublimation of HMDA at high temperatures. Later, a method was proposed for obtaining these compounds at relatively low temperatures by the fusion of GHC and HMDA in the presence of polyethylene glycol (PEG) [47]. However, with this method, it was impossible to achieve the required degree of purity and activity of the product. Preparation methods involving the stepwise heating of a suspension obtained by adding crystalline GHC to molten HMDA, followed by stirring and heating, have been reported. Although these methods allow one to obtain the final product with a sufficient degree of purity, the compound obtained has a wide molecular weight distribution, which negatively affects its antibacterial properties [48]. A preparation method has been reported, in which pre-crushed dicyanamide and ammonium chloride are fused at 200°C in the first stage, after which the melt is transferred to the second reactor, where the HMDA melt is gradually introduced at temperatures of 170–200°C. The disadvantage of this method is the presence of melamine in the product, which is formed by the thermal transformation

of dicyandiamide [49]. A synthesis method using equimolar amounts of HMDA and GHC has also been reported. Using this method, various derivatives with trilinear and cyclic or branched structures can be obtained (Fig. 4).

The main disadvantage of this method is the large number of products, which complicates the isolation of any particular compound.

Branched oligomers are obtained by the interaction of HMDA and GHC in the melt, in molar ratios of 1.0:1.0 to 1.0:1.2, at temperatures of 180–230°C, with a residence time in the range of 3–12 h [45].

In general, the existing methods for the synthesis of polyguanidines and their derivatives in bulk reactors have several disadvantages. In such methods, the heat- and mass-transfer rates are inadequate. This induces temperature and concentration anisotropies, which subsequently affect the molecular weight characteristics of the compound. Furthermore, large-volume reactors require a more sophisticated design to ensure explosion and fire safety, which leads to an increase in the process cost and the cost of the final product. Alternatively, one can consider the production of polyguanidines and their derivatives using microfluidic hardware.

MICROREACTOR TECHNOLOGIES

Historical development of microreactor technology

The first solid publications on the possibilities of using microfluidic technologies appeared in the second half of the 20th century. Among others, it is possible to highlight the manufacture and testing of

a gas chromatograph based on a microcircuit [50] and research carried out in the field of miniature analytical systems, which aroused the greatest interest in this area of technology [51]. The development became possible thanks to advances in the field of microelectronics, which became the prototypes of future microreactors.

A great contribution to the study of microfluidic technologies was made by the staff of the Massachusetts Institute of Technology (USA), as well as by scientists from the Mainz Institute of Microtechnology (Fraunhofer Institute for Microtechnology and Microsystems) (Germany) [52, 53].

Currently, microfluidic technologies are actively developing, the possibility of their implementation in the production of various substances and compounds is under discussion.

Technological principles of microreactor hardware operation

Microfluidics includes devices, systems, and methods for controlling fluid flows with characteristic length scales that are in the range of micrometers, and reaction volumes are in the range from nanoliter to microliter [54]. Microfluidic systems exhibit properties that are fundamentally different from generally known concepts of the behavior of liquids. Fluid flow will be driven by viscous forces and pressure gradients with low moment of inertia and thus inertial effects. The result is a laminar flow without turbulence. One of the parameters is the Reynolds number (Re), which is the ratio of inertial forces to viscous forces. At large Re, inertial forces prevail, and at small Re, viscosity

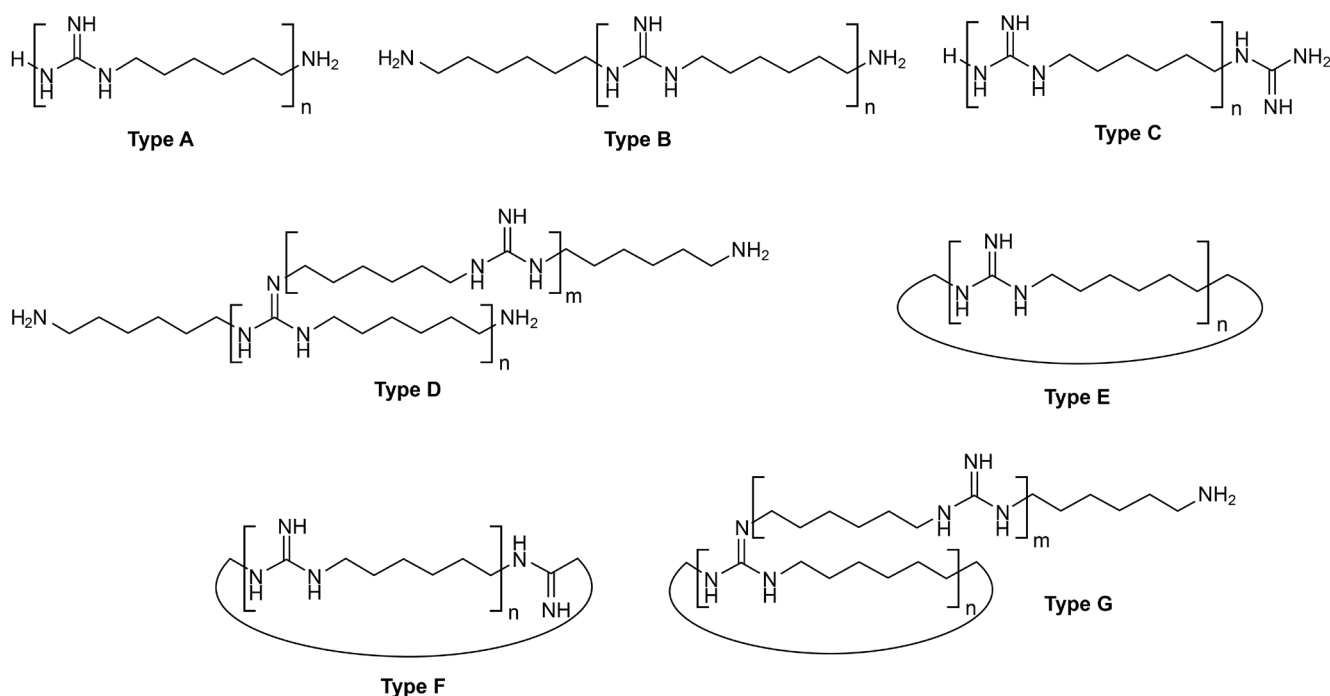


Fig. 4. Polyguanidine derivatives formed during synthesis: A, B, C (linear); D (branching); E, F (cyclic); G (cyclic branching).

forces prevail. Consequently, a decrease in the channel size has the same effect on the behavior of the liquid in terms of Re as an increase in the viscosity of the solution. In most microfluidic systems, the Re value for fluxes is much less than ten, and often less than one. With such a laminar fluid flow, the velocity at the center of the capillary is greater than at its walls due to the parabolic velocity profile [55], which leads to a nonuniform velocity distribution over the fluid flow. This adjusts, for example, the dwell time is distributed, which can reduce the yield and selectivity. However, the undeniable advantage is the absence of gradients of both concentration and temperature relative to volume and time.

It is also worth noting the high surface-to-volume ratio and small diffusion distances, which leads to a reduction in the diffusion time of particles, an increase in conversion, and the overall efficiency of the process [56]. One of the consequences of laminar flow is the fact that the mixing of molecules in a liquid is solely due to molecular diffusion. This can be a significant advantage when mixing in a particular process is undesirable. Diffusion plays an important role in the processes of mass transfer; in microreactor technologies, the diffusion distance is small.

The difference in the physical behavior of microscopic and macroscopic systems makes it possible to create functions that are difficult or even impossible to obtain on a macroscopic scale; therefore, it is necessary to strive for the development of microfluidic systems, proceeding from the design rules, considering the peculiarities of fluid physics, mechanics and diffusion in a confined space [57].

The advantage of using microreactor devices is associated with thermal processes and mass transfer. The large surface area to volume ratio ensures thermal uniformity in the reactor and fast heat transfer between the device and the liquid contained in it, which determines the high energy efficiency of the process [58]. Microreactor technologies make it possible to adjust the process temperature in a shorter time compared to bulk reactors. It should be noted that the use of microreactor technologies has a special economic advantage, since small volumes of expensive reagents are used, since the work is carried out with a minimum amount of substance [59].

Microfluidic reactors have intrinsic properties that enhance the safety of potentially hazardous reactions. Small instantaneous volumes mean that reactions involving toxic or explosive intermediates can be carried out safely [60]. In addition, the high surface area to volume ratio inside the channel allows rapid heat transfer during exothermic reactions [59].

In microreactors, the degree of control over the conditions allows the product to be selectively produced

with high accuracy [61]. This has several advantages: cleaning can be less stringent, more technologically simpler. During the synthesis, the reagents are continuously fed into the microreactor, and at the end of the process they are immediately separated from the initial mixture, which makes it possible to simplify the process itself, less time is required for the reaction to proceed, and more accurate process control can be provided.

As mentioned earlier, heat transfer in microfluidic reactors becomes more efficient as the reaction volumes decrease, that is, the amount of energy consumed to raise the temperature by one degree can be made very small, which is beneficial from an environmental point of view [59].

It is often claimed that microfluidic reactors allow “faster reactions” than bulk reactor reactions. It is noted that the product yield in microfluidic reactors is higher than in similar processes using bulk reactors [62].

An important advantage is that when glass or polymer parts are used, the uncontrolled decomposition of reaction mixtures at the reaction temperature is leveled [63].

Application of microreactor technologies in the chemical industry

Currently, microreactor technologies find their application in fine chemical technology, the synthesis of organic, inorganic and polymer particles, pigments, emulsions, in steam reforming. Since microfluidic reactors can be used in organic chemistry, they must be resistant to the action of various solvents, acids, bases, oxidants and reducing agents. It is important to maintain performance between -78 and 300°C . It should also be possible to carry out the initial purification of the reaction, for example, by extraction [59]. Thus, microreactors are actively used in carrying out a wide variety of reactions in compliance with all the above requirements, for example, in high-temperature processes, reactions with unstable intermediates that are difficult to scale with traditional synthesis methods, and reactions involving hazardous or toxic reagents, which in turn can be converted into a safer product [64]. In [59] it was indicated that microreactors are used in glycosylation reactions, Paal–Knorr synthesis, and for fluorination and perfluorination of organic compounds. The use of microfluidic reactors for multiphase processes [65] gives clear advantages over traditional methods (higher surface area to volume ratio).

Microfluidic technologies are also actively used to carry out various types of polymerization. In all examples of using microreactor technologies for carrying out polymerization reactions, a decrease in the polydispersity coefficient and an increase in yield are noted due to efficient heat transfer and a larger specific surface area. These advantages make it possible to

achieve a homogeneous chemical process and, as a result, to increase the homogeneity of the product. In [65], the product obtained in a microreactor had a lower viscosity compared to the product obtained in an ordinary batch reactor, while their other characteristics are comparable. In [67, 68], the polymers obtained in a microreactor tended to be branching, which was explained by the short diffusion path and the accelerated mass transfer during this. Another example illustrates how microfluidic devices can be used with aqueous solutions and with melts. As a result, a high selectivity of the process was achieved along with a low content of impurities [69].

Industrial research has led to the development of methods aimed at creating reliable microfluidic reactors with production facilities on an industrial scale. One of the important advantages of microfluidic reactors over traditional manufacturing methods is the ease of scaling up. Any microreactor can be used both for laboratory research and for industrial production [70]. The use of microfluidic reactors could also open new synthetic pathways for industry.

Microfluidic hardware in drug development and manufacturing

Microreactors have become more and more important over time in the pharmaceutical formulation industry due to their improved properties over batch reactors. It has been suggested [71] that chemicals, especially drugs, could be produced in miniature factories at points of use rather than in large factories.

Over the past few years, drip microfluidic systems have been widely used in drug discovery research. Microfluidic technologies enable very high throughput analyzes (up to thousands of samples per second). Drug screening, high-throughput analysis is one of the most exciting possibilities of microfluidic technology.

The use of microfluidic systems as a valuable tool for the discovery of new drugs is of great interest. Compared to equivalent bulk reactions, reactions carried out in a microreactor consistently give cleaner products in a much shorter time. Roberge *et al.* [72] believe that up to 50% of reactions in the fine chemical or pharmaceutical industries can benefit from a continuous process based mainly on microreactor technology, and for the majority (44%) a microreactor will be the preferred reaction device. After optimization of the microreactor, it can be easily introduced into industry [73].

Many large pharmaceutical companies, including *Roche* and *Pfizer* (USA), are investing in capillary microfluidic technologies for drug development. *RainDance Technologies* (Billerica, MA, USA) has developed commercial drip microfluidic systems that enable targeted DNA sequencing and digital PCR.

They announced a collaboration with *Roche* for a simple and cost-effective study of drug absorption, distribution, metabolism and excretion [74].

Microreactors are used in the synthesis of various drugs, for example, ibuprofen [75, 76] or an HIV protease inhibitor [77]. Using microfluidic technology, an antitumor drug docetaxel with an increased content of a hydrophobic active substance with optimal physicochemical characteristics is obtained [78].

Directions for the development of microfluidic technologies

The field of microfluidics is evolving and, until recently, was largely technology-driven. The focus was on the development of new functional components (pumps, valves, and new economical production technologies), as well as their functional demonstration. A wide range of components and manufacturing technologies are currently available, and while new technologies are emerging at a rapid pace, the focus in the future is likely to shift toward implementation, i.e., existing technologies will be transformed for new applications. Undoubtedly, microfluidics will play a critical role in the drug discovery process to develop drugs with ever-improving quality [57].

CONCLUSIONS

The fight against the resistance of pathogenic microflora to antibiotics requires special measures. One strategy involves reducing the use frequency of antibiotics and replacing them with antiseptic drugs everywhere. Antiseptics, as a rule, are obtained using volumetric reactors, which have drawbacks that affect the quality of the target compound. Microreactor technologies, considering their many advantages, are considered suitable alternatives. This article describes the advantages of microreactor systems over volumetric reactors and testifies to the expediency of their application in polycondensation and polymerization reactions. Thus, it can be concluded that microreactor technologies are applicable in the synthesis of promising polyguanidines and their derivatives. The proposed method allows for more accurate control of the conditions of the polycondensation reaction of the starting monomers. In addition, microreactor technologies can increase the yield and selectivity of the oligomers obtained, leading to an increase in the product purity and process efficiency, in contrast with other known methods.

Acknowledgments

We acknowledge the support of time and facilities from Ho Chi Minh City University of Technology (HCMUT), VNU-HCM for this study.

The author declares no conflicts of interests.

REFERENCES

1. Tsimmerman Ya.S. The problem of growing resistance of microorganisms to antibiotic therapy and prospects for *Helicobacter pylori* eradication. *Klinicheskaya meditsina = Clinical Medicine (Russ. J.)*. 2013;91(6):14–20 (in Russ.).
2. Cabeen M.T., Jacobs-Wagner C. Bacterial cell shape. *Nat. Rev. Microbiol.* 2005;3(8):601–610. <http://doi.org/10.1038/nrmicro1205>
3. Silhavy T.J., Kahne D., Walker S. The bacterial cell envelope. *Cold Spring Harb. Perspect. Biol.* 2010;2:a000414. <http://doi.org/10.1101/cshperspect.a000414>
4. Russell A.D. Bacterial Spores and Chemical Sporicidal Agents. *Clin. Microbiol. Rev. Apr.* 1990;3(2):99–119. <https://doi.org/10.1128/CMR.3.2.99>
5. Bowler P.G. Antibiotic resistance and biofilm tolerance: a combined threat in the treatment of chronic infections. *J. Wound Care.* 2018;27(5):273–277. <https://doi.org/10.12968/jowc.2018.27.5.273>
6. Stewart P.S., Franklin M.J. Physiological heterogeneity in biofilms. *Nat. Rev. Microbiol.* 2008;6(3):199–210. <https://doi.org/10.1038/nrmicro1838>
7. Kvashnina D.V., Kovalishena O.V. Prevalence of microbial resistance to chlorhexidine: a systematic review and analysis of regional monitoring. *Fundamental'naya i klinicheskaya meditsina = Fundamental and Clinical Medicine.* 2018;3(1):63–71 (in Russ.).
8. Akimkin V.G., Tutel'Yan A.V. Current directions of scientific researches in the field of infections, associated with the medical care, at the present stage. *Zdorov'e naseleniya i sreda obitaniya – ZNiSO = Public Health and Life Environment – PH&LE.* 2018;(4):46–50 (in Russ.).
9. Kultanova E.B., Turmukhambetova A.A., Kalieva D.K., Mukhamedzhan G.B. Nosocomial infections: a public health problem (literature review). *Vestnik Kazakhskogo Natsional'nogo meditsinskogo universiteta (Vestnik KazNMU).* 2018;(1):46–49 (in Russ.).
10. Exner M., et al. Antibiotic resistance: What is so special about multidrug-resistant Gram-negative bacteria? *GMS Hyg. Infect. Control.* 2017;12:Doc.05. <http://doi.org/10.3205/dgkh000290>
11. Privol'nev V.V., Zubareva N.A., Karakulina E.V. Topical therapy of wound infections: antiseptics or antibiotics? *Klinicheskaya mikrobiologiya i antimikrobnaya khimioterapiya = Clinical Microbiology and Antimicrobial Chemotherapy.* 2017;19(2):134–137 (in Russ.).
12. Tommasi R., Brown D.G., Walkup G.K., Manchester J.I., Miller A.A. ESKAPEing the labyrinth of antibacterial discovery. *Nat. Rev. Drug Discov.* 2015;14(8):529–542. <https://doi.org/10.1038/nrd4572>
13. Trombetta D., Saija A., Bisignano G., Arena S., Caruso S., Mazzanti G., Uccella N., Castelli F. Study on the Mechanisms of the Antibacterial Action of Some Plant α - β -unsaturated Aldehydes. *Letters in Applied Microbiology.* 2002;35:285–290.
14. Bakhir V.M., Vtorenko V.I., Leonov B.I., et al. Efficiency and safety of chemical solutions for disinfection, presterilization cleaning and sterilization. *Dezinfektsionnoe delo = Disinfection Affairs.* 2003;(1):29–36 (in Russ.).
15. Larson E.L., Morton H.E. Alcohols. In: Block S.S. (Ed.). *Disinfection, Sterilization, and Preservation.* 4th Ed. Philadelphia, PA: Lea and Febiger; 1991, pp. 191–203.
16. Aronson J.K. (Ed.). Phenols. In: *Meyler's Side Effects of Drugs.* 16th Ed. Elsevier; 2016, pp. 688–692. ISBN 9780444537164. <https://doi.org/10.1016/B978-0-444-53717-1.01259-2>
17. Lobanov S.M. Evaluation of effectiveness of chlorine-containing disinfectant in case of disinfection of poultry farm objects. *Problemy veterinarnoi sanitarii, gigieny i ekologii = Problems of Veterinary Sanitation, Hygiene and Ecology.* 2011;2(6):49–51 (in Russ.).
18. Jumbelic M.I., Hanzlick R., Cohle S. Alkylamine antihistamine toxicity and review of Pediatric Toxicology Registry of the National Association of Medical Examiners. Report 4: Alkylamines. *Am J Forensic Med Pathol.* 1997 Mar;18(1):65–9. <https://doi.org/10.1097/0000433-199703000-00012>
19. Popov N.I., Volkovskii G.D., Michko S.A., Griganova N.V. Bionol test results. *Veterinariya = Veterinary.* 2005;(2):12–14 (in Russ.).
20. Khudyakov, A.A. Effective disinfection and selection of a disinfectant. *Veterinariya = Veterinary.* 2010;(2):18–22 (in Russ.).
21. Shestopalov N.V., Panteleeva L.G., Sokolova N.F., Abramova I.M., Lukichev S.P. *Federal'nye klinicheskie rekomendatsii po vyboru khimicheskikh sredstv dezinfektsii i sterilizatsii dlya ispol'zovaniya v meditsinskikh organizatsiyakh (Federal clinical guidelines for the selection of disinfection and sterilization chemicals for use in medical organizations).* Moscow: 2015. 67 p. (in Russ.). https://www.dezsnab-trade.ru/media/content/information/rekomendaciy_po_vyboru_dezsredstv.pdf
22. Gotovskii D.G., Fomchenko I.V. Evaluation of the toxicity and biocidal properties of the disinfectant “Estadez with 3–2–1.” *Uchenye zapiski UO VGAVM.* 2012;48(1):18–22 (in Russ.).
23. Morozova N.S., Korzhenevskii S.V., Telenev A.V. The disinfection of microorganisms in the problem of nosocomial infections. *Vestnik assotsiatsii.* 2001;(3):15–17 (in Russ.).
24. Zhou Z., Wei D., Lu Y. Polyhexamethylene guanidine hydrochloride shows bactericidal advantages over chlorhexidine digluconate against ESKAPE bacteria. *Biotechnol. Appl. Biochem.* 2015;62(2):268–274. <https://doi.org/10.1002/bab.1255>
25. Lysytsya A., Mandygra M. The Antiviral Action of Polyhexamethylene Guanidine Derivatives. *J. Life Sci.* 2014;8(1):22–26.
26. Shandala M.G., Fedorova L.S., Pankratova G.P., Efimov K.M., Dityuk A.I., Snezhko A.G., Bogdanov A.I. Hygienic substantiation of the development and use of polyguanidines as antimicrobial prophylactic agents means of the innovative class. *Gigiena i sanitariya = Hygiene and Sanitation.* 2015;94(8):77–81 (in Russ.).
27. Belushkina N.N., Ivanov A.A., Krjukov L.N., Krjukova L.Ju., Moskaleva E.Ju., Pal'tsev M.A., Posypanova G.A., Severin E.S., Severin S.E., Torgun I.N., Fel'dman N.B., Khomjakov Ju.N. 2,2,6,6-tetrakis-(trifluoromethyl)-4-ethylamino-5,6-dihydro-1,3,5-oxadiazine (synthazin), method of its synthesis and pharmaceutical composition based on thereof: Pat. 2203892 RF. Publ. 10.05.2003. (in Russ.).
28. Ivanov I.S., Shatalov D.O., Kedik S.A., Sedishev I.P., Beliakov S.V., Trachuk K.N., Komarova V.V. An effective method for preparation of high purity oligohexamethylene guanidine salts. *Fine Chemical Technologies.* 2020;15(3):31–38. <https://doi.org/10.32362/2410-6593-2020-15-3-31-38>
29. Vointseva I.I. *Poliguanidiny – dezinfektsionnye sredstva i polifunktsional'nye dobavki v kompozitsionnye materialy (Polyguanidines are disinfectants and multifunctional additives in composite materials).* Moscow: LKMpress; 2009. 303 p. (in Russ.). ISBN 978-5-9901286-2-0
30. Gembitskii P.A., Vointseva I.I. *Polimernyi biotsidnyi preparat poligeksametilenguanidin (Polymer biocidal preparation polyhexamethylene guanidine).* Zaporozh'e: Poligraf; 1998. 42 p. (in Russ.).

31. Arzamastsev A.P., Popkov V.A., Krasnyuk I.I., Matyushina G.P., Zadereiko L.V., Abrikosova Yu.A. *Foaming composition for antiseptic treatment of the skin*: Pat. 2003102506 RF. Publ. 10.08.2004. (in Russ.).
32. Moksunov V.V., Shestopalov N.V. *Skin disinfection treatment agent*: Pat. 2521323 RF. Publ. 27.06.2014. (in Russ.).
33. Kukharenko O., Bardeau J.F., Zaets I., Ovcharenko L., et al. Promising low cost antimicrobial composite material based on bacterial cellulose and polyhexamethylene guanidine hydrochloride. *Eur. Polym. J.* 2014;60:247–254. <https://doi.org/10.1016/j.eurpolymj.2014.09.014>
34. Wangkui W., Yin W. *Pharmaceutical formula and preparation method of polyhexamethylene guanidine hydrochloride (PHMG)*: Pat. CN103705536A China. Publ. 09.04.2014.
35. Koffi-Nevry R., et al. Assessment of the antifungal activities of polyhexamethylene-guanidine hydrochloride (PHMGH)-based disinfectant against fungi isolated from papaya (*Carica papaya* L.) fruit. *African J. Microbiol. Res.* 2011;5(24):4162–4169.
36. Oulé M.K., Quinn K., Dickman M., Bernier A.M., Rondeau S., Moissac D.D., Boisvert A., Diop L. Akwatan, polyhexamethylene-guanidine hydrochloride-based sporicidal disinfectant: a novel tool to fight bacterial spores and nosocomial infections. *J. Med. Microbiol.* 2012;61(10):1421–1427. <https://doi.org/10.1099/jmm.0.047514-0>
37. Dilamian M., Montazer M., Masoumi J. Antimicrobial electrospun membranes of chitosan/poly(ethylene oxide) incorporating poly(hexamethylene biguanide) hydrochloride. *Carbohydrate Polymers.* 2013;94(1):364–371. <https://doi.org/10.1016/j.carbpol.2013.01.059>
38. Vitt A., Sofrata A., Slizen V., et al. Antimicrobial activity of polyhexamethylene guanidine phosphate in comparison to chlorhexidine using the quantitative suspension method. *Ann. Clin. Microbiol. Antimicrob.* 2015;14:36. <https://doi.org/10.1186/s12941-015-0097-x>
39. Vitt A., Gustafsson A., Ramberg P., Slizen V., Kazeko L. A., Buhlin K. Polyhexamethylene guanidine phosphate irrigation as adjunctive to scaling and root planing in the treatment of chronic periodontitis. *Acta Odontol. Scand.* 2019;77(4):290–295. <https://doi.org/10.1080/00016357.2018.1541099>
40. Sklyanova Yu.A., Ushakov R.V., Kazimirskii V.A., et al. Experimental grounding of phogutsid (anavidin) application in stomatology. *Byulleten' Vostochno-Sibirskogo nauchnogo tsentra SO RAMN = Bul. VSNTS SB RAMS.* 2006;4(50):344–346 (in Russ.).
41. Kha K.A., Grammatikova N.E., Vasilenko I.A., Kedik S.A. Comparative in vitro Antibacterial Activity of Polyhexamethylene Guanidine Hydrochloride and Polyhexamethylene Guanidine Succinate. *Antibiotiki i khimioterapiya = Antibiotics and Chemotherapy.* 2013;58(1–2):3–7 (in Russ.).
42. Guogang V. *Polyhexamethylene guanidine medicine for treating stomach disease and preparation method and application thereof*: Pat. CN105726491A China. Publ. 06.07.2016.
43. Khallyeva O.K., Dobysh V.A., Koktysh N.V., Belyasova N.A., Tarasevich V.A. Borne polyhexamethyleneguanidine salts. *Uspekhi v khimii i khimicheskoi tekhnologii = Advances in Chemistry and Chemical Technology.* 2016;30(1):11–13 (in Russ.).
44. Dobysh V.A., Koktysh N.V., Belyasova N.A., Kornei V.V. Study of structure and properties of the triple polymer-metal complex chitosan—Cu(II)—polyhexamethyleneguanidine. *Izvestiya vuzov. Prikladnaya khimiya i biotekhnologiya = Proceedings of Universities. Applied Chemistry and Biotechnology.* 2017;7(1):31–38 (in Russ.).
45. Ivanov I.S., Shatalov D.O., Kedik S.A., Sedishev I.P., Grammatikova N.E., Aidakova A.V., Trachuk K.N., Zazykova E.I. Study of the effect of the pharmaceutical substance branched oligohexamethylene guanidine hydrochloride in relation to microorganisms. *Antibiotiki i khimioterapiya = Antibiotics and Chemotherapy.* 2019;64(11–12):8–15 (in Russ.).
46. Kedik S.A., Sedishev I.P., Panov A.V., Zhavoronok E.S., Kha K.A. *Guanidine derivative based branched oligomers and disinfectant containing said oligomers*: Pat. RF 2443684C1. Publ. 27.02.2012. (in Russ.).
47. Safronov G.A., Gembitskii P.A., Kuznetsov O.Yu., Klyuev V.G., Kalinina T.A., Rodionov A.V. *Method of producing disinfecting agent*: Pat. SU-1616898 USSR. Publ. 30.12.1990.
48. Schmidt O. *Method for producing polyhexamethylene guanidine*: Pat. WO1999054291A1. Publ. 28.10.1991.
49. Popovkin V.V., Glukhov I.S., Antonov M.I. *Method of producing polyhexamethylene guanidine hydrochloride*: Pat. RF 2489452C1. Publ. 10.08.2013. (in Russ.).
50. Wei D., Ma Q., Guan Y., Hu F., Zheng A., Zhang X., Teng Z., Jiang H. Structural characterization and antibacterial activity of oligoguanidine (polyhexamethylene guanidine hydrochloride). *Mat. Sci. Eng.: C.* 2009;29(6):1776–1780. <https://doi.org/10.1016/j.msec.2009.02.005>
51. Terry S.C. A gas chromatography system fabricated on a silicon wafer using integrated circuit technology. PhD. Dissertation: Stanford University. ProQuest Dissertations Publishing; 1975.
52. Manz A., Graber N., Widmer H.M. Miniaturized total chemical analysis systems: A novel concept for chemical sensing. *Sensors and Actuators B.* 1990;1(1–6):244–248. [https://doi.org/10.1016/0925-4005\(90\)80209-1](https://doi.org/10.1016/0925-4005(90)80209-1)
53. Srinivasan R., et al. Chemical performance and high temperature characterization of micromachined chemical reactors. In: *Proceedings of International Solid State Sensors and Actuators Conference (Transducers 1997)*. 1997;1:163–166. <https://doi.org/10.1109/SENSOR.1997.613608>
54. Ehrfeld W., Golbig K., Hessel V., Löw, H. & Richter T. Characterization of mixing in micromixers by a test reaction: Single mixing units and mixer arrays. *Ind. Eng. Chem. Res.* 1999;38(3):1075–1082. <https://doi.org/10.1021/ie980128d>
55. Stone H.A., Stroock A.D., Ajdari A. Engineering flows in small devices. Microfluidics toward a lab-on-a chip. *Annu. Rev. Fluid Mech.* 2004;36(1):381–411. <https://doi.org/10.1146/annurev.fluid.36.050802.122124>
56. Reis M.H., Leibfarth F.A., Pitet LM. Polymerizations in Continuous Flow: Recent Advances in the Synthesis of Diverse Polymeric Materials. *ACS Macro Lett.* 2020;9(1):123–133. <https://doi.org/10.1021/acsmacrolett.9b00933>
57. Ivanov I.S., Kedik S.A., Shatalov D.O., et al. The Prospects of Application of Microfluidics for Synthesis of Compounds from the Alkylene Guanidine Series. *Polym. Sci. Ser. D.* 2021;14(2):305–311. <https://doi.org/10.1134/S1995421221020088>
58. Pihl J., Karlsson M., Chiu D.T. Microfluidic technologies in drug discovery. *Drug Discov. Today.* 2005;10(20):1377–1383. [https://doi.org/10.1016/S1359-6446\(05\)03571-3](https://doi.org/10.1016/S1359-6446(05)03571-3)
59. Schwalbe T., Autze V., Wille G. Chemical synthesis in microreactors. *CHIMIA. Int. J. Chem.* 2002;56(11):636–646. <https://doi.org/10.2533/000942902777679984>
60. Elvira K.S., Casadevall i Solvas X., Wootton R.C.R., DeMello A.J. The past, present and potential for microfluidic reactor technology in chemical synthesis. *Nature chemistry.* 2013;5:905–915. <https://doi.org/10.1038/NCHEM.1753>

61. Lee C-C., *et al.* Multistep synthesis of a radiolabeled imaging probe using integrated microfluidics. *Science*. 2005;310(5755):1793–1796. <https://doi.org/10.1126/science.1118919>
62. Asai T., *et al.* Switching reaction pathways of benzo[b]thiophen-3-yl lithium and benzo[b]furan-3-yl lithium based on high-resolution residence-time and temperature control in a flow microreactor. *Chem. Lett.* 2011;40(4):393–395. <https://doi.org/10.1246/cl.2011.393>
63. Illg T., Hessel V., Lob P., Schouten J.C. Continuous synthesis of tert-butyl peroxyvalerate using a single-channel microreactor equipped with orifices as emulsification units. *ChemSusChem*. 2011;4(3):392–398. <https://doi.org/10.1002/cssc.201000368>
64. Vörös A., Baán Z., Mizsey P., Finta Z. Formation of Aromatic Amidoximes with Hydroxylamine using Microreactor Technology. *Org. Proc. Res. Dev.* 2012;16(11):1717–1726. <https://doi.org/10.1021/op300113w>
65. Zhang X., Stefanick S., Villani F.J. Application of Microreactor Technology in Process Development. *Org. Proc. Res. Dev.* 2004;8(3):455–460. <https://doi.org/10.1021/op034193x>
66. Marre S., Roïg Y., Aymonier C. Supercritical microfluidics: Opportunities in flow-through chemistry and materials science. *J. Supercrit. Fluids*. 2012;66:251–264. <https://doi.org/10.1016/j.supflu.2011.11.029>
67. Narkevich I.A., Tarasov I.N., Golant Z.M., Alekhin A.V. Modern technologies for the synthesis of pharmaceutical substances: way to high-efficiency drug production. *Pharm. Chem. J.* 2016;49(11):760–764. <https://doi.org/10.1007/s11094-016-1366-5>
[Original Russian Text: Narkevich I.A., Tarasov I.N., Golant Z.M., Alekhin A.V. Modern technologies for the synthesis of pharmaceutical substances: way to high-efficiency drug production. *Khimiko-Farmatsevticheskii Zhurnal* 2015;49(11):36–40. <https://doi.org/10.30906/0023-1134-2015-49-11-36-40>]
68. Bally F., Serra C. A., Brochon C., Hadziioannou G. Synthesis of Branched Polymers under Continuous-Flow Microprocess: An Improvement of the Control of Macromolecular Architectures. *Macromol. Rapid Commun.* 2011;32(22):1820–1825. <https://doi.org/10.1002/marc.201100429>
69. Visaveliya N., Köhler J.M. Role of Self-Polarization in a Single-Step Controlled Synthesis of Linear and Branched Polymer Nanoparticles. *Macromol. Chem. Phys.* 2015;216(11):1212–1219. <https://doi.org/10.1002/macp.201500091>
70. Kuesters C.F., Stengel B.F., Benzinger W., Brandner J.J. *Microprocessing for preparing a polycondensate*: Pat. US9187574B2 Publ. 17.11.2015.
71. Kockmann N., Gottsponer M., Zimmermann B., Roberge D.M. Enabling continuous-flow chemistry in microstructured devices for pharmaceutical and fine-chemical production. *Chem. Eur. J.* 2008;14(25):7470–7477. <https://doi.org/10.1002/chem.200800707>
72. Fletcher P., Haswell S. Downsizing synthesis. *Chem. Brit.* 1999;35(11):38–41.
73. Roberge D.M., Durcy L., Bieler N., Cretton P., Zimmermann B. Microreactor technology: A revolution for the fine chemical and pharmaceutical industries? *Chem. Eng. Technol.* 2005;28(3):318–322. <https://doi.org/10.1002/ceat.200407128>
74. Šalić A., Tušek A., Zelić, B. Application of microreactors in medicine and biomedicine. *J. Appl. Biomed.* 2012;10(3):137–153. <https://doi.org/10.2478/v10136-012-0011-1>
75. Wang Y., Chen Z., Bian F., Shang L., Zhu K., Zhao Y. Advances of droplet-based microfluidics in drug discovery. *Expert Opin. Drug Discov.* 2020;15(8):969–979. <https://doi.org/10.1080/17460441.2020.1758663>
76. Bogdan A.R., Poe S.L., Kubis D.C., Broadwater S.J., McQuade D.T. The Continuous-Flow Synthesis of Ibuprofen. *Angew. Chem.* 2009;121(45):8699–8702. <https://doi.org/10.1002/ange.200903055>
77. Snead D.R., Jamison T.F. A three-minute synthesis and purification of ibuprofen: pushing the limits of continuous-flow processing. *Angew. Chem.* 2014;54(3):983–987. <https://doi.org/10.1002/anie.201409093>
78. Pinho V.D., Gutmann B., Miranda L.S.M., de Souza R.O.M.A., Kappe C.O. Continuous Flow Synthesis of α -Halo Ketones: Essential Building Blocks of Antiretroviral Agents. *J. Org. Chem.* 2014;79(4):1555–1562. <https://doi.org/10.1021/jo402849z>
79. Poltavets Yu.I. *Method for obtaining polymeric antitumor particles in flow microreactor and lyophilisate based on them*: Pat. RF 2681933C1. Publ. 03.14.2019. (in Russ.).

About the author:

Anh C. Ha, PhD, Dr. Sci. in Chemical Engineering, Faculty of Chemical Engineering, Ho Chi Minh City University of Technology (268 Ly Thuong Kiet Street, District 10, Ho Chi Minh City, Vietnam); Vietnam National University Ho Chi Minh City (Linh Trung Ward, Thu Duc District, Ho Chi Minh City, Vietnam). E-mail: hcanh@hcmut.edu.vn. Scopus Author ID 56485522100, <https://orcid.org/0000-0001-7919-4028>

Об авторе:

Ань К. Ха, PhD, к.х.н., Химико-технологический факультет, Технологический университет Хошимина (268 Ли Тхьонг Кьет ул., Район 10, г. Хошимин, Вьетнам); Вьетнамский национальный университет Хошимина (Линь Чунг Уорд, Район Тхэк, г. Хошимин, Вьетнам). E-mail: hcanh@hcmut.edu.vn. Scopus Author ID 56485522100, <https://orcid.org/0000-0001-7919-4028>

The article was submitted: October 18, 2021; approved after reviewing: December 03, 2021; accepted for publication: December 13, 2021.

The text was submitted by the author in English.

Edited for English language and spelling by Enago, an editing brand of Crimson Interactive Inc.

BIOCHEMISTRY AND BIOTECHNOLOGY

БИОХИМИЯ И БИОТЕХНОЛОГИЯ

ISSN 2686-7575 (Online)

<https://doi.org/10.32362/2410-6593-2021-16-6-476-489>



UDC 615.275.2

RESEARCH ARTICLE

Knockdown of *FLT4*, *Nup98*, and *Nup205* cellular genes as a suppressor for the viral activity of Influenza A/WSN/33 (H1N1) in A549 cell culture

Evgeny A. Pashkov^{1,2}, Evgeny B. Faizuloev², Ekaterina R. Korchevaya², Artem A. Rtishchev², Bogdan S. Cherepovich², Alexander V. Sidorov², Alexander V. Poddubikov², Elizaveta P. Bystritskaya², Yuliya E. Dronina^{1,3}, Anatoly S. Bykov², Oxana A. Svitich^{1,2}, Vitaliy V. Zverev^{1,2}

¹I.M. Sechenov First Moscow State Medical University (Sechenov University), Moscow, 119991 Russia

²I. Mechnikov Research Institute of Vaccines and Sera, Moscow, 105064 Russia

³N.F. Gamaleya National Research Center for Epidemiology and Microbiology, Moscow, 123098 Russia

@Corresponding author, e-mail: pashkov.j@yandex.ru

Abstract

Objectives. To evaluate the effect of cellular genes *FLT4*, *Nup98*, and *Nup205* on the reproduction of the influenza A virus in A549 human lung cancer cell line.

Methods. The work was carried out using the equipment of the center for collective use of the I.I. Mechnikov Research Institute of Vaccines and Sera (Russia). The virus-containing fluid was collected within three days from the moment of transfection and infection and the intensity of viral reproduction was assessed by viral titration and hemagglutination reaction. The viral RNA concentration was determined by real-time reverse-transcription polymerase chain reaction (RT-PCR). To calculate statistically significant differences between groups, the nonparametric Mann–Whitney test was used.

Results. In cells treated with small interfering RNAs (siRNAs) targeted at *FLT4*, *Nup98*, and *Nup205* genes, a significant decrease in their expression and indicators of viral reproduction (virus titer, hemagglutinating activity, viral RNA concentration) was observed at a multiplicity of infection (MOI) = 0.1. Additionally, it was found that a decrease in the expression of target genes using siRNA does not lead to a significant decrease in cell survival. The viral titer in cells treated with siRNA *FLT4.2*, *Nup98.1*, and *Nup205* on the first day was lower by an average of 1.0 lg, and on the second and third days, by 2.2–2.3 lg, compared to cells treated with nonspecific siRNA. During real-time RT-PCR, a significant decrease in the concentration of viral RNA was observed

with siRNA Nup98.1 (up to 190 times) and Nup205 (up to 30 times) on the first day, 26 and 29 times on the second day, and 6 and 30 times on the third day, respectively. For FLT4.2 siRNA, the number of viral RNA copies decreased by 23, 18, and 16 times on the first, second, and third days. Similar results were obtained when determining the hemagglutinating activity of the virus. The hemagglutinating activity on the third day most strongly decreased in cells treated with siRNA Nup205 and FLT4.2 (16 times). In cells treated with siRNA FLT4.1, Nup98.1, and Nup98.2, hemagglutinating activity decreased by 8 times.

Conclusions. In the present study, three cellular genes (FLT4, Nup98, and Nup205) were identified—the decrease in the expression of which effectively suppresses viral reproduction—and the original siRNA sequences were obtained. The results obtained are important for creating therapeutic and prophylactic medication, whose action is based on the RNA interference mechanism.

Keywords: influenza A virus, RNA interference, gene, messenger RNA, small interfering RNAs

For citation: Pashkov E.A., Faizuloev E.B., Korchevaya E.R., Rtishchev A.A., Cherepovich B.S., Sidorov A.V., Poddubikov A.V., Bystritskaya E.P., Dronina Yu.E., Bykov A.S., Svitich O.A., Zverev V.V. Knockdown of FLT4, Nup98, and Nup205 cellular genes as a suppressor for the viral activity of Influenza A/WSN/33 (H1N1) in A549 cell culture. *Tonk. Khim. Tekhnol. = Fine Chem. Technol.* 2021;16(6):476–489 (Russ., Eng.). <https://doi.org/10.32362/2410-6593-2021-16-6-476-489>

НАУЧНАЯ СТАТЬЯ

Нокдаун клеточных генов *FLT4*, *Nup98* и *Nup205* как супрессор вирусной активности гриппа A/WSN/33 (H1N1) в культуре клеток A549

Е.А. Пашков^{1,2,@}, Е.Б. Файзулоев², Е.Р. Корчевая², А.А. Ртищев²,
Б.С. Черепович², А.В. Сидоров², А.В. Поддубиков², Е.П. Быстрицкая²,
Ю.Е. Дронина^{1,3}, А.С. Быков¹, О.А. Свитич^{1,2}, В.В. Зверев^{1,2}

¹Первый Московский государственный медицинский университет им. И.М. Сеченова Минздрава России (Сеченовский Университет), Москва, 119991 Россия

²Научно-исследовательский институт вакцин и сывороток им. И.И. Мечникова Минздрава России, Москва, 105064 Россия

³Национальный исследовательский центр эпидемиологии и микробиологии им. почетного академика Н.Ф. Гамалеи Минздрава России, Москва, 123098 Россия

@ Автор для переписки, e-mail: pashkov.j@yandex.ru

Аннотация

Цели. Оценка влияния подавления экспрессии клеточных генов *FLT4*, *Nup98* и *Nup205* на динамику репродукции вируса гриппа А в культуре легочных клеток человека А549.

Методы. Работа выполнена с использованием оборудования центра коллективного пользования Научно-исследовательского института вакцин и сывороток им. И.И. Мечникова (Россия). Вирусосодержащую жидкость отбирали в течение трех дней с момента трансфекции и заражения и оценивали интенсивность вирусной репродукции методами титрования по цитопатическому действию и в реакции гемагглютинации. Концентрацию вирусной РНК определяли методом полимеразной цепной реакции (ПЦР) в реальном времени с обратной транскрипцией (ОТ-ПЦР-РВ). Для вычисления статистически значимых различий между группами использовали непараметрический критерий Манна–Уитни.

Результаты. В клетках, обработанных малыми интерферирующими РНК (миРНК) к генам *FLT4*, *Nip98* и *Nip205*, отмечалось достоверное подавление экспрессии целевых генов и показателей вирусной репродукции (титр вируса, гемагглютинирующая активность, концентрация вирусной РНК) при коэффициенте множественности заражения, равном 0.1. Дополнительно было установлено, что подавление экспрессии целевых генов с помощью миРНК не приводит к значительному снижению выживаемости клеток. Вирусный титр в клетках, обработанных миРНК *FLT4.2*, *Nip98.1* и *Nip205*, на первые сутки был меньше в среднем на 1.0 lg, а на вторые и третьи – на 2.2–2.3 lg, по сравнению с клетками, обработанными неспецифической миРНК. При проведении ОТ-ПЦР-РВ отмечено достоверное уменьшение концентрации вирусной РНК с миРНК *Nip98.1* (до 190 раз) и *Nip205* (до 30 раз) на первые сутки, в 26 и в 29 раз на вторые и в 6 и 30 раз на третьи сутки, соответственно. Для миРНК *FLT4.2* количество копий вирусной РНК уменьшилось в 23, 18 и 16 раз на первые, вторые и третьи сутки. Схожие результаты были получены при определении гемагглютинирующей активности вируса. Наиболее сильно, в 16 раз, гемагглютинирующая активность на третьи сутки снизилась в клетках, обработанных миРНК *Nip205* и *FLT4.2*. В клетках, обработанных миРНК *FLT4.1*, *Nip98.1* и *Nip98.2*, гемагглютинирующая активность уменьшилась в 8 раз.

Выводы. В ходе исследования были выявлены три клеточных гена (*FLT4*, *Nip98* и *Nip205*), подавление экспрессии которых позволяет эффективно уменьшить вирусную репродукцию, а также получены оригинальные последовательности миРНК. Полученные результаты имеют важное значение для создания терапевтических и профилактических препаратов, чье действие основано на механизме РНК-интерференции.

Ключевые слова: вирус гриппа А, РНК-интерференция, ген, матричная РНК, малые интерферирующие РНК

Для цитирования: Пашков Е.А., Файзулов Е.Б., Корчевая Е.Р., Ртищев А.А., Черепович Б.С., Сидоров А.В., Поддубиков А.В., Быстрицкая Е.П., Дронина Ю.Е., Быков А.С., Свитич О.А., Зверев В.В. Нокдаун клеточных генов *FLT4*, *Nip98* и *Nip205* как супрессор вирусной активности гриппа А/WSN/33 (H1N1) в культуре клеток А549. Тонкие химические технологии. 2021;16(6):476–489. <https://doi.org/10.32362/2410-6593-2021-16-6-476-489>

INTRODUCTION

Influenza infection is one of the most significant problems in global health today. According to the World Health Organization, up to 1 billion new cases of influenza are reported worldwide each year, with 3–5 million cases of severe illness and 0.5 million deaths [1]. Influenza viruses of the genus *Alphainfluenzavirus* (*Influenza A virus*, (HAV))—with high epidemiological significance and capable of causing pandemics—are of particular clinical significance [2]. In addition to causing respiratory system failure, influenza can cause complications in the cardiovascular system, central nervous system, and urinary system [3–7]. The risk of developing bacterial and fungal complications post influenza is no exception [8–10].

Despite the currently available specific anti-influenza drugs, their use is often unjustified since new viral strains resistant to these drugs are detected every year [11, 12]. The problem with the use of influenza vaccines is acute, as it is necessary to create

vaccines adapted to new strains of the influenza virus every year, and the development of a universal vaccine is far from complete [13–15]. In addition, influenza vaccination as prophylaxis is challenging for people who are allergic to chicken eggs [16].

To date, several etiotropic, symptomatic, and specific drugs are used to treat influenza. Currently, many influenza virus strains have 95% resistance to derivatives of the adamantane series [17]. Certain circulating strains are also known to be resistant to fusion inhibitors (*umifenovir*) [18]. In different epidemic seasons, the sensitivity of influenza A and B virus strains varied dramatically in relation to neuraminidase inhibitors. In 2008–2009, all circulating influenza A (H1N1) viruses were resistant to oseltamivir, but in 2018 they were fully susceptible to oseltamivir, peramivir, and zanamivir [19–21]. Thus, despite the widespread knowledge of biological function, structural organization, and pathogenesis of the influenza virus, no effective means of therapy and prevention exist as of yet [11, 12].

RNA interference (RNAi) is a sequential regulatory reaction in eukaryotic cells caused by an exogenous double-stranded RNA molecule [22]. A. Fire and C. Mell discovered RNAi in 1998 in the nematode *Caenorhabditis elegans*. They put forward several provisions on the properties of RNAi: mRNA degrades with it; the efficiency of double-stranded RNA (dsRNA) fragment, which determines the recognition of the complementary region of the target messenger RNA (mRNA), is higher than that of single-stranded RNA (ssRNA); a short dsRNA fragment is required to suppress gene expression [23].

The mechanism of RNAi is to cleave exogenous double-stranded RNA into small sequences ranging in size from 21 to 25 base pairs; small interfering RNAs (siRNAs). The size of the resulting siRNAs is small based on the fact that larger siRNAs increase the chance of interferon production. After the formation of siRNA, it binds to the RISC (RNA-induced silencing complex) complex, which consists of three proteins: *AGO2*, *PACT*, and *TRBP*. The resulting complex recognizes and cleaves the target mRNA [24–26].

Several antiviral drugs based on the RNAi mechanism are currently known and are at different stages of clinical trials, namely: *Miravirsen*, hepatitis C (*Santaris Pharma*); *ALN-RSV01*, respiratory syncytial viral infection (*Alnylam Pharmaceuticals*); and *pHIV7-shITAR-CCR5RZ*, HIV infection (*City of Hope Medical Center*) [27, 28]. Patisiran and Givosiran (*Alnylam Pharmaceuticals*) were also approved for clinical use to treat amyloid polyneuropathy and acute hepatic porphyria, respectively¹ [29].

A critical factor that compromises the efficiency of RNA interference might be the development of resistance to the siRNAs directed against viral genes [30]. To overcome the drug resistance ability of the influenza virus, the search for novel antiviral siRNAs with antiviral activity and targeted to host cell components is required for the replication of the virus.

This study has shown that using siRNAs directed to the cellular *FLT4*, *Nup98*, and *Nup205* genes can inhibit the reproduction of the influenza A virus in the A549 lung cancer cell line. Here the cellular gene *FLT4* plays a vital role in the process of endocytosis in the virus. While *Nup98* and *Nup205* encode proteins of the nuclear pore complex that are involved in the import and export of viral RNA segments into the nuclear cavity.

¹ Multi-Discipline Review. Center for Drug Evaluation and Research. Appl. No. 212194Orig1s000. 167 p. URL: https://www.accessdata.fda.gov/drugsatfda_docs/nda/2019/212194Orig1s000MultidisciplineR.pdf (Accessed August 24, 2021).

MATERIALS AND METHODS

Selecting target genes for suppressing viral reproduction

In this study, the criteria used to select genes that encode the expression of cellular factors necessary for viral reproduction are as follows: (i) genes reported as a potentially successful target for siRNA in publications related to siRNA screening; (ii) genes reported as effective in early independent studies; and (iii) genes showing low cytopathic effect from the temporary suppression their expression [26–28].

siRNA

The siRNA was selected from the web-based software, siDirect 2.0². All oligonucleotides were synthesized by *Syntol* (Russia). Oligoribonucleotides were diluted with water to a concentration of 100 pmol/μL. Then, complementary oligonucleotides were mixed, incubated in a thermostat at 60°C for 1 min, and then cooled to room temperature. Prepared RNA duplexes were stored at –80°C. All work with finished duplexes was carried out using a cold tripod. The sequences of the siRNAs are presented in Table 1. As a nonspecific control, we used siRNA *L2*, specific to the firefly luciferase gene and not affecting the life cycle of A549 cells.

Evaluation of the suppression of cellular gene expression

The expression level of the target genes was determined after siRNA transfection. The cells were treated with a lysis solution, and then cellular RNA was isolated using the MagnoSorb kit (*Interlabservice*, Russia), 24 h post-transfection. OT-1 reagent kit (*Syntol*, Russia) was used to set up the reverse-transcription reaction. Changes in gene expression dynamics were monitored using quantitative real-time PCR with a set of primers for the *FLT4*, *Nup98*, *Nup205*, and *GAPDH* genes [32]. To assess the effect of siRNAs on target genes, the relative expression level of the *FLT4*, *Nup98*, and *Nup205* genes was calculated according to the standard $2^{-\Delta\Delta CT}$ method.³ For each siRNA, primers were synthesized according to the gene regions affected by siRNA. Primers were selected using Integrated DNA Technologies website⁴ and synthesized by *Syntol* (Table 2).

Virus

The influenza virus used in this study is A/WSN/33 (**H1N1**) (St. Jude Children's Research Hospital, USA). Cultivation and determination of the virus titer were carried out on the culture of canine kidney cells (Madin-Darby Canine Kidney (MDCK)).

² <http://sirect2.mai.jp/> (Accessed February 02, 2021).

³ Bradburn S. How to Perform the Delta-Delta Ct Method. URL: <https://toptipbio.com/delta-delta-ct-pcr/> (Accessed August 27, 2021).

⁴ <https://eu.idtdna.com/> (Accessed March 02, 2021).

Table 1. siRNA sequences

siRNA	Sequence
<i>FLT4.1</i>	AAUGACAUCUGAAUCUCAGdGdG CUGAGAUUCAGAUGUCAUdTdA
<i>FLT4.2</i>	UGAAGUUCUGUUGAAAAAGdAdC CUUUUACAACAGAACUUCAdCdA
<i>Nup98.1</i>	AGUCUUUGUUUCAGAAAGCdGdC GCUUUCUGAAACAAAGACUdCdA
<i>Nup98.2</i>	UCCAAAUGUUGAAGUUGUGdCdC CACAACUUCAACAUUUGGAdCdA
<i>Nup205</i>	UCAAAAUCUUAUCAAGAAGdGdT CUUCUUGAUAAAGAUUUUGAdAdG
<i>L2</i> (nonspecific siRNA)	UUUCCGUCAUCGUCUUUCCdTdT GGAAAGACGAUGACGGAAAdTdT

Cell culture

MDCK cells (Institut Pasteur, France) and A549 human lung adenocarcinoma cells were used (ATCC® CCL-185, USA) in this study. MDCK cells were grown in minimum essential medium (MEM) (*PanEco*, Russia), supplemented with 5% fetal bovine serum (*Gibco*) (*ThermoFisher Scientific*, USA), 40 µg/mL gentamicin (*PanEco*), and 300 µg/mL L-glutamine (*PanEco*) at 37°C in a CO₂-incubator. A549 cells were grown in Dulbecco's modified Eagle's medium (DMEM) (*PanEco*), supplemented with 5% fetal bovine serum (*Gibco*), 40 µg/mL gentamicin (*PanEco*), and 300 µg/mL L-glutamine (*PanEco*) at 37°C in a CO₂-incubator.

MTT assay

The cell viability of A549 cells treated with siRNA was assessed with the MTT (methylthiazolyltetrazolium bromide) assay. On days 1, 2, 3 after transfection, 20 µL of MTT solution, 5 mg/mL (*PanEco*), was added to the wells containing cells in a 96-well plate and incubated at 37°C in a 5% CO₂ incubator for 2 h. Further, the supernatant and 100 µL of dimethyl sulfoxide (*Sigma-Aldrich*, cat. # D4540-1L) was added to each well. The optical density values were determined at 530 nm using a microplate reader Varioscan (*Thermo Fisher Scientific*, USA), with the background values set at 620 nm.

Transfection of siRNA cells with subsequent infection

For siRNA transfection, A549 cells were plated on 12-well plates at a density of 1 × 10⁵ cells/mL. After achieving 80% confluence, the cells were washed with phosphate-buffered saline and serum-free Opti-MEM medium (*Thermo Fisher Scientific*, USA). Then

a mixture of 24 µL Lipofectamine 2000 (*Thermo Fisher Scientific*) and 600 µL Opti-MEM (*Thermo Fisher Scientific*) was added to a solution of siRNA in Opti-MEM medium and incubated at room temperature for 20 min. The siRNA concentration required for gene knockdown was 40 pmol/µL per well. After incubation, the complexes were added to the wells. siRNA *L2* was used as a nonspecific control. The cells were then incubated at 37°C in a CO₂ incubator. Four hours later, the culture medium was removed from all wells, except for the negative control, and 1 mL of viral liquid consisting of DMEM, 0.001% chymotrypsin inhibitor (Tosyl phenylalanyl chloromethyl ketone (TPCK)) (*Sigma-Aldrich*, Germany), and 40 µg/mL gentamicin was added with a MOI of 0.1. After that, the cells were again placed in the CO₂ incubator. Over the next three days, supernatant samples were taken for the subsequent staging of the hemagglutination, titration, and Reverse Transcription Polymerase Chain Reaction (RT-PCR).

Detection of viral RNA

Viral RNA (vRNA) was isolated from the selected supernatants using the High Pure RNA Isolation Kit (*Roche*, Germany). OT-1 reagent kit (*Syntol*, Russia) was used to set up the reverse-transcription reaction. The concentration of viral RNA in the culture was measured using quantitative real-time RT-PCR with a set of primers and probes for the hemagglutination assay (HA) M-gene [33]. For real-time PCR, a reagent kit containing EVA Green dye, a reference ROX dye (*Syntol*), and a 2.5-fold reaction mixture (*Syntol*) were used. The working concentration of primers and probes was 10 and 5 pmol/µL, respectively. The real-time PCR reaction was carried out in a DT-96 thermal

cycler (*DNA-Technology*, Russia). The temperature-time regime for real-time PCR was as follows: 95°C–5 min (1 cycle); 62°C–40 s; 95°C–15 s (40 cycles). Table 2 shows primers and probes synthesized by *Syntol*.

Determination of HAV hemagglutinating titer

Saline (50 µL) was added to each well of a 96-well round-bottom plate. Then, 50 µL of samples were added to the wells, and subsequent 2-fold dilutions were made. After that, 50 µL of 0.5% erythrocyte mixture was added to the wells and left at room temperature for 40 min. The viral titer was expressed in agglutinating units.⁵

Virus titration at the endpoint of the cytopathic effect

The viral titer was determined using the endpoint assay to assess the cytopathic effect in the MDCK cells. MDCK cells were seeded in 96-well plates at a density

of (1×10^4 cells/mL). After 2 days, the nutrient medium was removed from the wells; 10-fold serial dilutions of viral samples were added in a support medium without trypsin and incubated for 4 days in a CO₂ incubator at 37°C. On the fourth day, the titration results were visually recorded under a microscope for the presence of a specific cytopathic effect for the influenza virus (change, deformation, detachment of dead cells from the bottom of the well). The viral titer was calculated according to the method described in [34] and was expressed as the logarithm of tissue cytotoxic doses—TCD_{50/mL}.

Statistical data processing

The statistical significance of the results obtained was assessed using the Mann-Whitney test. The difference was considered significant if $0.01 \leq p \leq 0.05$. Reliability indicators were calculated using Psychol-ok⁶.

Table 2. Primers for real-time RT-PCR for the IAV M-gene

Primer	Sequence
<i>FLT4.1F</i>	AAUGACAUCUGAAUCUCAGdGdG
<i>FLT4.1R</i>	CUGAGAUUCAGAUGUCAUUdTdA
<i>FLT4.2F</i>	UGAAGUUCUGUUGAAAAAGdAdC
<i>FLT4.2R</i>	CUUUUCAAACAGAACUUCAdCdA
<i>Nup98.1F</i>	UGAGUAUGUUAGACUAUUGdAdT
<i>Nup98.1R</i>	CAAUAGUCUAACAUCUCAdCdC
<i>Nup98.2F</i>	AUUAAGGUUCUCAAACCCdAdA
<i>Nup98.2R</i>	GGUUUUGAAGAACCUUAAUdAdA
<i>Nup205F</i>	UUAUUCACAUCAAUCUGUGdAdC
<i>Nup205R</i>	CACAGAUUGAUGUGAAUAAdTdG
<i>IAV M F:</i>	GGAATGGCTAAAGACAAGACCAAT
<i>IAV M R:</i>	GGGCATTTTGGACAAAGCGTCTAC
<i>IAV M Pr: FAM</i>	AGTCCTCGCTCACTGGGCACGGTG-BHQ1
<i>GAPDH F</i>	AGCCACATCGCTCAGACAC
<i>GAPDH R</i>	GCCAATACG ACCAAATCC

⁵ MU 3.3.2.1758–03 Methods for determining the quality indicators of immunobiological drugs for the prevention and diagnosis of influenza. https://www.rospotrebnadzor.ru/documents/details.php?ELEMENT_ID=4727 (Accessed August 27, 2021).

⁶ <https://www.psychol-ok.ru/statistics/mann-whitney/> (Accessed August 05, 2021).

RESULTS

Justification for the choice of siRNA targets

Three target genes were selected for siRNA experiments. All three genes actively interact with the influenza virus at several stages of its reproduction. The *FLT4* gene encodes the Epidermal Growth Factor (*EGF*) receptor protein of the tyrosine kinase receptor. According to Eierhoff, the *EGF* protein is actively involved in the process of viral endocytosis [35]. Proteins *Nup98* and *Nup205* (encoded by genes of the same name) import and export viral mRNA from nucleoplasm [36, 37].

We tested the ability of the synthesized siRNAs to suppress the expression of their target genes. Compared to cells treated with nonspecific siRNA *L2*, gene expression decreased by more than 80% on the first day for each of the five siRNAs. Figure 1 shows the efficiency of mRNA knockdown in A549 cells. Evaluation of the suppression of gene expression was carried out using the $2^{-\Delta\Delta CT}$ method.⁷

Influence of siRNA on the survival of transfected cells

The survival rate of A549 cells transfected with siRNA was measured within three days (Table 3). The survival threshold was set at 70%, according to a similar study [26]. After 24 h, the viability of cells treated with siRNA remained practically unchanged. On the second day, the survival rate of cells treated with all siRNAs, except for *Nup205* and siRNA *L2*, decreased by 14–21%. The survival rate of untransfected cells was taken as 100%. All values were normalized to the mean optical density of untransfected cells at each time interval following transfection. Treatment of cells with siRNA did not decrease cell survival compared with the negative control.

Influence of siRNA on hemagglutinating activity

Table 4 shows the changes in the hemagglutinating titer of the influenza virus on day 3 in the hemagglutination assay (HA). The hemagglutinating activity in cells treated with siRNAs *Nup205* and *FLT4.2* decreased 16 times compared to 8 times in cells treated with siRNAs *FLT4.1*, *Nup98.1*, and *Nup98.2*.

Influence of siRNA on the titer of the virus

The next step was to determine whether the change in the infectious titer of the virus was due to the siRNA's effect on the target genes. Within three days after transfection, the supernatant was removed and then titrated on a monolayer of MDCK cells in 96-well plates. It was found that the use of all siRNAs at MOI = 0.1 led to a significant decrease in viral reproduction compared to siRNA *L2*. As seen in Fig. 1, virus titers increased

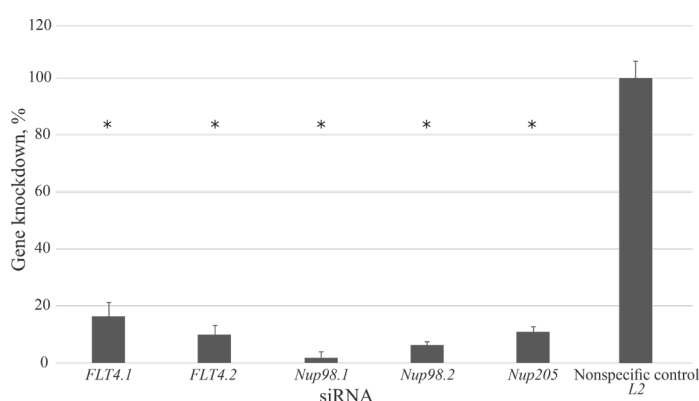


Fig. 1. Influence of siRNA on the expression of genes *FLT4*, *Nup98*, and *Nup205*.

with time in nontransfected cell culture, reaching peak values at 48 and 72 hours. The same was observed in cells transfected with nonspecific siRNA *L2*. When the *FLT4* gene expression was suppressed using *FLT4.1* siRNA, the viral titer decreased by about 0.9–1.0 lg TCD_{50/mL} compared to the control on the first, second, and third day. With siRNA *FLT4.2*, there was a decrease by 1.0 lg TCD_{50/mL} on the first day; however, there was a decrease by 2.2 lg TCD_{50/mL} on the second and third day, compared to the control groups. Upon transfection of siRNA to the *Nup205* gene, the viral titer decreased by 1.0 lg TCD_{50/mL} on the 1st day and by 2.3 lg TCD_{50/mL} on the next day relative to the control and nonspecific control. In cells treated with *Nup98.1* siRNA, a significant decrease in the virus titer was observed (2.3 lg TCD_{50/mL}) on the 2nd day compared to the controls, while for *Nup98.2*, it was 2.2 lg TCD_{50/mL} on the 3rd day, compared to the controls. The dynamics of changes in the viral titer are shown in Fig. 2.

Influence of siRNA on the concentration of viral RNA

The effect of siRNA on the concentration of viral RNA is shown in Fig. 3. On the first day, a decrease in the concentration of viral RNA was observed with *Nup98.1* siRNA (up to 190 times) and *Nup205* siRNA (up to 30 times) during real-time RT-PCR. A 29-fold decrease in the vRNA concentration for *Nup205* and 26-fold for *Nup98.1* was noted on the second day. While on the third day, the vRNA concentration decreased by 6 and 30 times for *Nup98.1* siRNA and *Nup205* siRNA, respectively. For *FLT4.2* siRNA, the viral RNA concentration decreased by 23, 18, and 16 times on the first, second, and third day, respectively. In contrast, there was no significant decrease in the concentration of viral RNA using *FLT4.1* siRNA on the first, second, and third days.

⁷ Bradburn S. How to Perform the Delta-Delta Ct Method. URL: <https://toptipbio.com/delta-delta-ct-pcr/> (Accessed August 27, 2021).

Table 3. Cell survival after siRNA transfection in percentage, %

siRNA	1st day	2nd day	3rd day
<i>FLT4.1</i>	96	81	74
<i>FLT4.2</i>	94	80	81
<i>Nup98.1</i>	100	79	79
<i>Nup98.2</i>	97	86	87
<i>Nup205</i>	94	95	94
<i>L2</i>	94	99	99
<i>K</i> -(untranslated)	100	100	100

Table 4. Viral reproduction on the 3rd day according to HA data

siRNA	Viral reproduction to HA (log ₂)
	A/WSN/33 (MOI = 0.1)
<i>FLT4.1</i>	1:8
<i>FLT4.2</i>	1:4
<i>Nup98.1</i>	1:8
<i>Nup98.2</i>	1:8
<i>Nup205</i>	1:4
<i>K</i> -(<i>L2</i>)	1:64
<i>K-IAV</i>	1:64

DISCUSSION

Influenza is an acute infectious respiratory disease caused by viruses of the *Orthomyxoviridae* family. Diseases caused by the influenza virus are one of the most pressing global public health problems today. The search for new anti-influenza medication is relevant because the influenza virus rapidly develops resistance to known specific anti-influenza drugs [38].

In this work, we performed a series of cell culture experiments to assess the anti-influenza activity of small interfering RNAs directed at *FLT4*, *Nup98*, and *Nup205* genes. A pronounced antiviral activity of siRNAs directed to the mRNA of these genes was observed, and consistent data were obtained on the

correlation between the expression of cellular genes and viral reproduction, assessed by different methods (virus titration by cytopathic effect, real-time RT-PCR, HA).

An important factor for the successful use of siRNA is that the knockdown of the target gene should not affect the vital activity of cells. siRNAs targeting the genes *FLT4*, *Nup98*, and *Nup205* did not decrease cell viability below the threshold level of 70%, by analogy with the paper [26].

The use of siRNAs to suppress the expression of cellular genes to reduce viral reproduction has an advantage over siRNAs directed to the whole viral genome. This is due to the fact that influenza viruses have a higher tendency for mutational variability that often leads to substitutions of nucleotide sequences in their genome [39]. This can cause siRNA to be ineffective

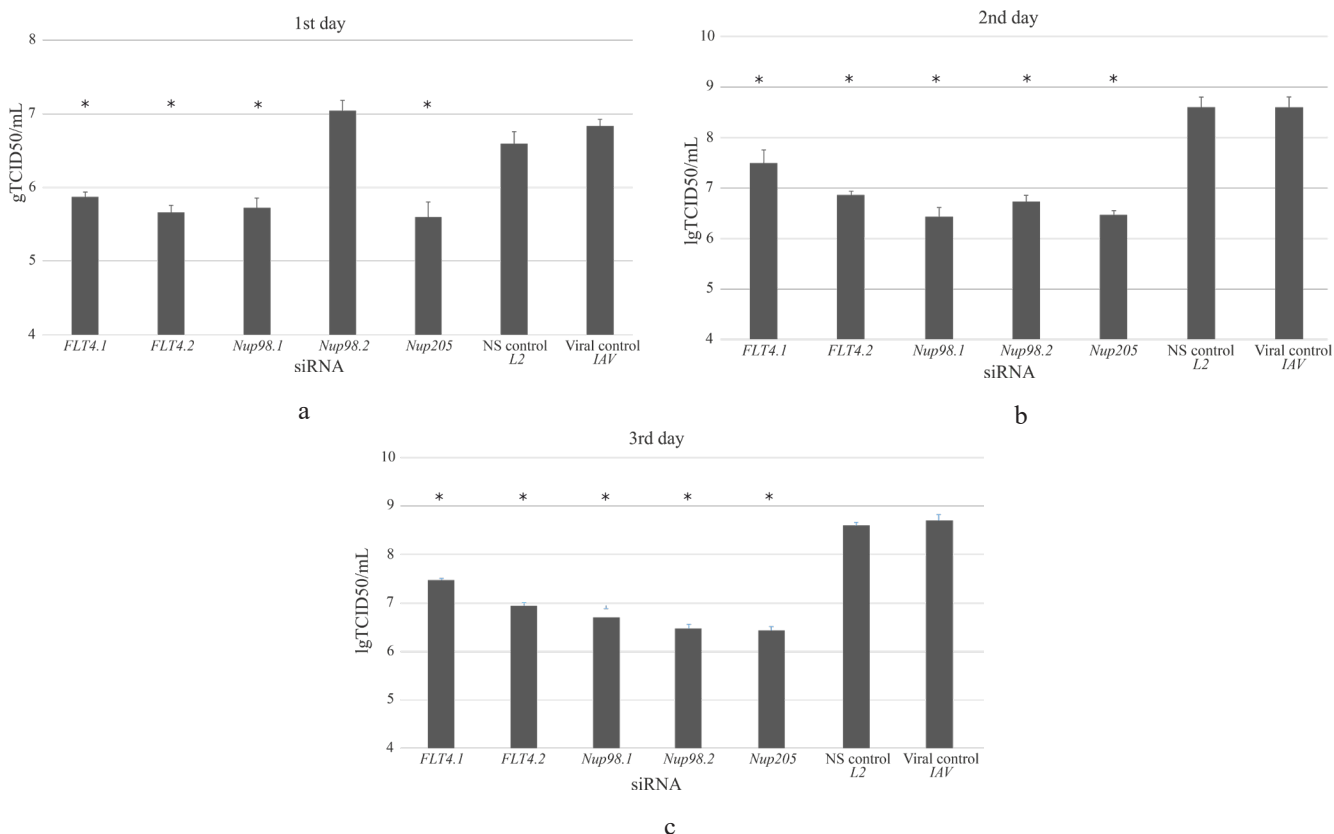


Fig. 2. Effect of siRNAs directed to the *FLT4*, *Nup98*, and *Nup205* genes on the reproduction of the influenza virus (MOI = 0.1). (a) 1st day post infection (p.i.), (b) 2nd day p.i., and (c) 3rd day p.i.

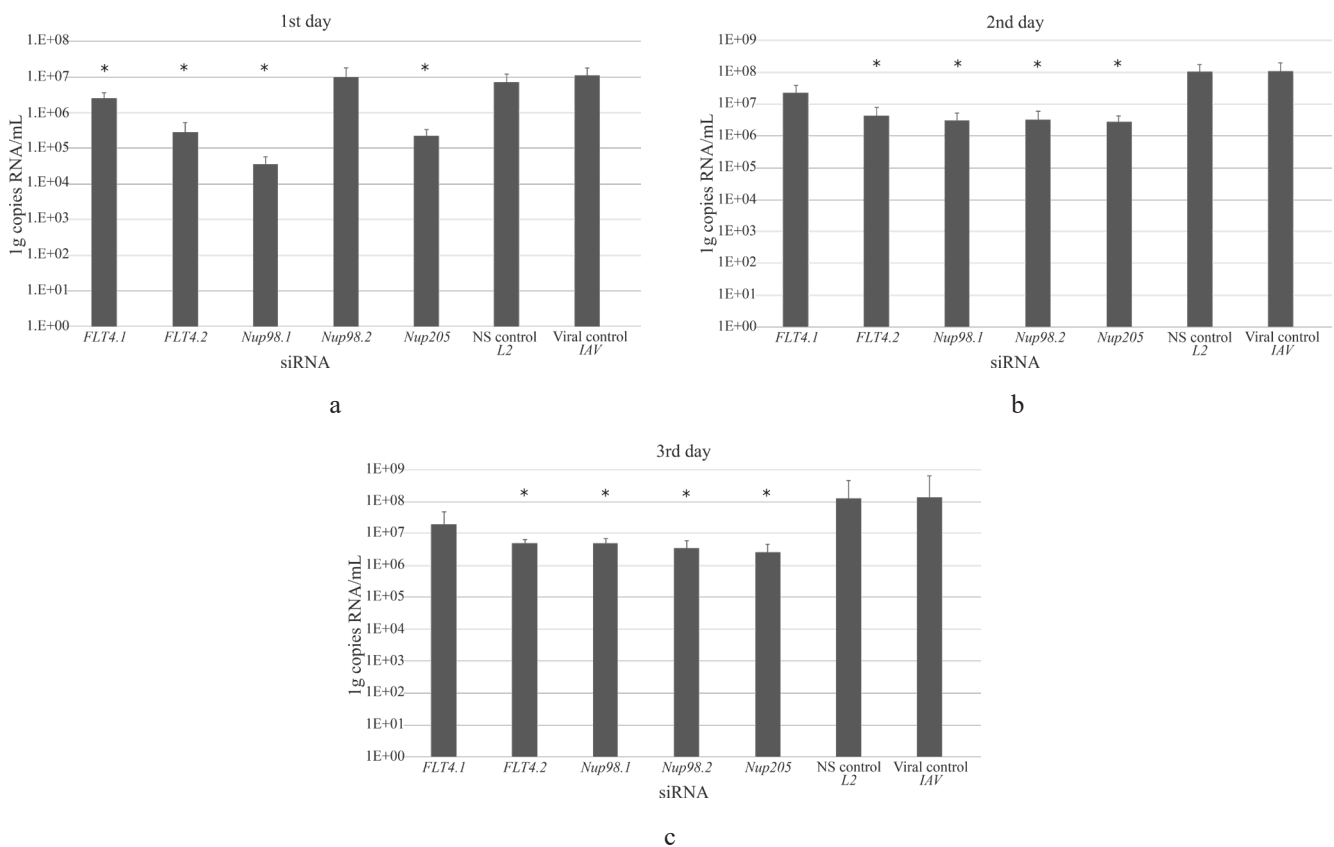


Fig. 3. The effect of siRNA on the concentration of viral RNA. (a) 1st day post infection (p.i.), (b) 2nd day p.i., and (c) 3rd day p.i.

toward the virus since even a single substitution in the target RNA sequence can completely neutralize the action of siRNA [43]. For example, the ability to elude the action of siRNA was experimentally demonstrated in a model of HIV-1 infection, where nucleotide substitutions occurred in the *tat*, *nef*, *int*, and *att* genes [41]. In view of this, A. Karlas and M. Lesch suggest that using siRNAs directed at the cellular genome is more justified since the possibility of an alternate viral reproduction pathway is very low [30]. The promise of this approach—based on the suppression of the activity of cellular genes necessary for the reproduction of the influenza virus—has been shown in several independent studies [26, 30, 42, 43].

CONCLUSIONS

Currently, there remains a need to create highly effective drugs to treat influenza and its complications. The present study shows that siRNAs directed to cellular genes that play essential roles in viral endocytosis and nuclear import and export of vRNA significantly reduce

the reproduction of the influenza virus *in vitro*. These data confirm that the investigated human genes *FLT4*, *Nup98*, and *Nup205* are promising targets for developing anti-influenza drugs. The findings of this study give hope that siRNA medication will be implemented in the future.

Acknowledgments

The authors are grateful to the Center for Shared Use of the I.I. Mechnikov Research Institute of Vaccines and Sera. The study was not sponsored.

Authors' contributions

E.A. Pashkov, E.R. Korchevaya, A.A. Rtishchev, and B.S. Cherepovich – conducting the experiments;

E.A. Pashkov, E.P. Bystritskaya, and Yu.E. Dronina – writing the text of the article and the analysis of the obtained results;

E.B. Fayzuloev, A.V. Poddubikov, and A.V. Sidorov – scientific editing;

A.S. Bykov, O.A. Svitich, and V.V. Zverev – idea of the study and general management.

The authors declare no obvious and potential conflicts of interest related to the publication of this article.

REFERENCES

- Hussain M., Galvin H.D., Haw T.Y., Nutsford A.N., Husain M. Drug resistance in influenza A virus: the epidemiology and management. *Infect. Drug Resist.* 2017 Apr 20;10:121–134. <https://doi.org/10.2147/IDR.S105473>
- Peasah S.K., Azziz-Baumgartner E., Breese J, Meltzer M.I., Widdowson MA. Influenza cost and cost-effectiveness studies globally – a review. *Vaccine.* 2013;31(46):5339–5348. <https://doi.org/10.1016/j.vaccine.2013.09.013>
- Rezkalla S.H., Kloner R.A. Influenza-related viral myocarditis. *WMJ.* 2010;109(4):209–213. PMID: 20945722. URL: <https://wmjonline.org/wp-content/uploads/2010/109/4/209.pdf>
- Nguyen J.L., Yang W., Ito K., Matte T.D., Shaman J., Kinney P.L. Seasonal Influenza Infections and Cardiovascular Disease Mortality. *JAMA Cardiol.* 2016;1(3):274–281. PMID: 27438105; PMCID: PMC5158013 <https://doi.org/10.1001/jamacardio.2016.0433>
- Ekstrand J.J. Neurologic complications of influenza. *Semin. Pediatr. Neurol.* 2012;19(3):96–100. <https://doi.org/10.1016/j.spn.2012.02.004>

- Edet A., Ku K., Guzman I., Dargham H.A. Acute Influenza Encephalitis/Encephalopathy Associated with Influenza A in an Incompetent Adult. *Case Rep. Crit. Care.* 2020;2020:6616805. <https://doi.org/10.1155/2020/6616805>
- Err H., Wiwanitkit V. Emerging H6N1 influenza infection: renal problem to be studied. *Ren. Fail.* 2014;36(4):662. <https://doi.org/10.3109/0886022X.2014.883934>
- Leneva I.A., Egorov A.Yu., Falynskova I.N., Makhmudova N.R., Kartashova N.P., Glubokova E.A., Vartanova N.O., Poddubikov A.V. Induction of secondary bacterial pneumonia in mice infected with pandemic and laboratory strains of the H1N1 influenza virus. *Zhurnal mikrobiologii, epidemiologii i immunobiologii = Journal of Microbiology, Epidemiology and Immunobiology.* 2019;1(1):68–74 (in Russ.). <https://doi.org/10.36233/0372-9311-2019-1-68-74>
- Metersky M.L., Masterton R.G., Lode H., File T.M. Jr., Babinchak T. Epidemiology, microbiology, and treatment considerations for bacterial pneumonia complicating influenza. *Int. J. Infect. Dis.* 2012;16(5):e321–31. <https://doi.org/10.1016/j.ijid.2012.01.003>

10. Vanderbeke L., Spriet I., Breynaert C., Rijnders B.J.A., Verweij P.E., Wauters J. Invasive pulmonary aspergillosis complicating severe influenza: epidemiology, diagnosis and treatment. *Curr. Opin. Infect. Dis.* 2018;31(6):471–480. <https://doi.org/10.1097/QCO.0000000000000504>
11. Van der Vries E., Schutten M., Fraaij P., Boucher C., Osterhaus A. Influenza virus resistance to antiviral therapy. *Adv. Pharmacol.* 2013;67:217–246. <https://doi.org/10.1016/B978-0-12-405880-4.00006-8>
12. Han J., Perez J., Schafer A., Cheng H., Peet N., Rong L., Manicassamy B. Influenza Virus: Small Molecule Therapeutics and Mechanisms of Antiviral Resistance. *Curr. Med. Chem.* 2018;25(38):5115–5127. <https://doi.org/10.2174/0929867324666170920165926>
13. Looi Q.H., Foo J.B., Lim M.T., Le C.F., Show P.L. How far have we reached in development of effective influenza vaccine? *Int. Rev. Immunol.* 2018;37(5):266–276. <https://doi.org/10.1080/08830185.2018.1500570>
14. Pleguezuelos O., James E., Fernandez A., Lopes V., Rosas L.A., Cervantes-Medina A., Cleath J., Edwards K., Neitzey D., Gu W., Hunsberger S., Taubenberger J.K., Stoloff G., Memoli M.J. Efficacy of FLU-v, a broad-spectrum influenza vaccine, in a randomized phase IIb human influenza challenge study. *NPJ Vaccines.* 2020;5(1):22. <https://doi.org/10.1038/s41541-020-0174-9>
15. Wang F., Chen G., Zhao Y. Biomimetic nanoparticles as universal influenza vaccine. *Smart Mater. Med.* 2020;1:21–23. <https://doi.org/10.1016/j.smaim.2020.03.001>
16. Smith M. Vaccine safety: medical contraindications, myths, and risk communication. *Pediatr. Rev.* 2015;36(6):227–238.
17. Wang J., Wu Y., Ma C., Fiorin G., Wang J., Pinto L.H., *et al.* Structure and inhibition of the drug-resistant S31N mutant of the M2 ion channel of influenza A virus. *Proc. Natl. Acad. Sci. USA.* 2013;110(4):1315–1320. <https://doi.org/10.1073/pnas.1216526110>
18. Leneva I.A., Russell R.J., Boriskin Y.S., Hay A.J. Characteristics of arbidol-resistant mutants of influenza virus: Implications for the mechanism of anti-influenza action of arbidol. *Antiviral Res.* 2009;81(2):132–140. <https://doi.org/10.1016/j.antiviral.2008.10.009>
19. Hurt A.C., Ernest J., Deng Y.M., Iannello P., Besselaar T.G., Birch C., *et al.* Emergence and spread of oseltamivir-resistant influenza A (H1N1) viruses in Oceania, Southeast Asia and South Asia. *Antiviral Res.* 2009;83(1):90–93. <https://doi.org/10.1016/j.antiviral.2009.03.003>
20. Hurt A.C. The epidemiology and spread of drug resistant human influenza viruses. *Curr. Opin. Virol.* 2014;8:22–29. <https://doi.org/10.1016/j.coviro.2014.04.009>
21. Lampejo T. Influenza and antiviral resistance: an overview. *Eur. J. Clin. Microbiol. Infect. Dis.* 2020;39(7):1201–1208. <https://doi.org/10.1007/s10096-020-03840-9>
22. Fire A.Z. Gene silencing by double-stranded RNA. *Cell Death Differ.* 2007;14(12):1998–2012. <https://doi.org/10.1038/sj.cdd.4402253>
23. Fire A., Xu S.Q., Montgomery M.K., Kostas S.A., Driver S.E., Mell C.C. Potent and specific genetic interference by double-stranded RNA in *Caenorhabditis elegans*. *Nature.* 1998;391(6669): 806–811. <https://doi.org/10.1038/35888>
24. Faizuloev E.B., Nikonova A.A., Zverev V.V. Prospects for the development of antiviral drugs based on small interfering RNAs. *Voprosy virusologii = Problems of Virology.* 2013;(S1):155–169 (in Russ.). URL: <https://cyberleninka.ru/article/n/perspektivy-sozdaniya-protivovirusnyh-preparatov-na-osnove-malyh-interferiruyuschih-rnk/viewer>
25. McManus M.T., Sharp P.A. Gene silencing in mammals by small interfering RNAs. *Nat. Rev. Genet.* 2002;3(10):737–747. <https://doi.org/10.1038/nrg908>
26. Estrin M.A., Hussein I.T.M., Puryear W.B., Kuan A.C., Artim S.C., Runstadler J.A. Host-directed combinatorial RNAi improves inhibition of diverse strains of influenza A virus in human respiratory epithelial cells. *PLoS One.* 2018;13(5):e0197246. <https://doi.org/10.1371/journal.pone.0197246>
27. Janssen H.L., Reesink H.W., Lawitz E.J., Zeuzem S., Rodriguez-Torres M., Patel K., van der Meer A.J., Patick A.K., Chen A., Zhou Y., Persson R., King B.D., Kauppinen S., Levin A.A., Hodges M.R. Treatment of HCV infection by targeting microRNA. *N. Engl. J. Med.* 2013;368(18):1685–1394. <https://doi.org/10.1056/nejmoa1209026>
28. Qureshi A., Tantray V.G., Kirmani A.R., Ahangar A.G. A review on current status of antiviral siRNA. *Rev. Med. Virol.* 2018;28(4):e1976. <https://doi.org/10.1002/rmv.1976>
29. Hoy S.M. Patisiran: First Global Approval. *Drugs.* 2018;78(15):1625–1631. <https://doi.org/10.1007/s40265-018-0983-6>
30. Lesch M., Luckner M., Meyer M., Weege F., Gravenstein I., Raftery M., Sieben C., Martin-Sancho L., Imai-Matsushima A., Welke R.W., Frise R., Barclay W., Schönrich G., Herrmann A., Meyer T.F., Karlas A. RNAi-based small molecule repositioning reveals clinically approved urea-based kinase inhibitors as broadly active antivirals. *PLoS Pathog.* 2019;15(3):e1007601. <https://doi.org/10.1371/journal.ppat.1007601>
31. Karlas A., Machuy N., Shin Y., Pleissner K.P., Artarini A., Heuer D., *et al.* Genome-wide RNAi screen identifies human host factors crucial for influenza virus replication. *Nature.* 2010;463(7282):818–822. <https://doi.org/10.1038/nature08760>
32. Arenas-Hernandez M., Vega-Sanchez R. Housekeeping gene expression stability in reproductive tissues after mitogen stimulation. *BMC Res. Notes.* 2013;6:285. <https://doi.org/10.1186/1756-0500-6-285>
33. Lee H.K., Loh T.P., Lee C.K., Tang J.W., Chiu L., Koay E.S. A universal influenza A and B duplex real-time RT-PCR assay. *J. Med. Virol.* 2012;84(10):1646–1651. <https://doi.org/10.1002/jmv.23375>
34. Ramakrishnan M.A. Determination of 50% endpoint titer using a simple formula. *World J. Virol.* 2016;5(2):85–86. <https://doi.org/10.5501/wjv.v5.i2.85>
35. Eierhoff T., Hrinčius E.R., Rescher U., Ludwig S., Ehrhardt C. The Epidermal Growth Factor Receptor (EGFR) promotes uptake of influenza A viruses (IAV) into host cells. *PLoS Pathog.* 2010;6(9):e1001099. <https://doi.org/10.1371/journal.ppat.1001099>
36. Shaw M.L., Stertz S. Role of Host Genes in Influenza Virus Replication. In: Tripp R., Tompkins S. (Eds.). Roles of Host Gene and Non-coding RNA Expression in Virus Infection. *Current Topics in Microbiology and Immunology.* 2017;419:151–189. https://doi.org/10.1007/82_2017_30

37. Watanabe T., Watanabe S., Kawaoka Y. Cellular networks involved in the influenza virus life cycle. *Cell Host & Microbe*. 2010;7(6):427–439. <https://doi.org/10.1016/j.chom.2010.05.008>
38. Hussain M., Galvin H.D., Haw T.Y., Nutsford A.N., Husain M. Drug resistance in influenza A virus: the epidemiology and management. *Infect. Drug Resist.* 2017;10:121–134. <https://doi.org/10.2147/IDR.S105473>
39. Sanjuán R., Domingo-Calap P. Mechanisms of viral mutation. *Cell. Mol. Life Sci.* 2016;73(23):4433–4448. <https://doi.org/10.1007/s00018-016-2299-6>
40. Preslold J.B., Novella I.S. RNA viruses and RNAi: quasispecies implications for viral escape. *Viruses*. 2015;7(6):3226–3240. <https://doi.org/10.3390/v7062768>
41. Das A.T., Brummelkamp T.R., Westerhout E.M., Vink M., Madiredjo M., Bernards R., et al. Human immunodeficiency virus type 1 escapes from RNA interference-mediated inhibition. *J. Virol.* 2004;78(5):2601–5. <https://doi.org/10.1128/JVI.78.5.2601-2605.2004>
42. Rupp J.C., Locatelli M., Grieser A., Ramos A., Campbell P.J., Yi H., et al. Host cell copper transporters CTR1 and ATP7A are important for Influenza A virus replication. *Virology*. 2017;14(1):11. <https://doi.org/10.1186/s12985-016-0671-7>
43. Wang R., Zhu Y., Zhao J., Ren C., Li P., Chen H., et al. Autophagy Promotes Replication of Influenza A Virus *In Vitro*. *J. Virol.* 2019;93(4):e01984–18. <https://doi.org/10.1128/JVI.01984-18>

About the authors:

Evgeny A. Pashkov, Postgraduate Student, Department of Microbiology, Virology and Immunology, I.M. Sechenov First Moscow State Medical University (Sechenov University) (8, Trubetskaya ul., Moscow, 119991, Russia); Junior Researcher, Laboratory of Molecular Immunology, Federal State Budgetary Scientific Institution “I. Mechnikov Research Institute of Vaccines and Sera” (5A, Malyi Kazennyi pereulok, Moscow, 105064, Russia). E-mail: pashkov.j@yandex.ru, <https://orcid.org/0000-0002-5682-4581>

Evgeny B. Faizuloev, Cand. Sci. (Biol.), Head of the Laboratory of Molecular Virology, Federal State Budgetary Scientific Institution “I. Mechnikov Research Institute of Vaccines and Sera” (5A, Malyi Kazennyi pereulok, Moscow, 105064, Russia). E-mail: faizuloev@mail.ru, <https://orcid.org/0000-0001-7385-5083>

Ekaterina R. Korchevaya, Junior Researcher, Laboratory of Molecular Virology, Federal State Budgetary Scientific Institution “I. Mechnikov Research Institute of Vaccines and Sera” (5A, Malyi Kazennyi pereulok, Moscow, 105064, Russia). E-mail: c.korchevaya@gmail.com, <https://orcid.org/0000-0002-6417-3301>

Artem A. Rtishchev, Junior Researcher, Laboratory of RNA viruses, Federal State Budgetary Scientific Institution “I. Mechnikov Research Institute of Vaccines and Sera” (5A, Malyi Kazennyi pereulok, Moscow, 105064, Russia). E-mail: rtishchevartiom@gmail.com, <https://orcid.org/0000-0002-4212-5093>

Bogdan S. Cherepovich, Junior Researcher, Laboratory of RNA viruses, Federal State Budgetary Scientific Institution “I. Mechnikov Research Institute of Vaccines and Sera” (5A, Malyi Kazennyi pereulok, Moscow, 105064, Russia). E-mail: bogdancherepovich@mail.ru, <https://orcid.org/0000-0002-5803-6263>

Alexander V. Sidorov, Cand. Sci. (Biol.), Head of the Laboratory of DNA viruses, Federal State Budgetary Scientific Institution “I. Mechnikov Research Institute of Vaccines and Sera” (5A, Malyi Kazennyi pereulok, Moscow, 105064, Russia). E-mail: sashasidorov@yandex.ru, <https://orcid.org/0000-0001-8962-4765>

Alexander A. Poddubikov, Cand. Sci. (Biol.), Head of the Laboratory of Microbiology of Opportunistic Pathogenic Bacteria, Federal State Budgetary Scientific Institution “I. Mechnikov Research Institute of Vaccines and Sera” (5A, Malyi Kazennyi pereulok, Moscow, 105064, Russia). E-mail: poddubikov@yandex.ru, <https://orcid.org/0000-0001-8962-4765>

Elizaveta P. Bystritskaya, Junior Researcher, Laboratory of Molecular Immunology, Federal State Budgetary Scientific Institution “I. Mechnikov Research Institute of Vaccines and Sera” (5A, Malyi Kazennyi pereulok, Moscow, 105064, Russia). E-mail: lisabystritskaya@gmail.com, <https://orcid.org/0000-0001-8430-1975>

Yuliya E. Dronina, Cand. Sci. (Med.), Associate Professor, Department of Microbiology, Virology and Immunology, I.M. Sechenov First Moscow State Medical University (Sechenov University) (8, Trubetskaya ul., Moscow, 119991, Russia); Senior Researcher, Laboratory of Legionellosis, N.F. Gamaleya National Research Center for Epidemiology and Microbiology (The Gamaleya National Center) (18, Gamaleya ul., Moscow, 123098, Russia). E-mail: droninayu@mail.ru, <https://orcid.org/0000-0002-6269-2108>

Anatoly S. Bykov, Dr. Sci. (Med.), Professor, Department of Virology and Immunology, I.M. Sechenov First Moscow State Medical University (Sechenov University) (8, Trubetskaya ul., Moscow, 119991, Russia). E-mail: 9153183256@mail.ru, <https://orcid.org/0000-0002-8099-6201>

Oxana A. Svitich, Corresponding Member of the Russian Academy of Sciences, Dr. Sci. (Med.), Head of the Federal State Budgetary Scientific Institution "I. Mechnikov Research Institute of Vaccines and Sera," Head of the Laboratory of Molecular Immunology, Federal State Budgetary Scientific Institution "I. Mechnikov Research Institute of Vaccines and Sera" (5A, Malyi Kazennyi pereulok, Moscow, 105064, Russia); Professor, Department of Microbiology, Virology and Immunology, I.M. Sechenov First Moscow State Medical University (Sechenov University) (8, Trubetskaya ul., Moscow, 119991, Russia). E-mail: svitichoa@yandex.ru, <https://orcid.org/0000-0003-1757-8389>

Vitaliy V. Zverev, Full Member of the Russian Academy of Sciences, Dr. Sci. (Biol.), Scientific Director of the Federal State Budgetary Scientific Institution "I. Mechnikov Research Institute of Vaccines and Sera" (5A, Malyi Kazennyi pereulok, Moscow, 105064, Russia); Head of the Department of Microbiology, Virology and Immunology, I.M. Sechenov First Moscow State Medical University (Sechenov University) (8, Trubetskaya ul., Moscow, 119991, Russia). E-mail: vitalyzverev@outlook.com, <https://orcid.org/0000-0002-0017-1892>

Об авторах:

Пашков Евгений Алексеевич, аспирант, кафедра микробиологии, вирусологии и иммунологии, Первый Московский государственный медицинский университет им. И.М. Сеченова Минздрава России (Сеченовский Университет), (119991, Россия, Москва, ул. Трубецкая, д. 8, с. 2); младший научный сотрудник, лаборатория молекулярной иммунологии, Научно-исследовательский институт вакцин и сывороток им. И.И. Мечникова (105064, Россия, Москва, Малый Казенный переулок, д. 5А). E-mail: pashckov.j@yandex.ru, <https://orcid.org/0000-0002-5682-4581>

Файзулов Евгений Бахтиёрович, к.б.н., заведующий лабораторией молекулярной вирусологии, Научно-исследовательский институт вакцин и сывороток им. И.И. Мечникова (105064, Россия, Москва, Малый Казенный переулок, д. 5А). E-mail: faizuloev@mail.ru, <https://orcid.org/0000-0001-7385-5083>

Корчевая Екатерина Романовна, младший научный сотрудник, лаборатория молекулярной вирусологии, Научно-исследовательский институт вакцин и сывороток им. И.И. Мечникова (105064, Россия, Москва, Малый Казенный переулок, д. 5А). E-mail: c.korchevaya@gmail.com, <https://orcid.org/0000-0002-6417-3301>

Ртищев Артём Андреевич, младший научный сотрудник, лаборатория РНК-содержащих вирусов, Научно-исследовательский институт вакцин и сывороток им. И.И. Мечникова (105064, Россия, Москва, Малый Казенный переулок, д. 5А). E-mail: rtishchevartyom@gmail.com, <https://orcid.org/0000-0002-4212-5093>

Черепович Богдан Сергеевич, младший научный сотрудник, лаборатория РНК-содержащих вирусов, Научно-исследовательский институт вакцин и сывороток им. И.И. Мечникова (105064, Россия, Москва, Малый Казенный переулок, д. 5А). E-mail: bogdancherepovich@mail.ru, <https://orcid.org/0000-0002-5803-6263>

Сидоров Александр Викторович, к.б.н., заведующий лабораторией ДНК-содержащих вирусов, Научно-исследовательский институт вакцин и сывороток им. И.И. Мечникова (105064, Россия, Москва, Малый Казенный переулок, д. 5А). E-mail: sashasidorov@yandex.ru, <https://orcid.org/0000-0001-8962-4765>

Поддубиков Александр Владимирович, к.б.н., заведующий лабораторией микробиологии условно-патогенных бактерий, Научно-исследовательский институт вакцин и сывороток им. И.И. Мечникова (105064, Россия, Москва, Малый Казенный переулок, д. 5А). E-mail: poddubikov@yandex.ru, <https://orcid.org/0000-0001-8962-4765>

Быстрицкая Елизавета Петровна, младший научный сотрудник, лаборатория молекулярной вирусологии, Научно-исследовательский институт вакцин и сывороток им. И.И. Мечникова (105064, Россия, Москва, Малый Казенный переулок, д. 5А). E-mail: lisabystritskaya@gmail.com, <https://orcid.org/0000-0001-8430-1975>

Дронина Юлия Евгеньевна, к.м.н., доцент кафедры микробиологии, вирусологии и иммунологии, Первый Московский государственный медицинский университет им. И.М. Сеченова Минздрава России (Сеченовский Университет), (119991, Россия, Москва, ул. Трубецкая, д. 8, с. 2); старший научный сотрудник, лаборатория легионеллеза, Национальный исследовательский центр эпидемиологии и микробиологии им. почетного академика Н.Ф. Гамалеи (123098, Россия, Москва, ул. Гамалеи, д. 18). E-mail: droninayu@mail.ru, <https://orcid.org/0000-0002-6269-2108>

Быков Анатолий Сергеевич, д.м.н., профессор кафедры микробиологии, вирусологии и иммунологии, Первый Московский государственный медицинский университет им. И.М. Сеченова Минздрава России (Сеченовский Университет), (119991, Россия, Москва, ул. Трубецкая, д. 8, с. 2). E-mail: 9153183256@mail.ru, <https://orcid.org/0000-0002-8099-6201>

Свитич Оксана Анатольевна, чл.-корр. РАН, д.м.н., директор, заведующий лабораторией молекулярной иммунологии, Научно-исследовательский институт вакцин и сывороток им. И.И. Мечникова (105064, Россия, Москва, Малый Казенный переулок, д. 5А); профессор кафедры микробиологии, вирусологии и иммунологии, Первый Московский государственный медицинский университет им. И.М. Сеченова Минздрава России (Сеченовский Университет), (119991, Россия, Москва, ул. Трубецкая, д. 8, с. 2). E-mail: svitichoa@yandex.ru, <https://orcid.org/0000-0003-1757-8389>

Зверев Виталий Васильевич, академик РАН, д.б.н., научный руководитель Научно-исследовательского института вакцин и сывороток им. И.И. Мечникова (105064, Россия, Москва, Малый Казенный переулок, д. 5А); заведующий кафедрой микробиологии, вирусологии и иммунологии, Первый Московский государственный медицинский университет им. И.М. Сеченова Минздрава России (Сеченовский Университет), (119991, Россия, Москва, ул. Трубецкая, д. 8, с. 2). E-mail: vitalyzverev@outlook.com, <https://orcid.org/0000-0002-0017-1892>

The article was submitted: October 30, 2021; approved after reviewing: November 13, 2021; accepted for publication: December 03, 2021.

Translated from Russian into English by H. Moshkov

Edited for English language and spelling by Enago, an editing brand of Crimson Interactive Inc.

**SYNTHESIS AND PROCESSING OF POLYMERS
AND POLYMERIC COMPOSITES**

**СИНТЕЗ И ПЕРЕРАБОТКА ПОЛИМЕРОВ
И КОМПОЗИТОВ НА ИХ ОСНОВЕ**

ISSN 2686-7575 (Online)

<https://doi.org/10.32362/2410-6593-2021-16-6-490-501>



UDK 678

RESEARCH ARTICLE

Influence of emulgator nature on dispersity and stability of artificial polymer suspensions based on polycarbonate and polymethyl methacrylate

Aleksandr N. Stuzhuk[@], Aleksandr V. Shkolnikov, Pavel S. Gorbatov, Inessa A. Gritskova

MIREA – Russian Technological University (M.V. Lomonosov Institute of Fine Chemical Technologies), Moscow, 119571 Russia

[@]Corresponding author, e-mail: aleksandr-stuzhuk@mail.ru

Abstract

Objectives. To create stable artificial polymer suspensions with a positive charge of particles based on polycarbonate and polymethyl methacrylate using cationic surfactants and organosilicon surfactants.

Methods. The size of droplets and polymer suspension particles was determined by photon correlation spectroscopy (dynamic light scattering) using a Zetasizer NanoZS laser particle analyzer (Malvern, UK).

Results. Domestic cationic surfactants Katamin-AB and Azol-129 were found to be capable of producing stable artificial polycarbonate and polymethyl methacrylate suspensions. Based on the polymer, the optimal surfactant concentration was 6 wt %. The effect of polymer concentration in solution on the stability and particle size of final polymer suspensions was shown. It was determined that the polymer concentration in the solution should not exceed 10%. When obtaining a highly dispersed suspension during dispersion, a higher concentration causes an increase in the viscosity of emulsions. As a result of a synergistic effect formation, we used mixtures of cationic surfactants (Katamin-AB/Azol-138 and Azol-129/Azol-138) to enhance the stability of the final polymer suspensions. The optimal surfactant ratio was 9:1. The total concentration of the mixture is 10 wt %, based on the polymer. Polymer suspensions were stabilized with each of 2:1 mixtures of cationic surfactants Katamin-AB and Azol-129 with an organosilicon surfactant U-851. The total mixture concentration was 9 wt %, based on the polymer.

Conclusions. *New methods of producing artificial polycarbonate and polymethyl methacrylate suspensions in the presence of domestically produced cationic surfactants, as well cationic-organosilicon surfactants mixtures, were proposed. The colloidal-chemical properties of the obtained polymer suspensions were considered. It was found that using a 2:1 mixture of cationic and organosilicon surfactants produces polymer suspensions that are stable during production and storage.*

Keywords: *organosilicon surfactants, artificial polymer suspension, cationic surfactants, polycarbonate, polymethyl methacrylate, structural and mechanical barrier*

For citation: Stuzhuk A.N., Shkolnikov A.V., Gorbatov P.S., Gritskova I.A. Influence of emulgator nature on dispersity and stability of artificial polymer suspensions based on polycarbonate and polymethyl methacrylate. *Tonk. Khim. Tekhnol. = Fine Chem. Technol.* 2021;16(6):490–501 (Russ., Eng.). <https://doi.org/10.32362/2410-6593-2021-16-6-490-501>

НАУЧНАЯ СТАТЬЯ

Влияние природы эмульгатора и концентрации полимера на дисперсность и устойчивость искусственных полимерных суспензий на основе поликарбоната и полиметилметакрилата

А.Н. Стужук[@], А.В. Школьников, П.С. Горбатов, И.А. Грицкова

МИРЭА – Российский технологический университет (Институт тонких химических технологий им. М.В. Ломоносова), Москва, 119571 Россия

[@]Автор для переписки, e-mail: aleksandr-stuzhuk@mail.ru

Аннотация

Цели. Создание агрегативно устойчивых искусственных полимерных суспензий с положительным зарядом частиц на основе поликарбоната и полиметилметакрилата с использованием катионных поверхностно-активных веществ (КПАВ), а также их смесей с кремнийорганическим поверхностно-активным веществом (КОПАВ).

Методы. Размер капель и частиц полимерных суспензий определяли методом фотонной корреляционной спектроскопии (динамического светорассеяния) с помощью лазерного анализатора частиц Zetasizer NanoZS (Malvern, Великобритания).

Результаты. Было установлено, что для получения устойчивых искусственных поликарбонатных и полиметилметакрилатных суспензий могут быть использованы отечественные КПАВ Катамин АБ и Азол-129. Оптимальная концентрация ПАВ составила 6 мас. % в расчете на полимер. Показано влияние концентрации полимера в растворе на устойчивость и размер частиц конечных полимерных суспензий. Определено, что концентрация полимера в растворе не должна превышать 10%. Дальнейшее повышение концентрации приводит к повышению вязкости эмульсий при получении высокодисперсной суспензии в процессе диспергирования. Использованы смеси КПАВ Катамин АБ/Азол-138 и Азол-129/Азол-138 для повышения устойчивости конечных полимерных суспензий за счет образования синергетического эффекта. Оптимальное массовое соотношение ПАВ составило 9:1. Общая концентрация смеси 10 мас. % в расчете на полимер. Получены полимерные суспензии, стабилизированные смесями КПАВ Катамин АБ/КОПАВ U-851 и КПАВ Азол-129/КОПАВ U-851 в соотношении 2:1 каждой смеси в расчете на полимер. Общая концентрация смеси составила 9 мас. % в расчете на полимер.

Выводы. Предложены новые способы получения искусственных поликарбонатных и полиметилметакрилатных суспензий, полученных в присутствии КПАВ отечественного производства, а также их смесей и смесей КПАВ с КОПАВ. Рассмотрены коллоидно-химические свойства полученных полимерных суспензий и показано, что при использовании смеси КПАВ и КОПАВ, взятых в объемном соотношении 2:1, образуются устойчивые в процессе получения и хранения полимерные суспензии.

Ключевые слова: кремнийорганические ПАВ, искусственная полимерная суспензия, катионные ПАВ, поликарбонат, полиметилметакрилат, структурно-механический барьер

Для цитирования: Стужук А.Н., Школьников А.В., Горбатов П.С., Грицкова И.А. Влияние природы эмульгатора и концентрации полимера на дисперсность и устойчивость искусственных полимерных суспензий на основе поликарбоната и полиметилметакрилата. *Тонкие химические технологии*. 2021;16(6):490–501. <https://doi.org/10.32362/2410-6593-2021-16-6-490-501>

INTRODUCTION

Recently, artificial polymer suspensions have become increasingly important because they are used in a wide range of industries, including the rubber industry (films, coatings, gloves, rubber threads, etc.), light industry (adhesives and textile materials), food industry (protective coatings on food), pulp and paper industry, construction industry (binders, sealants, compounds), agricultural industry (soil protection against erosion), and other industries.

Artificial polymer suspensions (artificial latexes) are obtained by emulsifying polymer solutions in an organic solvent in the presence of different surfactants, followed by replacing the organic phase with an aqueous phase, solvent distillation, and concentration to attain the required polymer content. In the preparation process, it is essential to maintain stability at all stages. For this, cationic surfactants of various structures are used. It is well established in the literature that combining different types of surfactants is the best way of obtaining stable polar polymer suspensions. The preparation of artificial polymer suspensions has not been described in the literature. It was best to rely on the fact that synthetic polar polymer suspension stability is characterized by high stability when using a mixture of different surfactants.

In this work, mixtures of different surfactants were used to enhance polymer suspension stability. This ensured the formation of structural-mechanical and electrostatic stabilization barriers, according to Rebinder [1].

This study aims at obtaining stable artificial polycarbonate and polymethyl methacrylate suspensions with a positive particle charge in the presence of cationic surfactants and their mixtures with other surfactants.

MATERIALS AND METHODS

The feedstocks selected were granular polycarbonate from the Makrolon brand (*Bayer*, Germany) and polymethyl methacrylate from the Acrypet VH 001 brand (*Mitsubishi Chemical Corporation*, Japan).

Without additional purification, chloroform (reagent grade) was used as a solvent.

The surfactants used were cationic surfactants synthesized at *Kotlas Chemical Plant*: Katamin AB (alkyldimethylbenzylammonium chloride, where alkyl is a mixture of normal C10–C16 alkyl radicals); Azol-129 (quaternary ammonium base of coconut oil *tert*-alkylamine acids and benzyl chloride with a hydrocarbon radical of coconut oil fatty acids C8–C14 as a substituent; active substance content is 75%); Azol-138 (*N,N,N*-trimethyl-*N*-(alkyl 12–14) ammonium methyl phosphite); Azol-139 (quaternary ammonium base from dicocoalkyldimethylamine and dimethyl phosphonate with a hydrocarbon radical of coconut oil fatty acids C12–C14). We also used an organosilicon surfactant (U-851 α,ω -bis[3-methylsiloxy]polydimethylmethyl-(10-carboxydecyl) siloxane) synthesized at the N.S. Enikolopov Institute of Synthetic Polymeric Materials of the Russian Academy of Sciences.

The size of droplets and polymer suspension particles was determined by photon correlation spectroscopy (dynamic light scattering) using a Zetasizer NanoZS laser particle analyzer (Malvern, UK) [2].

Dynamic light scattering (DLS) is a combination of the following phenomena: a change in frequency (Doppler shift) and an intensity and in motion direction of light transmitted through a medium of moving (Brownian) particles. It is a method for measuring particles that are up to 6 μm in diameter. The Brownian motion of particles is measured by DLS and correlated with their size. Elastic (Rayleigh) scattering occurs when a light beam passes through a suspension. In DLS, coherent and monochromatic laser radiation is used. The autocorrelation function, which is determined from the time variation of scattered radiation intensity, is the quantity being measured:

$$G(t_d) = 1/N \sum_r I(t_i)I(t_i - t_d) = (I(t)I(t - t_d)),$$

where $G(t_d)$ is the autocorrelation function; N is the number of measurements performed at time t_i ; $I(t_i - t_d)$ is the light scattering intensity after a certain delay time t_d .

Suspensions were prepared by combining a hydrocarbon phase (a polymer dissolved in a solvent) with a surfactant aqueous solution in a 1:1 ratio. The first stage involved using a magnetic stirrer to prepare a low-dispersed emulsion. The droplet size ranged from 20 to 100 μm . The second stage involves using a rotor-stator homogenizer DIAX-900 (Heidolph, Germany) to disperse a low-dispersed emulsion to obtain a highly dispersed emulsion. Dispersion

speed: 24000 rpm, dispersion time: 7–10 min. A rotary evaporator RV 10 (IKA, Germany) was used to distill the solvent.

RESULTS AND DISCUSSION

According to the published data, the emulsion dispersity (expressed by the polydispersity index, PdI), average particle diameter (d_{av}), and charge (ζ -potential) are the main parameters that determine suspensions stability [3–5].

Investigations began with the study of the colloidal-chemical properties of the polycarbonate (PC) and polymethyl methacrylate (PMMA) suspensions obtained in the presence of different cationic surfactants.

Artificial polymer suspensions were obtained using a 5% polymer solution. For the polymer, the concentration of the surfactant was 6 wt %.

Tables 1 and 2 and Figs 1 and 2 show the colloidal-chemical properties of the polycarbonate and polymethyl methacrylate suspensions obtained using Katamin AB and Azol-129 in different concentrations.

Table 1 and Fig. 1 show the number-average particle diameters of polycarbonate artificial polymer suspensions determined using Katamin AB, Azol-129, Azol-138, and Azol-139. The polymer suspension sample obtained using Katamin AB as a stabilizer had great stability, a narrow particle size distribution, and particle diameters ranging from 500 nm to 700 nm (80% of the particles by number). The samples stabilized with Azol-129 and Azol-138 had the largest diameter and particle size distribution. In the presence of Azol-139, it is impossible to obtain stable artificial polymer suspensions. A significant

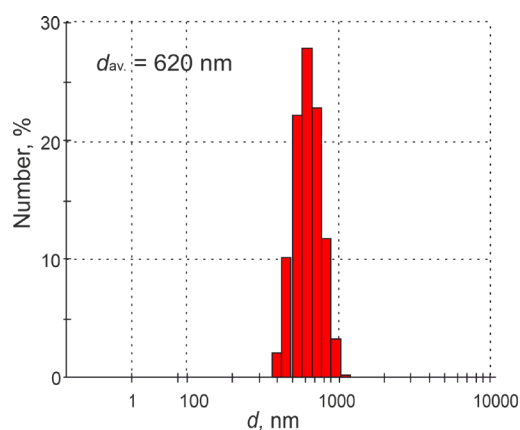
Table 1. Comparative analysis of the colloidal-chemical properties of artificial polycarbonate polymer suspensions stabilized by Katamin AB, Azol-129, Azol-138, and Azol-139, taken at different concentrations

Polymer	Surfactant	d_{av} , nm	PdI	ζ -potential, mV	Coagulum, wt %
PC	Katamin AB	620	0.140	+30	–
	Azol-129	830	0.290	+24	–
	Azol-138*	1050	0.330	+25	10
	Azol-139	–	–	–	100

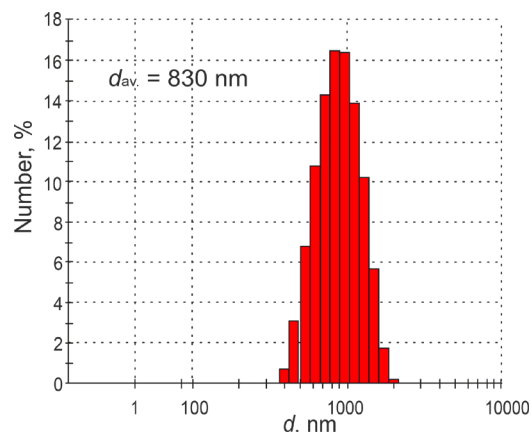
*The size of the coagulum-free polymer suspension.

Table 2. Comparative analysis of the colloidal-chemical properties of artificial polymethyl methacrylate PS stabilized by Katamin AB, Azol-129, Azol-138, and Azol-139

Polymer	Surfactant	d_{av} , nm	PdI	ζ -potential, mV	Coagulum, wt %
PMMA	Katamin AB	260	0.270	+39	–
	Azol-129	300	0.359	+28	–
	Azol-138	310	0.375	+23	–
	Azol-139	–	–	–	100



a



b

Fig. 1. The number-average particle size distributions of polycarbonate artificial polymer suspensions when used in the production process as a surfactant: (a) Katamin AB, (b) Azol-129.

part of the polymer coagulated when the solvent was removed under vacuum. This could be due to the poor stability of the particles in the presence of the atypical cationic surfactant with two alkyl radicals with a chain length of C12–C14 in the hydrophobic part of the surfactant molecule. The most stable suspensions were obtained using Katamin AB. The fact that it has a higher surface activity than the other stabilizers presented [6] explains this outcome.

Data on the stability of the polymethyl methacrylate polymer suspensions using different surfactants revealed that Katamin AB allows for the narrowest particle size distribution (Table 3 and Fig. 2).

The polymer concentration effect in the initial chloroform solution at all the preparation stages was evaluated using the final properties of the polymer suspensions. The polymer concentration in the solution was varied from 5% to 20% (Table 4).

As shown, the suspensions obtained using polymer solutions with concentrations of 5% and 10% are stable. The average particle diameters and PdI increase as polymer concentration increases.

The viscosity of solutions with a polymer concentration of more than 10% was high. As a result, polymer suspension emulsification, degassing, and concentration was difficult.

According to the literature, a synergistic effect, which significantly affects the colloidal-chemical properties of polymer suspensions, can occur when using mixtures of surfactants in a certain volume ratio of components [6].

Azol-129/Azol-138 and Katamin AB/Azol-138 were selected as the surfactant mixtures. The colloidal-chemical properties of the polymer suspensions obtained in the presence of these mixtures are presented in Tables 5 and 6 and Fig. 4.

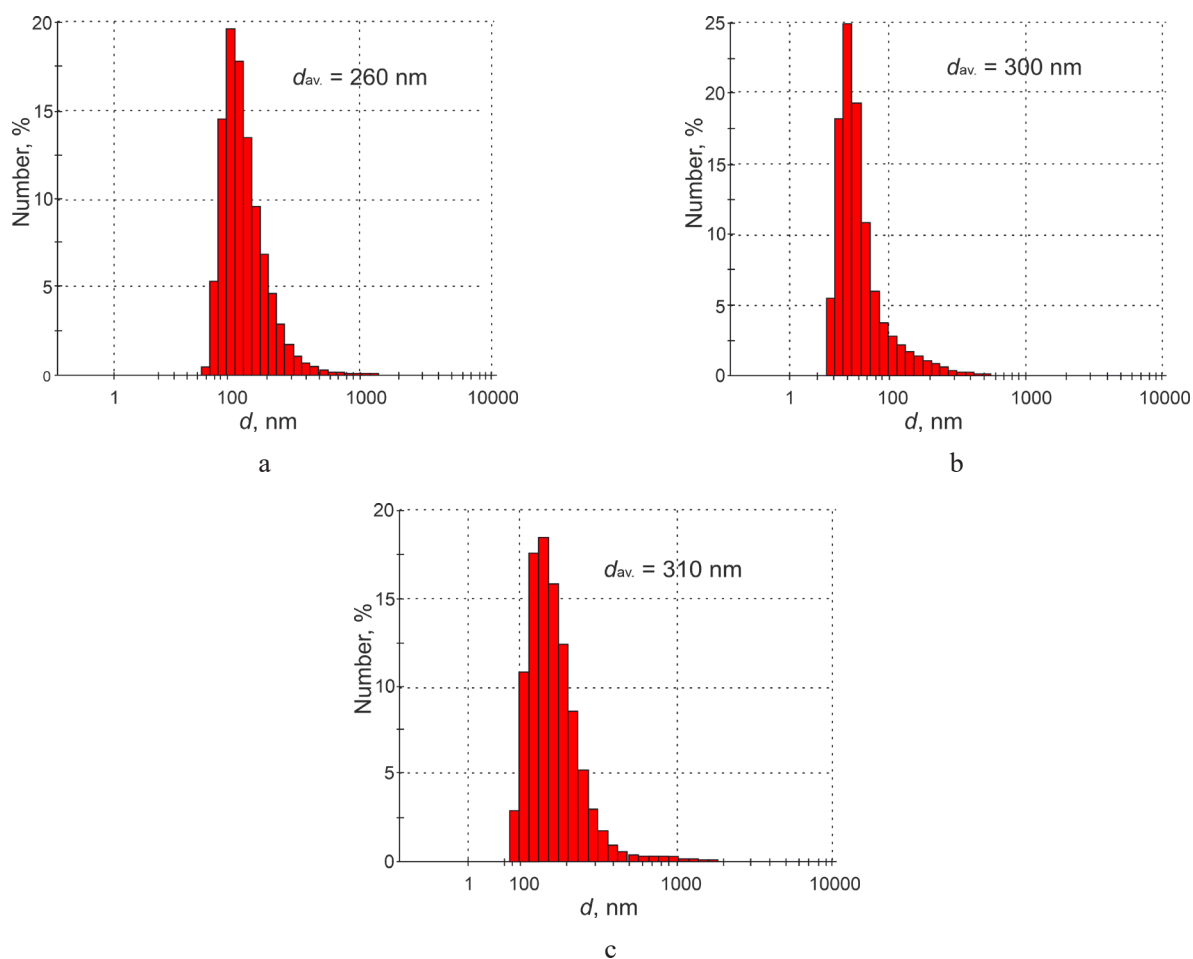


Fig. 2. The number-average particle size distributions of polymethyl methacrylate artificial polymer suspensions when the following surfactants were used in the production process: (a) Katamin AB, (b) Azol-129, and (c) Azol-138.

Table 3. The stability of artificial polycarbonate and polymethyl methacrylate polymer suspensions depending on the polymer concentration

Polymer concentration in solution	Stability in time	
	PC	PMMA
5	+	+
10	+	+
20	+/-	+/-

The conducted study reveals that it is necessary to use a mixture of surfactants Azol-129/Azol-138 and Katamin AB/Azol-138 in a ratio of 9:1, respectively, to achieve the maximum effect (to reduce the particle diameter). When using Azol-129/Azol-138 and Katamin AB/Azol-138 mixtures, there is a significant increase in stability compared to polymer suspensions where these surfactants are used separately.

Polymer suspensions stabilized with Azol-129 were characterized by low stability and an average particle diameter of about 800 nm. By adding one mass part of Azol-138 to the system, the polymer suspension stability was greatly improved, and the particle diameter was reduced to 580 nm. The addition of AB Azol-138 to Katamin AB allowed for a reduction in the average diameter (from 620 nm to 400 nm).

Table 4. Colloidal-chemical properties of polycarbonate suspensions stabilized using Katamin AB and obtained at various polymer concentrations in solution

Concentration, %	d_{av} , nm	<i>PdI</i>	Coagulum, wt %
5	620	0.140	–
10	1260	0.330	–
20	840	0.270	50

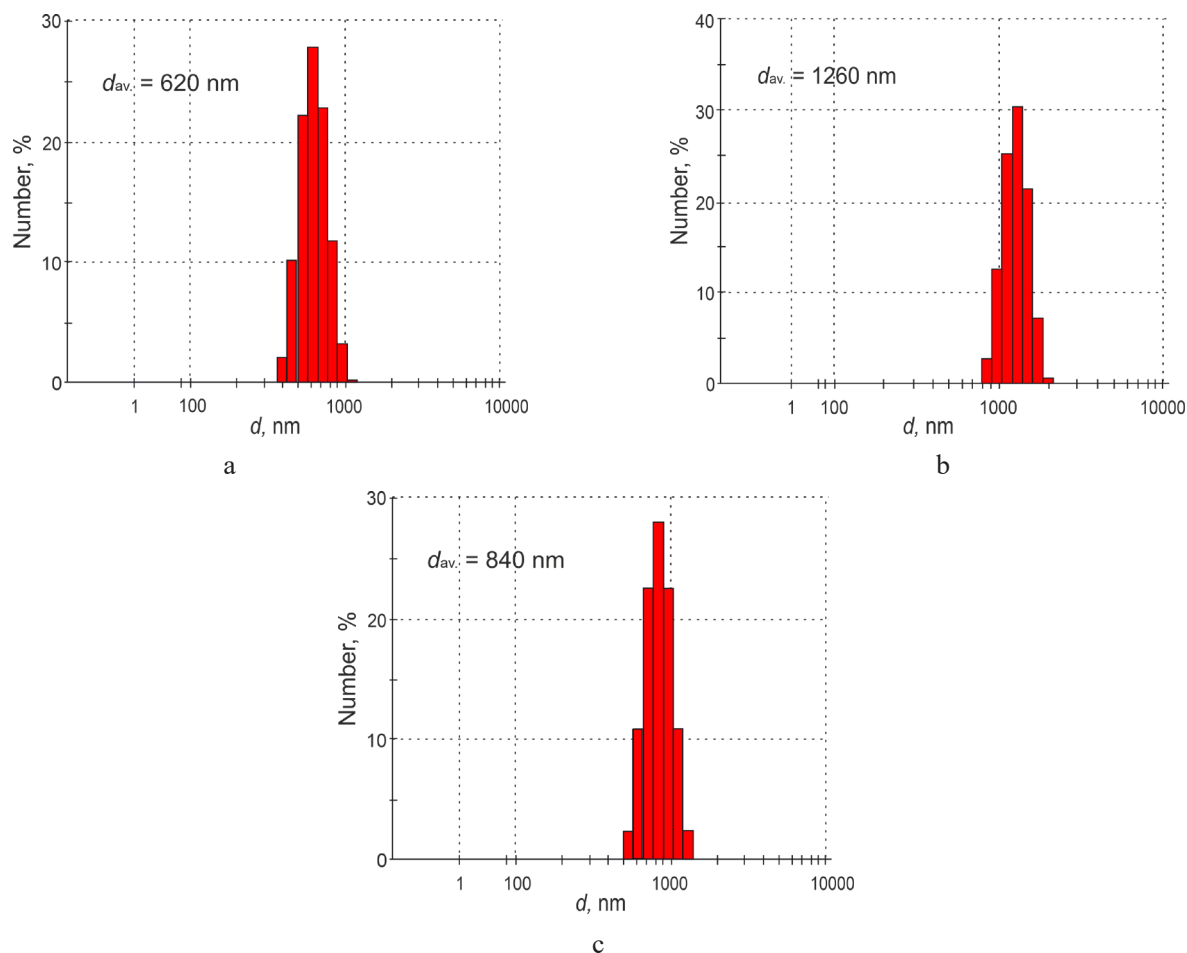
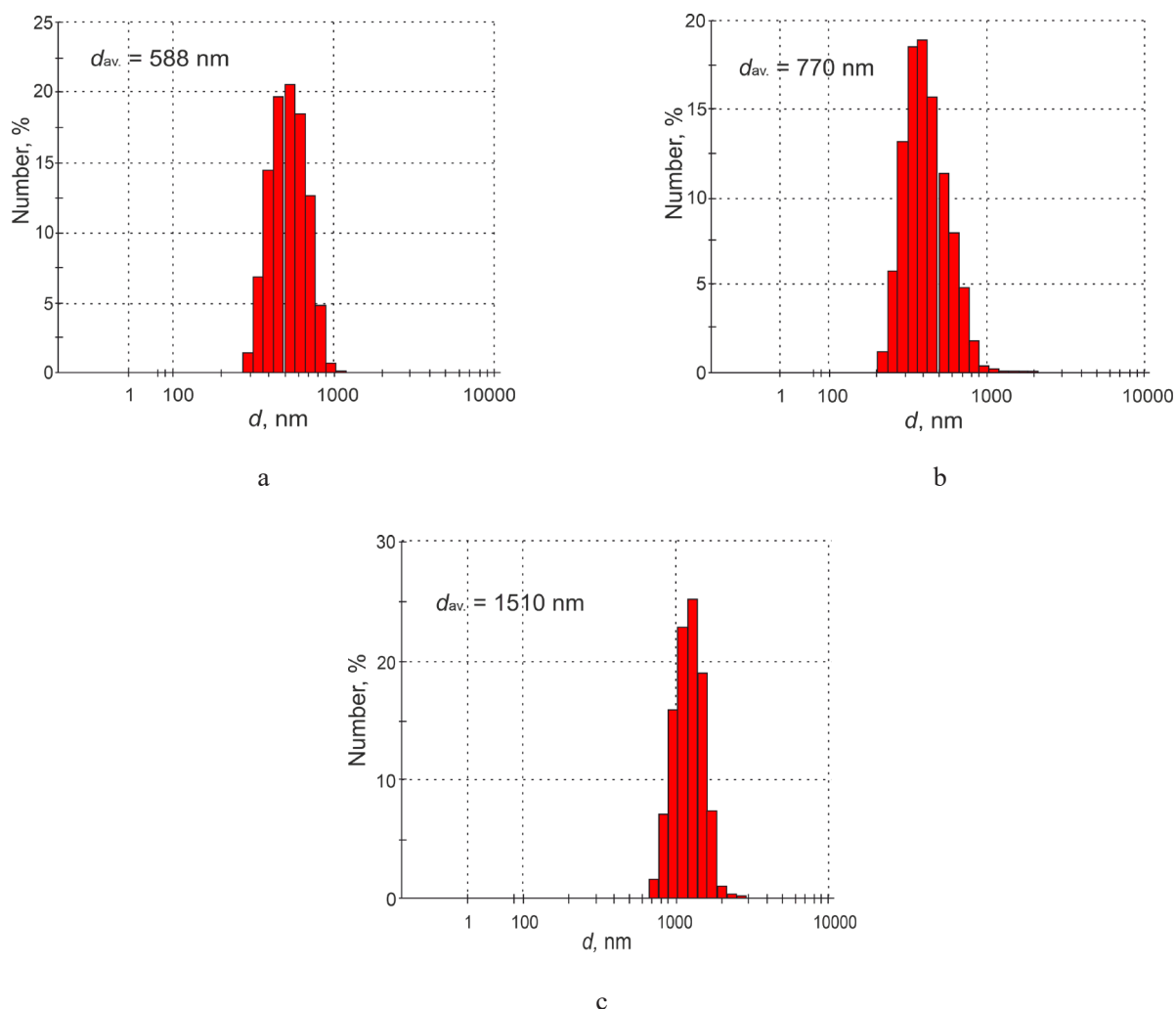

Fig. 3. Numerical distributions of particle size in polymer suspensions for the suspensions presented in Table 3: (a) 5%, (b) 10%, and (c) 20%.

Table 5. Colloidal-chemical properties of polycarbonate polymer suspensions obtained using varied ratios of the surfactants Azol-129/Azol-138

Surfactants	Surfactants ratio	d_{av} , nm	<i>PdI</i>	ζ -potential, mV	Coagulum, wt %
Azol-129/Azol-138	9:1	588	0.101	+22	нет no
Azol-129/Azol-138	3:1	770	0.331	+16	–
Azol-129/Azol-138	2:1	1510	0.255	+6	10

Table 6. Colloidal-chemical properties of polycarbonate polymer suspensions stabilized with Katamin AB/Azol-138 in different mass ratios

Surfactants	Surfactants ratio	d_{av} , nm	PdI	ζ -potential, mV	Coagulum, wt %
Katamin AB/Azol-138	9:1	402	0.136	+32	no
Katamin AB/Azol-138	3:1	607	0.320	+13	5
Katamin AB/Azol-138	2:1	694	0.382	+7	10

**Fig. 4.** Numerical distributions of polymer suspension particle size for suspensions presented in Table 4: (a) 9:1, (b) 3:1, and (c) 2:1.

Recently, there have been interests in water-insoluble organosilicon surfactants, owing to the possibility of obtaining aggregate-stable polymer suspensions through the polymerization of vinyl monomers [7, 8].

The formation of an interfacial adsorption layer on particle surfaces in their presence was found to be

different from that observed in the presence of water-soluble surfactants.

This difference is due to the formation of a thick strong interphase layer, which is due to the adsorption of a water-insoluble surfactant from the monomer phase. These results were demonstrated when studying the colloidal-chemical properties of different organosilicon surfactants [9–16].

Carboxyl-containing organosilicon surfactant α,ω -bis(trimethylsiloxy-oligodimethylmethyl-(10-carboxydecyl)siloxane (U-851) and its mixture with the cationic surfactants Azol-129 and Katamin AB were used.

The surfactants mixture had a concentration of 9 wt % calculated for the polymer, with a cationic surfactant/organosilicon surfactant ratio of 2:1. The concentration of U-851 was calculated to be 3 mass fractions for the polymer.

In these works, it was found that the formation of an interfacial adsorption layer on the surface of particles in their presence is fundamentally different from that observed in the presence of water-soluble surfactants [3,7].

To obtain stable polymer suspensions, we used a mixture of the cationic surfactants Katamin AB and Azol-129 with the carboxyl-containing organosilicon surfactant U-851.

The surfactants mixture had a concentration of 9 mass fractions calculated for the polymer, with a cationic surfactant/organosilicon surfactant ratio of 2:1. The concentration of the surfactant U-851 in the suspension stabilized only with it was 6 mass fractions calculated for the polymer.

The stability properties of the obtained suspensions and their colloidal-chemical properties are presented in Tables 7 and 8 and Fig. 5.

Table 7. Stability of polycarbonate suspensions over time when a mixture of a cationic surfactant and an organosilicon surfactant is used

Surfactant	Stability over time
Katamin AB/U-851	+
Azol-129/U-851	+
U-851	-

Table 8. Colloidal-chemical properties of artificial polycarbonate suspensions obtained using U-851 and its mixture with a cationic surfactant

Surfactant	d_{av} , nm	<i>PdI</i>	ζ -potential, mV	Coagulum, wt %
Katamin AB/U-851	360	0.240	+32	-
Azol-129/U-851	410	0.287	+25	-
U-851	-	-	-	100

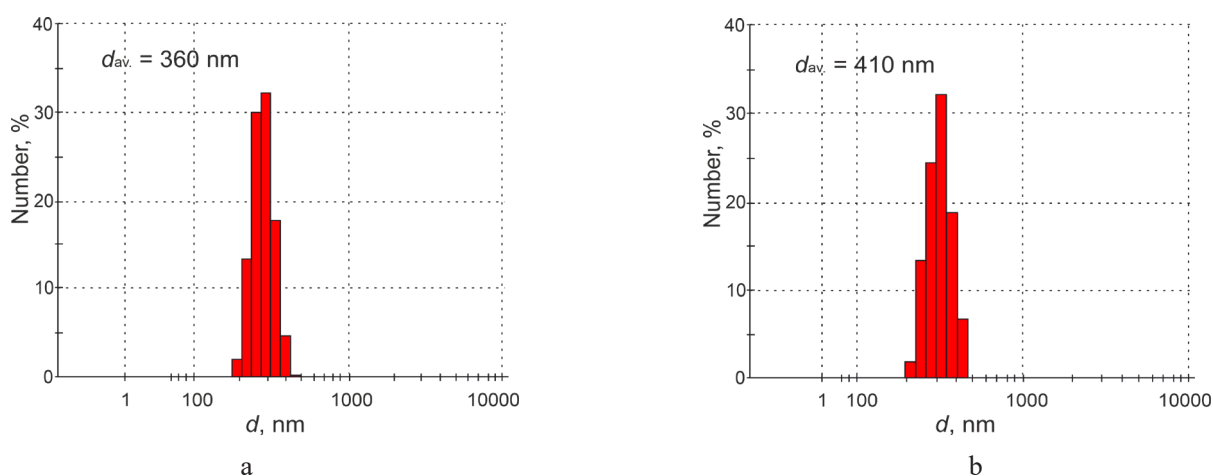


Fig. 5. Numerical distributions of polycarbonate suspensions particle sizes depending on the choice of surfactant mixtures: (a) Katamin AB/U-851 and (b) Azol-129/U-851.

Both suspensions were characterized by a rather narrow particle size distribution, with an average particle diameter of 360 nm and a charge of +32 mV for the Katamin AB/U-851 mixture, and an average particle diameter of 410 nm and a charge of 25 mV for the Azol-129/U-851 mixture.

CONCLUSIONS

The article proposed a methodology for obtaining stable artificial polycarbonate and polymethyl methacrylate polymer suspensions with a positive particle charge. It was shown that to obtain them, domestically produced cationic surfactants with a concentration of 6 wt % calculated for the polymer can be used. It is proposed to use a 9:1 mixture of surfactants: Azol-129 and Azol-138; Katamin AB and Azol-138, with a total surfactant concentration of 10 wt % calculated for the polymer to form a more durable electrostatic stability barrier in the interfacial adsorption layers. It is possible to increase stability over time using Katamin AB/U-851 and Azol-129/U-851 mixtures because of the formation of structural-mechanical and electrostatic stability

barriers in the interfacial adsorption layers of polymer particles.

Acknowledgments

The reported study was funded by the Russian Foundation for Basic Research, project No. 19-33-90128\19.

Authors' contributions

A.N. Stuzhuk – development of a method for obtaining aggregate-stable artificial polymethylmethacrylate and polycarbonate suspensions with a positive charge of particles, writing and editing the text of the article, and preparing a manuscript for publication;

A.V. Shkolnikov – collecting and processing the material, synthesis of aggregate-stable artificial polymethyl methacrylate and polycarbonate suspensions with a positive particle charge;

P.S. Gorbatov – synthesis of artificial polymethylmethacrylate suspensions with a positive particle charge, and statistical processing of research results;

I.A. Gritskova – developing the scientific concept, offering consultation on the research methodology, writing and editing the text of the article.

The authors declare no conflicts of interest.

REFERENCES

- Manson J., Sperling L. *Polimernye smesi i kompozity (Polymer mixtures and composites: trans. from Engl.)*. Godowsky Yu.K. (Ed.). Moscow: Khimiya; 1979. 440 p. (in Russ.).
[Manson J., Sperling L. *Polymer blends and composites*. NY: Plenum Press; 1976. 513 p.]
- Tscharnuter W. Photon correlation spectroscopy in particle sizing. In: Meyers R.A. (Ed.) *Encyclopedia of Analytical Chemistry*. 2000. P. 5469–5485.
- Gritskova I.A., Kopylov V.M., Simakova G.A., Gusev S.A., Markuze I.Yu. Polymerization of styrene in the presence of surface-active organosilicon substances of various nature. *Polym. Sci. Ser. B*. 2010;52(9):1689–1695. <https://doi.org/10.1134/S1560090410090046>
- Gritskova I.A., Botova O.I., Shitov R.O., Grinfeld E.A. Preparation of artificial latexes based on isoprene-styrene thermoplastic elastomers. *Fine Chemical Technologies*. 2014;9(5):61–63 (in Russ.)
- Larsson M., Hill A., Duffy J. Suspension stability; why particle size, zeta potential and rheology are important. *Annu. Trans. Nord. Rheol. Soc.* 2012;12:209–214.
- Holmberg K., Jönsson Yu., Kronberg B., Lindman B. *Poverkhnostno-aktivnye veshchestva i polimery v vodnykh rastvorakh (Surfactants and polymers in aqueous solutions)*. Moscow: Laboratoriya znaniy; 2020. 531 p. (in Russ.). ISBN 978-5-00101-767-7

СПИСОК ЛИТЕРАТУРЫ

- Мэнсон Дж., Сперлинг Л. *Полимерные смеси и композиты*: пер. с англ., под ред. Ю.К. Годовского. М.: Химия; 1979. 440 с.
- Tscharnuter W. Photon correlation spectroscopy in particle sizing. In: Meyers R.A. (Ed.) *Encyclopedia of Analytical Chemistry*. 2000. P. 5469–5485.
- Грицкова И.А., Копылов В.М., Симакова Г.А., Гусев С.А., Маркузе И.Ю. Полимеризация стирола в присутствии поверхностно-активных кремнийорганических веществ различной природы. *Высокомолекулярные соединения. Серия Б*. 2010;52(9):1689–1695.
- Грицкова И.А., Ботова О.И., Шитов Р.О., Гринфельд Е.А. Получение искусственных латексов на основе изопрен-стирольного термоэластопласта. *Тонкие химические технологии*. 2014;9(5):61–63.
- Larsson M., Hill A., Duffy J. Suspension stability; why particle size, zeta potential and rheology are important. *Annu. Trans. Nord. Rheol. Soc.* 2012;12:209–214.
- Холмберг К., Йёнссон Ю., Кронберг Б., Линдман Б. *Поверхностно-активные вещества и полимеры в водных растворах*. М.: Лаборатория знаний; 2020. 531 с. ISBN 978-5-00101-767-7
- Жданов А.А., Грицкова И.А., Чирикова О.В., Щеголихина О.И. Кремнийорганические ПАВ – стабилизаторы частиц полистирольных суспензий. *Коллоидный журнал*. 1995;57(1):30–33.

- [Holmberg K., Jönsson Yu., Kronberg B., Lindman B. *Surfactants and polymers in aqueous solutions*. John Wiley & Sons; 2003. 562 p.]
7. Zhdanov A.A., Gritskova I.A., Chirikova O.V., Shegolikina O.I. Organosilicon surfactants as stabilizers of polystyrene suspensions particles. *Kolloidnyi zhurnal = Colloid J.* 1995;57(1):30–33 (in Russ.).
 8. Semchikov Yu.D. *Vysokomolekulyarnye soedineniya (High-molecular compounds)*. Moscow, N. Novgorod: NSTU: Publishing Center "Academy"; 2003. 368 p. (in Russ.).
 9. Lee V.Ya. *Organosilicon Compounds: Theory and Experiment (Synthesis)*. Academic Press; 2017. 758 p. ISBN 978-0-12-801981-8
 10. Salages J.L. Surfactants. Types and Uses. FIRP Booklet 300 A; 2002. 49 p. URL: <https://dokumen.tips/documents/surfactants-types-and-uses.html>
 11. Srividhya M., Chandrasekar K., Baskar G., Reddy B.S.R., Physico-chemical properties of siloxane surfactants in water and their surface energy characteristics. *Polymer.* 2007;48(5):1261–1268. <https://doi.org/10.1016/j.polymer.2007.01.015>
 12. Curstedt T., Calkovska A., Johansson J. New Generation Synthetic Surfactants. *Neonatology.* 2013;103(4): 327–330. <https://doi.org/10.1159/000349942>
 13. Shinoda K., Nakagawa T., Tamamushi B., Isemura T. *Kolloidnye poverhnostno-aktivnye veshchestva. Fiziko-khimicheskie svoistva (Colloidal Surfactants. Some Physicochemical Propertiestrans: trans. from Engl.)*. Taubman A.B. (Ed.). Moscow: Mir; 1966. 319 p. (in Russ.).
 - [Shinoda K., Nakagawa T., Tamamushi B., Isemura T. *Colloidal Surfactants: Some Physicochemical Propertiestrans*. New-York: Academic Press; 1963. 310 p. ISBN 978-1-4832-2923-2]
 14. Zimon A.D. *Adgeziya zhidkosti i smachivanie*. M.: Himiya; 1974. 416 p. (in Russ.).
 15. Liu J., Zhang F.F., Song Y.H., Lv K. Zhang N., Li Y.C. The synthesis of nonionic hyperbranched organosilicone surfactant and characterization of its wetting ability. *Coatings.* 2021;11(1). <https://doi.org/10.3390/coatings11010032>
 16. Aveyard B. *Surfactants. In: Solution, at Interfaces and in Colloidal Dispersions*. Oxford, New-York: Oxford University Press; 2019. 576 p. ISBN 978-0-19-882860-0
 8. Семчиков Ю.Д. *Высокомолекулярные соединения*. Москва, Н. Новгород: Изд-во НГТУ: Издательский центр «Академия»; 2008. 368 с. ISBN 978-5-7695-5389-9,5-7695-3028-6.
 9. Lee V.Ya. *Organosilicon Compounds: Theory and Experiment (Synthesis)*. Academic Press; 2017. 758 p. ISBN 978-0-12-801981-8
 10. Саладжес Д.Л. Поверхностно-активные вещества – виды и применение. Буклет FIRP 300 A, 2002. 49 с.
 11. Srividhya M., Chandrasekar K., Baskar G., Reddy B.S.R., Physico-chemical properties of siloxane surfactants in water and their surface energy characteristics. *Polymer.* 2007;48(5):1261–1268. <https://doi.org/10.1016/j.polymer.2007.01.015>
 12. Curstedt T., Calkovska A., Johansson J. New Generation Synthetic Surfactants. *Neonatology.* 2013;103(4): 327–330. <https://doi.org/10.1159/000349942>
 13. Шинода К., Накагава Т., Тамамуси Б., Исемура Т. *Коллоидные поверхностно-активные вещества*. пер. с англ., под ред. А.Б. Таубмана, М.: Мир, 1966. 319 с.
 14. Зимон А.Д. *Адгезия жидкости и смачивание*. М.: Химия; 1974. 416 с.
 15. Liu J., Zhang F.F., Song Y.H., Lv K. Zhang N., Li Y.C. The synthesis of nonionic hyperbranched organosilicone surfactant and characterization of its wetting ability. *Coatings.* 2021;11(1). <https://doi.org/10.3390/coatings11010032>
 16. Aveyard B. *Surfactants: In Solution, at Interfaces and in Colloidal Dispersions*. Oxford, New-York: Oxford University Press; 2019. 576 p. ISBN 978-0-19-882860-0

About the authors:

Alexander N. Stuzhuk, Postgraduate Student, S.S. Medvedev Department of Chemistry and Technology of Macromolecular Compounds, M.V. Lomonosov Institute of Fine Chemical Technologies, MIREA – Russian Technological University (86, Vernadskogo pr., Moscow, 119571, Russia). E-mail: aleksandr-stuzhuk@mail.ru. <http://orcid.org/0000-0001-6593-3045>

Alexander V. Shkolnikov, Postgraduate Student, S.S. Medvedev Department of Chemistry and Technology of Macromolecular Compounds, M.V. Lomonosov Institute of Fine Chemical Technologies, MIREA – Russian Technological University (86, Vernadskogo pr., Moscow, 119571, Russia). E-mail: sashka513@mail.ru. <https://orcid.org/0000-0002-3320-3344>

Pavel S. Gorbatov, Postgraduate Student, S.S. Medvedev Department of Chemistry and Technology of Macromolecular Compounds, M.V. Lomonosov Institute of Fine Chemical Technologies, MIREA – Russian Technological University (86, Vernadskogo pr., Moscow, 119571, Russia). E-mail: refazer@mail.ru. <https://orcid.org/0000-0003-4925-7176>

Inessa A. Gritskova, Dr. Sci. (Chem.), Professor, S.S. Medvedev Department of Chemistry and Technology of Macromolecular Compounds, M.V. Lomonosov Institute of Fine Chemical Technologies, MIREA – Russian Technological University (86, Vernadskogo pr., Moscow, 119571, Russia). E-mail: inessagritskova@gmail.com. <http://orcid.org/0000-0002-4358-1998>

Об авторах:

Стужук Александр Николаевич, аспирант кафедры химии и технологии высокомолекулярных соединений Института тонких химических технологий им. М.В. Ломоносова ФГБОУ ВО «МИРЭА – Российский технологический университет» (119571, Россия, Москва, пр-т Вернадского, д. 86). E-mail: aleksandr-stuzhuk@mail.ru. <http://orcid.org/0000-0001-6593-3045>

Школьников Александр Васильевич, аспирант кафедры химии и технологии высокомолекулярных соединений Института тонких химических технологий им. М.В. Ломоносова ФГБОУ ВО «МИРЭА – Российский технологический университет» (119571, Россия, Москва, пр-т Вернадского, д. 86). E-mail: sashka513@mail.ru. <https://orcid.org/0000-0002-3320-3344>

Горбатов Павел Сергеевич, аспирант кафедры химии и технологии высокомолекулярных соединений Института тонких химических технологий им. М.В. Ломоносова ФГБОУ ВО «МИРЭА – Российский технологический университет» (119571, Россия, Москва, пр-т Вернадского, д. 86). E-mail: refazer@mail.ru. <https://orcid.org/0000-0003-4925-7176>

Грицкова Инесса Александровна, д.х.н., профессор кафедры химии и технологии высокомолекулярных соединений Института тонких химических технологий им. М.В. Ломоносова ФГБОУ ВО «МИРЭА – Российский технологический университет» (119571, Россия, Москва, пр-т Вернадского, д. 86). E-mail: inessagritskova@gmail.com. <http://orcid.org/0000-0002-4358-1998>

The article was submitted: August 18, 2021; approved after reviewed: October 27, 2021; accepted for publication: November 22, 2021.

Translated from Russian into English by M. Povorin

Edited for English language and spelling by Enago, an editing brand of Crimson Interactive Inc.

ISSN 2686-7575 (Online)

<https://doi.org/10.32362/2410-6593-2021-16-6-502-511>



UDC 546.723 + 661.872.2

RESEARCH ARTICLE

Heterophase synthesis of cobalt ferrite

Elena E. Nikishina

MIREA – Russian Technological University (M.V. Lomonosov Institute of Fine Chemical Technologies),
Moscow, 119571 Russia

@Corresponding author, e-mail: nikishina@mirea.ru

Abstract

Objectives. The study aimed to develop new methods for the synthesis of cobalt ferrite (CoFe_2O_4), which is a precursor for the synthesis of CoFe_2O_4 -based functional materials, as well as to study the physicochemical properties of the obtained phases.

Methods. Two methods were used for the synthesis of CoFe_2O_4 : (1) heterophase interaction of hydrated iron oxide with cobalt(II, III) oxide and (2) heterophase interaction of hydrated iron oxide with an aqueous solution of cobalt(II) sulfate ($C_{\text{Co}} = 0.147 \text{ mol/L}$, solid/liquid = 1:43). In both cases, the precursor was hydrated iron oxide (Fe_2O_3 , 84.4 wt %), which was obtained by the heterophase interaction of iron(III) chloride with a concentrated ammonia solution (6.0–9.5 mol/L). The resulting intermediate products were subjected to thermal treatment at 750°C (synthesis **1**) and at 900°C (synthesis **2**) for 10–30 h in increments of 10 h. The synthesized phases and products of their thermolysis were studied by differential thermal analysis and differential thermogravimetry (DTA–DTG), X-ray diffraction analysis (XRDA), and granulometry.

Results. The hydrated iron oxide sample remained amorphous even up to the crystallization temperature of 445°C, which corresponds to the exothermic effect on the DTA curve. Further heating led to the α -modification of iron(III) oxide of the hexagonal system ($a = b = 5.037 \pm 0.002 \text{ \AA}$; $c = 13.74 \pm 0.01 \text{ \AA}$), which has an average particle size of 1.1 μm . XRDA results showed that a synthesis temperature of 750°C (synthesis **1**) and a heat treatment duration of 30 h were sufficient for the formation of a single-phase cobalt ferrite ($a = 8.388 \pm 0.002 \text{ \AA}$) with an average particle diameter of 1.9 μm . For synthesis **2**, a higher temperature of 900°C was

used because sample weight loss (about 12.5%) was observed in the temperature range of 720–810 °C based on the DTA results, which was due to the removal of SO_2 and SO_3 . Moreover, when synthesis temperature and duration were at 900 °C and 30 h, respectively, CoFe_2O_4 with $a = 8.389 \pm 0.002 \text{ \AA}$ was formed. The results of the granulometric analysis showed that particles of different diameters were formed. The smallest particle size (1.5 μm) of cobalt ferrite was obtained by the heterophase interaction of hydrated iron(III) oxide (Fe_2O_3 , 84.4 wt %) with an aqueous solution of cobalt sulfate with $C_{\text{Co}} = 0.147 \text{ mol/L}$.

Conclusions. Depending on the method used for the synthesis of cobalt ferrite, particles of different diameters are formed. The smallest particle size of cobalt ferrite was obtained from the heterophase interaction of hydrated iron(III) oxide with an aqueous solution of cobalt(II) sulfate.

Keywords: iron, cobalt, ferrite, oxides, thermal analysis, X-ray phase analysis, particle size analysis

For citation: Nikishina E.E. Heterophase synthesis of cobalt ferrite. *Tonk. Khim. Tekhnol. = Fine Chem. Technol.* 2021;16(6):502–511 (Russ., Eng.). <https://doi.org/10.32362/2410-6593-2021-16-6-502-511>

НАУЧНАЯ СТАТЬЯ

Гетерофазный синтез феррита кобальта

Е.Е. Никишина

МИРЭА – Российский технологический университет (Институт тонких химических технологий им. М.В. Ломоносова), Москва, 119571 Россия

@Автор для переписки, e-mail: nikishina@mirea.ru

Аннотация

Цели. Разработка новых методов синтеза феррита кобальта (CoFe_2O_4), являющегося предшественником для синтеза функциональных материалов на его основе, а также исследование физико-химических свойств полученных фаз.

Методы. Гидратированный оксид железа и феррит кобальта получали гетерофазным методом. Синтезированные фазы и продукты их термолиты изучали методами дифференциально-термического анализа и дифференциальной термогравиметрии (ДТА–ДТГ), рентгенофазового анализа (РФА) и гранулометрии.

Результаты. В статье изложены результаты двух методов синтеза феррита кобальта (CoFe_2O_4) и исследования полученных фаз. В обоих случаях в качестве предшественника выступал гидратированный оксид железа(III) с содержанием Fe_2O_3 – 84.4 мас. %, полученный гетерофазным взаимодействием хлорида железа(III) с концентрированным раствором аммиака (6.0–9.5 моль/л). Первый способ заключался во взаимодействии гидратированного оксида железа(III) с оксидом кобальта(II, III), второй – во взаимодействии гидратированного оксида железа(III) с водным раствором сульфата кобальта(II) с концентрацией $C_{\text{Co}} = 0.147 \text{ моль/л}$ ($T : \text{Ж} = 1 : 43$). Получившиеся промежуточные продукты подвергали термической обработке при 750 °C (синтез **1**) и 900 °C (синтез **2**) в течение 10–30 ч с шагом 10 ч.

Выводы. Феррит кобальта (CoFe_2O_4) получен двумя способами. С использованием комплекса методов (РФА, ДТА–ДТГ, гранулометрии) исследованы физико-химические свойства синтезированных образцов. Установлено, что гидратированный оксид железа(III) вплоть до температуры кристаллизации ($445\text{ }^\circ\text{C}$), соответствующей экзотермическому эффекту на кривой ДТА, остается рентгеноаморфным. Дальнейшее нагревание его приводит к образованию α -модификации оксида железа(III) гексагональной сингонии ($a = b = 5.037 \pm 0.002\text{ \AA}$; $c = 13.74 \pm 0.01\text{ \AA}$), средний размер частиц которой равен 1.1 мкм . Согласно данным РФА, в синтезе **1** при $750\text{ }^\circ\text{C}$ и продолжительности термообработки 30 ч образуется однофазный феррит кобальта ($a = 8.388 \pm 0.002\text{ \AA}$) со средним диаметром частиц 1.9 мкм . В интервале температур $720\text{--}810\text{ }^\circ\text{C}$ в образце наблюдается убыль массы (около 12.5%), связанная с удалением SO_2 и SO_3 . Поэтому в синтезе **2** температуру нагревания увеличивали до $900\text{ }^\circ\text{C}$. Показано, что при $900\text{ }^\circ\text{C}$ и продолжительности синтеза 30 ч также образуется феррит кобальта (CoFe_2O_4) ($a = 8.389 \pm 0.002\text{ \AA}$). Результаты гранулометрического анализа указывают на зависимость диаметра образующихся частиц от способа получения феррита кобальта. Наименьший размер частиц (1.5 мкм) обнаружен у феррита кобальта, полученного гетерофазным взаимодействием гидратированного оксида железа(III) ($\text{Fe}_2\text{O}_3 - 84.4\text{ мас. \%}$) с водным раствором сульфата кобальта с концентрацией $C(\text{Co}^{2+}) = 0.147\text{ моль/л}$.

Ключевые слова: железо, кобальт, феррит, оксиды, термический анализ, рентгенофазовый анализ, гранулометрический анализ

Для цитирования: Никишина Е.Е. Гетерофазный синтез феррита кобальта. Тонкие химические технологии. 2021;16(6):502–511. <https://doi.org/10.32362/2410-6593-2021-16-6-502-511>

INTRODUCTION

Due to their unique properties, spinel-structured ferrites are widely used in various fields of science and technology. This class of magnetic ceramics is used in various applications, such as information storage systems, magnetic fluids, gas sensors, catalysts, rechargeable lithium batteries, magnetic cores, microwave absorbers, medical diagnostics and therapy, wastewater treatment, and biosensors [1–7].

The ferrite formula can be represented as AB_2O_4 . It has a spinel structure (Fig. 1), where the tetrahedral A-position is occupied by ions in the oxidation state of +2 (e.g., Mg^{2+} , Fe^{2+} , Ni^{2+} , Co^{2+} , and Mn^{2+}). The octahedral B-position is mainly occupied by Fe^{3+} ions, but they can be replaced by other ions in the oxidation state of +3 (e.g., Al^{3+} , Cr^{3+}). If the A-position is occupied by ions in the +3 oxidation state and the B-position is equally populated by ions in the +2 and +3 oxidation states, the spinel structure is called reversed [8, 9].

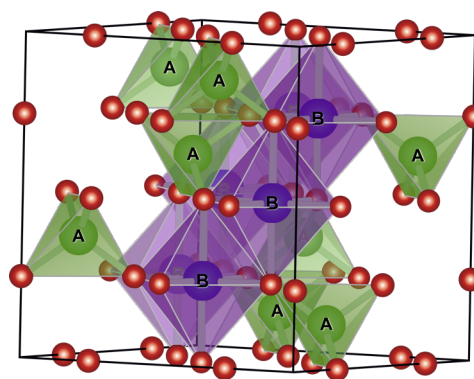


Fig. 1. Ferrite spinel structure [9].

One of the representatives of this class of materials is cobalt ferrite (CoFe_2O_4), a well-known magnetic hard material with a high coercive force associated with a small size of crystalline grains and strong magnetocrystalline

anisotropy and moderate magnetization. It has an inverted spinel structure, where all or most of the Co^{2+} ions occupy an octahedral B-position and Fe^{3+} ions occupy both tetrahedral (A) and octahedral (B) positions.

These properties, along with high chemical stability, make it possible to use cobalt ferrite in various applications, such as medicine, catalysis, magnetic data carriers in audio and video cassettes, high-density digital recording discs, various sensors, recording devices, and solar cells [10–13]. The purpose of this work was to develop methods for the synthesis of cobalt ferrite, which is a precursor for the synthesis of CoFe_2O_4 -based functional materials, as well as to study the physicochemical properties of the obtained phases.

MATERIALS AND METHODS

Iron(III) chloride hexahydrate, which was used as the starting material in the study, cobalt(II, III) oxide, and cobalt sulfate were supplied by *Merck*, Germany, while aqueous ammonia was sourced from *Himmed*, Russia.

Hydrated iron(III) oxide was obtained by the heterophase interaction of iron(III) chloride with a concentrated solution of ammonia hydrate (6.0–9.5 mol/L).

Cobalt ferrite was synthesized using two heterophase synthesis methods.

Synthesis 1. Samples of hydrated iron(III) oxide and cobalt(II,III) oxide in the ratio of 1.5:1 were placed in a glass flask with a lapped stopper. The hydrated iron oxide to cobalt oxide ratio used was based on the oxide content of hydrated iron oxide and CoFe_2O_4 . Distilled water was poured into the flask with the substance, and the flask containing the reaction mixture was shaken on a vibrating apparatus at room temperature ($22 \pm 2^\circ\text{C}$) for 10 h. The resulting suspension was transferred to a crucible and subjected to slow evaporation. Then, the intermediate product obtained was subjected to heat treatment at 750°C for 10–30 h in increments of 10 h.

Synthesis 2. A suspension of hydrated iron(III) oxide was placed in a glass flask with a lapped stopper, to which a solution of cobalt(II) sulfate with $C_{\text{Co}} = 0.147$ mol/L (solid/liquid = 1:43) was added. Then, the flask was shaken on a vibrating apparatus at room temperature for 10 h. The resulting suspension was transferred to a crucible and subjected to slow evaporation, and the intermediate product obtained was subjected to heat treatment at 900°C for 30 h in increments of 10 h.

The oxide content in hydrated iron(III) oxide was determined by gravimetric analysis.

Differential thermal analysis and differential thermogravimetry (DTA–DTG) of the samples was conducted on a Q-1500 D air derivatograph (*MOM*, Hungary) with simultaneous recording of four curves: differential (DTA), temperature (T), differential thermogravimetric (DTG), and integrated mass change (TG) curves using a hardware–software complex in LabVIEW 8.21 (*National Instruments*, USA). The temperature was measured with a platinum–platinum rhodium thermocouple (PP-1) with an error of $\pm 5^\circ\text{C}$ in the temperature range of 20– 1000°C , using $\alpha\text{-Al}_2\text{O}_3$ as a standard.

X-ray diffraction analysis (XRDA) was carried out on a D8 Advance diffractometer (*Bruker*, Germany) under SiK_α radiation with continuous rotation of the sample ($1^\circ/\text{min}$, step-by-step $2\theta = 0.02^\circ$, exposure 0.5 s) and modes in the angle range $2\theta = 5^\circ\text{--}80^\circ$. An ICDD card file was used for phase identification.

Granulometric analysis (determination of the particle size distribution function) was performed using a DelsaNano laser particle analyzer (*Beckman Coulter*, USA). Specific surface area and pore size were measured using a SA 3100 analyzer (*Beckman Coulter*, USA). Surface area was calculated from adsorption isotherms using the Brunauer–Emmett–Teller (BET) method. A nonporous sample ASX_1_4 (specific surface area according to BET was 4.18 m^2/g) GSO 9735_2010¹ (a set of standard samples of nanostructured aluminum oxide ASX_1) was used as a standard. The measurement range of the specific surface was $0.1\text{--}2000$ m^2/g . The resolution of the pressure sensor was 0.0062 kPa. The limit of the permissible relative error of the analyzer when measuring the specific surface was $\pm 5\%$. Preliminary degassing of the samples was carried out for 1 h at $t = 70^\circ\text{C}$ and a pressure of 0.1 Pa.

Heat treatment of the samples was conducted in a TK-12.1250.N.1F laboratory furnace with a Thermomatic-N automatic temperature controller that has an error of $\pm 1^\circ\text{C}$ at nominal temperature.

RESULTS AND DISCUSSION

The heterophase synthesis of hydrated iron(III) oxide involves the interaction of solid ferric chloride with a concentrated ammonia solution (6.0–9.5 mol/L). The synthesis proceeded at a high rate at room temperature. Simultaneously, a well-filtered hydrated iron(III) oxide powder with a high content of Fe_2O_3 (84.4 wt %) was obtained, which was easily

¹ https://gso.ru/wp-content/uploads/2016/08/catalog_gso_2020_3.pdf

washed off from impurities and retained a high reactivity. When obtaining hydrated iron(III) oxide, the prewashing operation is important, and it was conducted by the repeated treatment of the sediment with distilled water. Washing removes chloride ions in hydrated iron(III) oxide precipitate, thereby lowering its content to less than 0.05 wt %. Figure 2 shows the particle size distribution of hydrated iron(III) oxide. On the histogram (Fig. 2), there is a pronounced maximum corresponding to the maximum amount of powder particles with a size of 0.8–1.2 μm . Hence, it can be assumed that the hydrated iron(III) oxide was a relatively monodisperse powder. About 95% was accounted for by particles with a size of 0.7–2.0 μm .

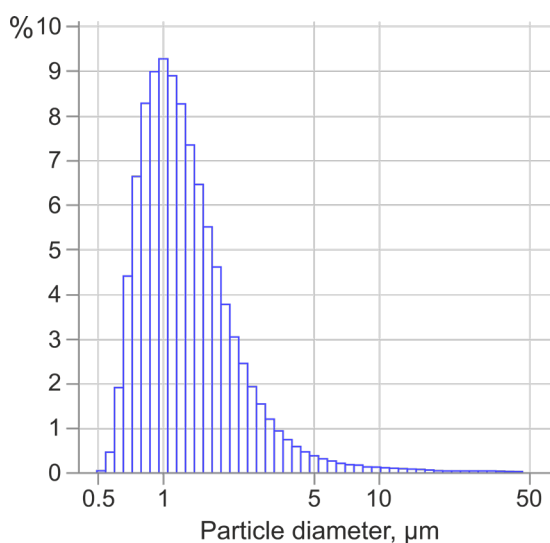


Fig. 2. Particle size distribution of hydrated iron(III) oxide.

Studies have shown that the average particle size is 1.1 μm . The specific surface area of hydrated iron(III) oxide measured by the BET method was 76.72 m^2/g .

Thermolysis of hydrated iron(III) oxide was studied in the temperature range of 20–1000°C. Figure 3 shows the results of the DTA. It was found that the loss of the bulk of water in hydrated iron(III) oxide at temperatures as high as 200°C corresponds to the endothermic effect on the DTA curve (Fig. 3). The resulting phase remains amorphous, which was confirmed by the results of XRDA. With a further increase in temperature, there are no other endoeffects that could indicate a stepwise dehydration. The exoeffect at 445°C corresponds to the transition from an amorphous state to a crystalline state. Further heating above the specified temperature is accompanied by the formation of crystalline oxide Fe_2O_3 . Figure 4 shows the diffractogram of the thermolysis products of hydrated iron(III) oxide at 500°C. Obviously, at 500°C, a hexagonal α -modification of iron(III) oxide was formed. The parameters of the α - Fe_2O_3 lattice are as follows: $a = b = 5.037 \pm 0.002 \text{ \AA}$ and $c = 13.74 \pm 0.01 \text{ \AA}$.

To establish the effect of the precursor on the phase composition of cobalt ferrite, two synthesis methods were conducted with hydrated iron(III) oxide acting as a precursor in both. Either cobalt oxide Co_3O_4 (synthesis 1) was added to it, or an aqueous solution of cobalt(II) sulfate ($C_{\text{Co}} = 0.147 \text{ mol/L}$, synthesis 2).

Figures 5 and 6 show the results of the thermal analysis of the intermediate products obtained during syntheses after evaporation of suspensions.

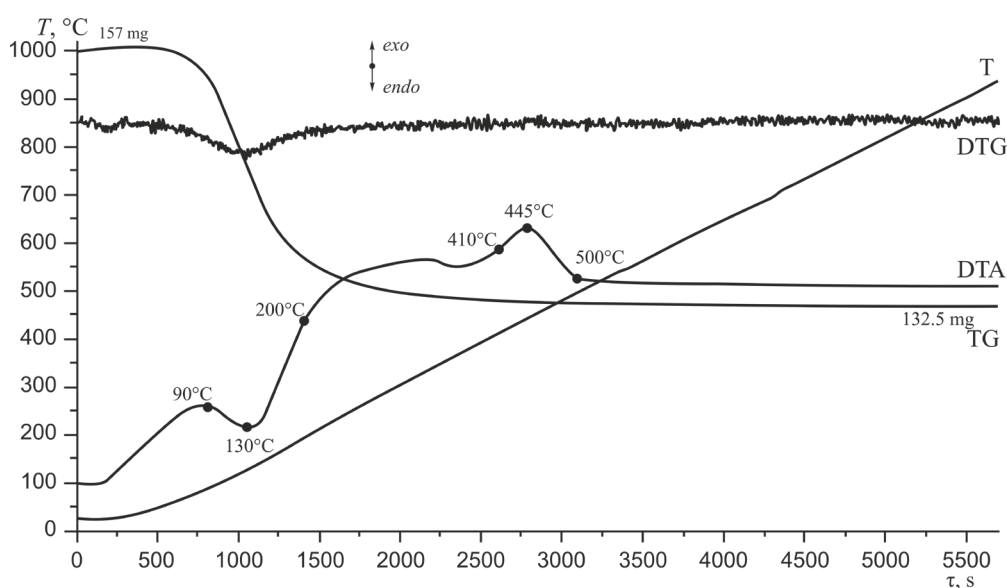


Fig. 3. Thermogravigram of hydrated iron(III) oxide (Fe_2O_3 , 84.4 wt %).

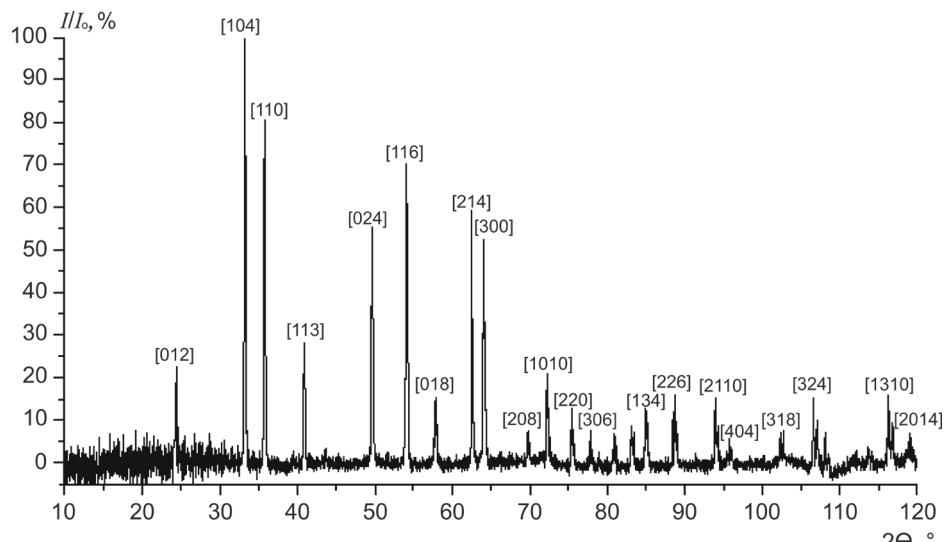


Fig. 4. X-ray diffraction pattern of the thermal decomposition product of hydrated iron(III) oxide, $T = 500^{\circ}\text{C}$.

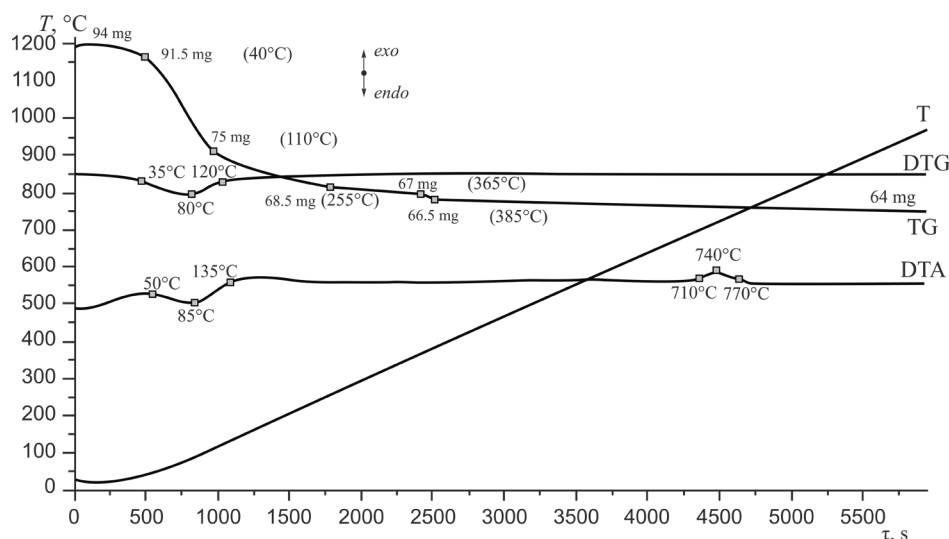


Fig. 5. Thermogravimogram of the intermediate product obtained by the interaction of hydrated iron(III) oxide with cobalt(II, III) oxide (synthesis 1).

Thermogravimograms showed an endothermic effect associated with the dehydration processes ($50\text{--}135^{\circ}\text{C}$, Fig. 5; $75\text{--}160^{\circ}\text{C}$ and $275\text{--}330^{\circ}\text{C}$, Fig. 6) and with the removal of SO_2 and SO_3 ($725\text{--}805^{\circ}\text{C}$ and $805\text{--}870^{\circ}\text{C}$ [15], Fig. 6). In both cases, there was no exothermic effect at 445°C that corresponds to the crystallization of individual hydrated iron(III) oxide. On the thermogravimogram of the intermediate product obtained by the interaction of hydrated iron(III) oxide with cobalt(II, III) oxide (Fig. 5), an exoeffect was observed at $710\text{--}770^{\circ}\text{C}$, which can be associated with the formation of a compound of a given composition, but the sample annealed at 710°C was amorphous.

The resulting intermediates were subjected to heat treatment. In the case of synthesis 1, a temperature of 750°C was used, corresponding to the

exothermic effect on the DTA curve (Fig. 5), and the synthesis duration was 10–30 h in increments of 10 h. In all cases, fine crystalline powder of CoFe_2O_4 (cubic syngony) was obtained, which is confirmed by the results of XRDA (ICDD 79-1744: $a = 8.390 \text{ \AA}$). However, in the case of 10-h annealing, the diffraction peaks of unreacted iron and cobalt oxides were observed on the diffractogram (Fig. 7). Annealing for 30 h turned out to be the most optimal—pronounced peaks of only one phase are present on the diffractogram, which is cubic (CoFe_2O_4 , Fig. 8). The calculated lattice parameter of the synthesized cobalt ferrite is $a = 8.388 \pm 0.002 \text{ \AA}$.

In synthesis 2, an annealing temperature of 900°C was selected. This is due to the fact that up to a temperature of 870°C , there was a decrease in

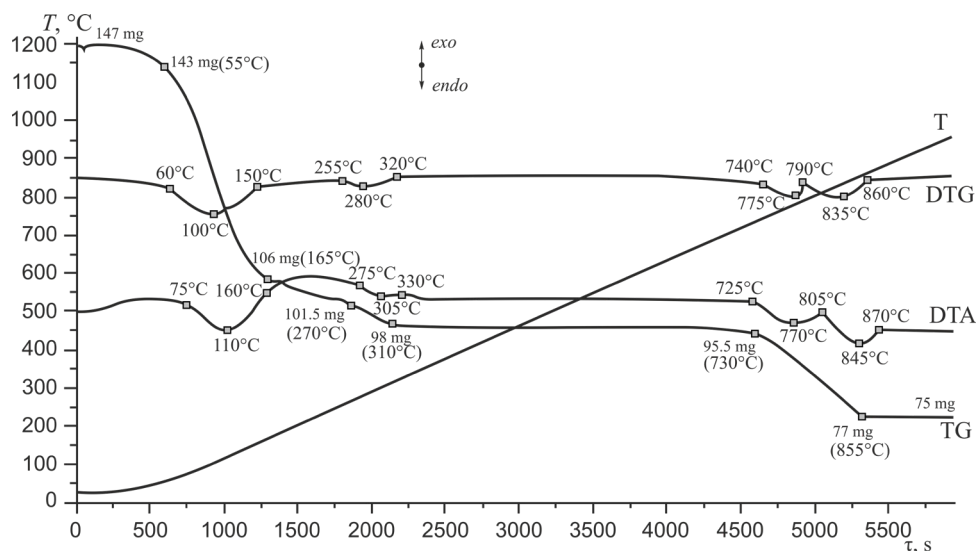


Fig. 6. Thermogravimogram of the intermediate product obtained by the interaction of hydrated iron(III) oxide with a solution of cobalt(II) sulfate (synthesis 2).

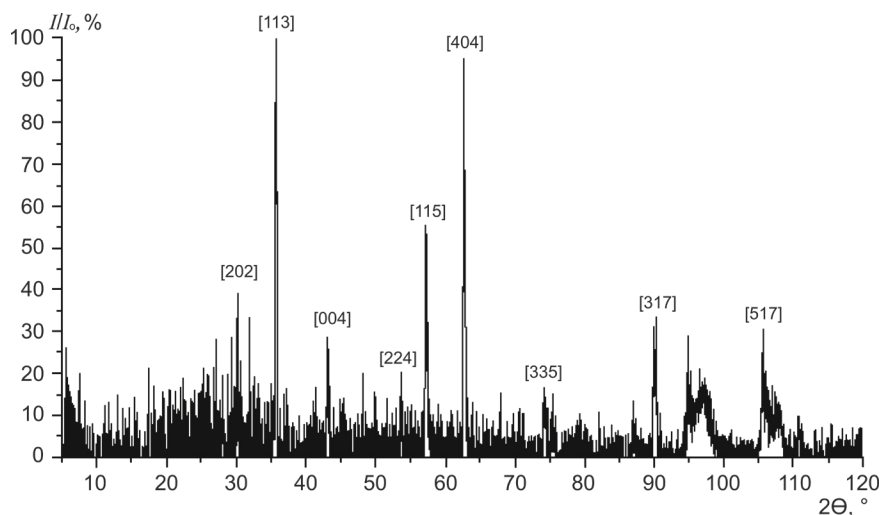


Fig. 7. X-ray diffraction pattern of cobalt ferrite synthesized at 750°C and annealed for 10 h (synthesis 1).

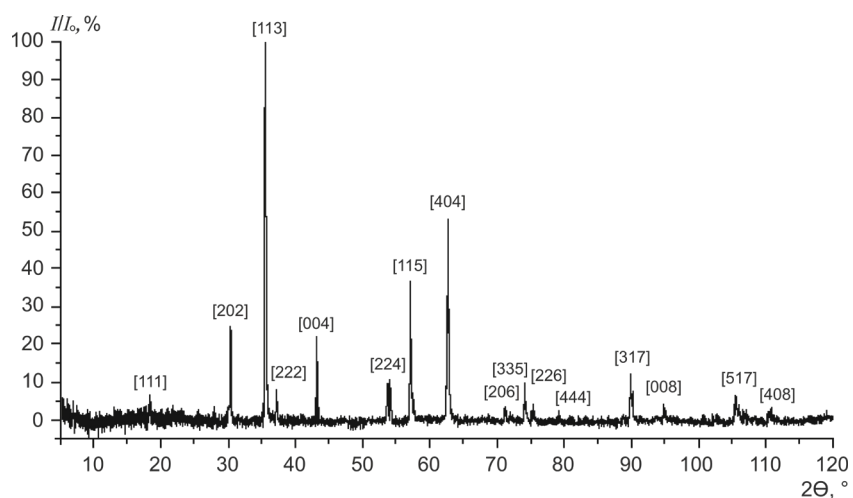


Fig. 8. X-ray diffraction pattern of cobalt ferrite synthesized at 750°C and annealed for 30 h (synthesis 1).

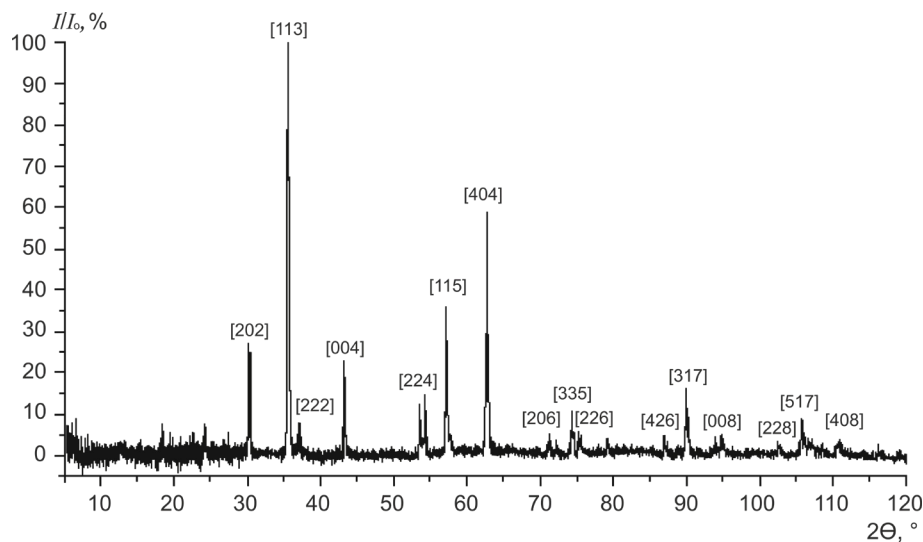


Fig. 9. X-ray diffraction pattern of cobalt ferrite synthesized at 900°C and annealed for 30 h (synthesis 2).

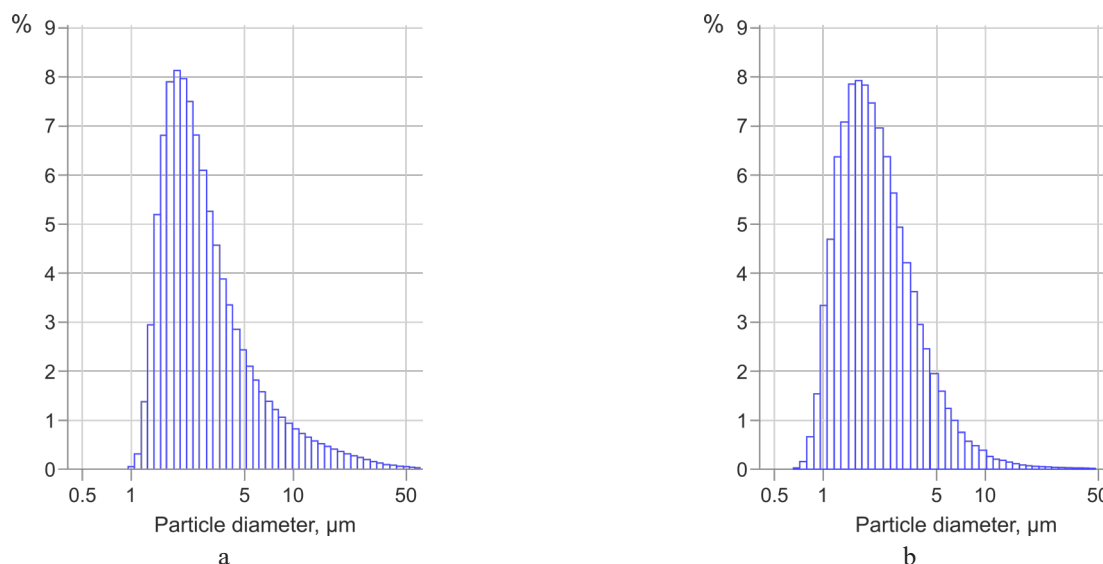


Fig. 10. Particle size distribution of cobalt ferrite: (a) synthesis 1, 750°C, 30 h; (b) synthesis 2, 900°C, 30 h.

sample mass (about 12.5%, Fig. 6). The duration of annealing was 30 h. Figure 9 shows the diffractogram of the resulting product. The lattice parameter of the synthesized cobalt ferrite is $a = 8.389 \pm 0.002 \text{ \AA}$.

The influence of the choice of precursors on the size of cobalt ferrite particles has been studied. Figure 10a shows the size distribution of cobalt ferrite particles (synthesis 1, 750°C, 30 h). On the histogram (Fig. 10a), there is a pronounced maximum corresponding to the maximum presence of powder particles with a size of 1.5–3.0 μm. The main fraction consisted of particles with a size of 1.0–5.0 μm (~85%) with an average diameter of 1.9 μm (for the initial hydrated iron(III) oxide, it was 1.1 μm).

Figure 10b shows the size distribution of cobalt ferrite particles (synthesis 2, 900°C, 30 h). In this case, it is obvious from the histogram that a maximum

number of cobalt ferrite powder particles have a size of 1.2–3.0 μm, and the average particle diameter was 1.5 μm.

As can be seen from the distributions, the smallest particles were formed in cobalt ferrite obtained by the heterophase interaction of hydrated iron(III) oxide (Fe_2O_3 , 84.4 wt %) with an aqueous solution of cobalt(II) sulfate with $C_{\text{Co}} = 0.147 \text{ mol/L}$.

CONCLUSIONS

CoFe_2O_4 was synthesized in two ways. The first method is the heterophase interaction of hydrated iron(III) oxide with cobalt(II, III) oxide with subsequent thermal treatment at 750°C for 30 h (synthesis 1), and the second method is the heterophase interaction of hydrated iron(III) oxide

(Fe₂O₃, 84.4 wt %) with an aqueous solution of cobalt(II) sulfate ($C_{\text{Co}} = 0.147 \text{ mol/L}$) with subsequent heat treatment at 900°C for 30 h (synthesis 2).

Using various methods (XRDA, DTA–DTG, and granulometry), the physicochemical properties of the synthesized samples were investigated. The results of the studies on hydrated iron(III) oxide showed that up to the crystallization temperature of 445°C, which corresponds to the exothermic effect on the DTA curve, the sample remained amorphous. Further heating led to the α -modification of iron(III) oxide hexagonal syngony ($a = b = 5.037 \pm 0.002 \text{ \AA}$; $c = 13.74 \pm 0.01 \text{ \AA}$), which has an average particle size of 1.1 μm .

Using the XRD method, it was found that in the case of synthesis 1, a temperature of 750°C and a heat treatment for 30 h were sufficient to form a single-phase cobalt ferrite ($a = 8.388 \pm 0.002 \text{ \AA}$) with an average particle diameter of 1.9 μm . The temperature used in synthesis 2 was increased to 900°C due to a decrease in sample mass (about 12.5%) observed during synthesis in the temperature range of 720–810°C based on the results of differential thermal analysis.

Loss in sample mass was due to the removal of SO₂ and SO₃. Using a synthesis temperature and a synthesis duration of 900°C and 30 h, respectively, CoFe₂O₄ with $a = 8.389 \pm 0.002 \text{ \AA}$ was formed.

Depending on the synthesis method, cobalt ferrite particles of different diameters were formed. The smallest particle size of cobalt ferrite (1.5 μm) was obtained by the heterophase interaction of hydrated iron(III) oxide (Fe₂O₃, 84.4 wt %) with an aqueous solution of cobalt(II) sulfate with $C_{\text{Co}} = 0.147 \text{ mol/L}$.

Acknowledgments

This work was performed using the equipment of the Joint Science and Training Center for Collective Use and supported by The Ministry of Education and Science of the Russian Federation.

Author's contribution

Elena E. Nikishina – conducting research, preparing a manuscript.

The author declares no conflicts of interest.

REFERENCES

1. Yan Z., Gao J., Li Y., Zhang M., Guo M. Hydrothermal synthesis and structure evolution of metal-doped magnesium ferrite from saprolite laterite. *RSC Advances*. 2015;5:92778–92787. <https://doi.org/10.1039/C5RA17145H>
2. Kefeni K.K., Mamba B.B., Msagati T.A.M. Application of spinel ferrite nanoparticles in water and wastewater treatment: A review. *Sep. Purif. Technol.* 2017 Nov;188:399–422. <https://doi.org/10.1016/j.seppur.2017.07.015>
3. Rashdan S.A., Hazeem L.J. Synthesis of spinel ferrites nanoparticles and investigating their effect on the growth of microalgae *Picochlorum* sp. *Arab J. Basic Appl. Sci.* 2020 Feb;27(1):134–141. <https://doi.org/10.1080/25765299.2020.1733174>
4. Amiri M., Salavati-Niasari M., Akbari A. Magnetic nanocarriers: Evolution of spinel ferrites for medical applications. *Adv. Colloid Interface Sci.* 2019 Mar;265:29–44. <https://doi.org/10.1016/j.cis.2019.01.003>
5. Vedrtnam A., Kalauni K., Dubey S., Kumar A. A comprehensive study on structure, properties, synthesis and characterization of ferrites. *AIMS Materials Science*. 2020;7(6):800–835. <https://doi.org/10.3934/mat.2020.6.800>
6. Zhou J., Shu X., Wang Y., Ma J. *et al.* Enhanced Microwave Absorption Properties of (1-x)CoFe₂O₄/xCoFe Composites at Multiple Frequency Bands. *J. Magn. Magn. Mater.* 2020 Jun;493:165699–165708. <https://doi.org/10.1016/j.jmmm.2019.165699>
7. Bartunek V., Sedmidubsky D., Hube, S., Svecov, M., Ulbrich P., Jankovsky O. Synthesis and properties of nanosized stoichiometric cobalt ferrite spinel. *Materials*. 2018 Jul;11(7):1241–1251. <https://doi.org/10.3390/ma11071241>
8. Zhou Z., Zhang Y., Wang Z., Wei W., *et al.* Electronic structure studies of the spinel CoFe₂O₄ by X-ray photoelectron spectroscopy. *Appl. Surf. Sci.* 2008 Aug;254(21):6972–6975. <https://doi.org/10.1016/j.apsusc.2008.05.067>
9. Das D., Biswas R., Ghosh S. Systematic analysis of structural and magnetic properties of spinel CoB₂O₄ (B=Cr, Mn and Fe) compounds from their electronic structures. *J. Phys.: Condens. Matter*. 2016 Nov;28(44):446001–446010. <https://doi.org/10.1088/0953-8984/28/44/446001>
10. Swatsitang E., Phokha S., Hunpratub S., Usher B., Bootchanont A., Maensiri S., *et al.* Characterization and magnetic properties of cobalt ferrite nanoparticles. *J. Alloys Compd.* 2016 Apr;664:792–797. <https://doi.org/10.1016/j.jallcom.2015.12.230>

11. Kazemi M., Ghobadi M., Mirzaie A. Based on: Cobalt ferrite nanoparticles (CoFe₂O₄ MNPs) as catalyst and support: Magnetically recoverable nano-catalysts in organic synthesis. *Nanotechnol. Rev.* 2017 Jan;7(1):1–50. <https://doi.org/10.1515/ntrev-2017-0138>

12. Srinivasan S.Y., Paknikar K.M., Bodas D., Gajbhiye V. Applications of cobalt ferrite nanoparticles in biomedical nanotechnology. *Nanomedicin.* 2018 Jun;13(10):1221–1238. <https://doi.org/10.2217/nnm-2017-0379>

13. Chagas C.A., de Souza E.F., de Carvalho M.C.N.A., Martins R.L., Schmal M. Cobalt ferrite nanoparticles for the preferential oxidation of CO. *Appl. Catal. A-Gen.* 2016;519C:139–145. <https://doi.org/10.1016/j.apcata.2016.03.024>

14. Tatarchuk T., Bououdina M., Vijaya J.J., Kennedy L.J. Spinel Ferrite Nanoparticles: Synthesis, Crystal Structure, Properties, and Perspective Applications. In: *International Conference on Nanotechnology and Nanomaterials. NANO 2016: Nanophysics, Nanomaterials, Interface Studies, and Applications.* 2016 Aug:305–325. https://doi.org/10.1007/978-3-319-56422-7_22

15. Mu J., Perimutte D.D. Thermal Decomposition of Inorganic Sulfates and Their Hydrates. *Ind. Eng. Chem. Process Des. Dev.* 1981 Oct;20(4):640–646. <https://doi.org/10.1021/i200015a010>

About the author:

Elena E. Nikishina, Assistant Professor, Department of Chemistry and Technology Rare Elements, M.V. Lomonosov Institute of Fine Chemical Technologies, MIREA – Russian Technological University (86, Vernadskogo pr., Moscow, 119571, Russia). E-mail: nikishina@mirea.ru. Scopus Author ID 6602839662, ResearcherID O-7115-2014, <http://orcid.org/0000-0003-3579-2194>

Об авторе:

Никишина Елена Евгеньевна, доцент кафедры химии и технологии редких элементов Института тонких химических технологий им. М.В. Ломоносова ФГБОУ ВО «МИРЭА – Российский технологический университет» (119571, Россия, Москва, пр-т Вернадского, д. 86). E-mail: nikishina@mirea.ru. Scopus Author ID 6602839662, ResearcherID O-7115-2014, <http://orcid.org/0000-0003-3579-2194>

The article was submitted: October 05, 2021; approved after reviewing: October 26, 2021; accepted for publication: November 26, 2021.

Translated from Russian into English by N. Isaeva

Edited for English language and spelling by Enago, an editing brand of Crimson Interactive Inc.

**ANALYTICAL METHODS IN CHEMISTRY
AND CHEMICAL TECHNOLOGY**
**АНАЛИТИЧЕСКИЕ МЕТОДЫ
В ХИМИИ И ХИМИЧЕСКОЙ ТЕХНОЛОГИИ**

ISSN 2686-7575 (Online)

<https://doi.org/10.32362/2410-6593-2021-16-6-512-525>



UDC 535.33/34:547.77

RESEARCH ARTICLE

Ion mobility spectrometry of *N*-methylimidazole and possibilities of its determination

Daria A. Aleksandrova^{1,@}, Tatiana B. Melamed¹, Elena P. Baberkina¹, Anatolii A. Fenin¹, Ekaterina S. Osinova¹, Aleksei E. Kovalenko¹, Roman V. Yakushin¹, Yulia R. Shaltaeva², Vladimir V. Belyakov², Daria I. Zykova³

¹Mendeleev University of Chemical Technology of Russia, Moscow, 125047 Russia

²National Research Nuclear University "MEPHI," Moscow, 115230 Russia

³Moscow Aviation Institute (National Research University), Moscow, 125080 Russia

@Corresponding author, e-mail: dasha-25.2012@yandex.ru

Abstract

Objectives. To determine the ion mobility of *N*-methylimidazole, establish the structure of ions corresponding to characteristic signals, and determine the detection limit of *N*-methylimidazole on the ion-drift detector Kerber.

Methods. Ion mobility spectrometry was used to study the ionization processes. The enthalpies of the reactions of monomer and dimer ions were calculated in the ORCA 4.1.1 software by the B3LYP density functional method with a set of basic functions 6-31G (d, p).

Results. The drift time and ion mobility values of *N*-methylimidazole were determined. A method for mathematical processing of spectra and a program for its implementation was developed. The changing peculiarities of the ion mobility spectrum during measurement at a given time were studied. According to the interpretation of the spectrum signals, the structure of the generated ions was proposed, and the enthalpies of ion formation were determined.

Conclusions. The characteristic signal of the *N*-methylimidazole ion protonated at the nitrogen atom of the pyridine type was revealed. It was found that two signals in the ion mobility spectra of *N*-methylimidazole correspond to the presence of the monomer and dimer ions. The detection limit of *N*-methylimidazole on the ion-drift detector Kerber was determined, amounting to 3 pg.

Keywords: ion mobility spectrometry (IMS), characteristic signal, protonation, heterocyclic nitrogen compounds, pyridine, imidazole, N-methylimidazole

For citation: Aleksandrova D.A., Melamed T.B., Baberkina E.P., Fenin A.A., Osinova E.S., Kovalenko A.E., Yakushin R.V., Shaltaeva Yu.R., Belyakov V.V., Zyкова D.I. Ion mobility spectrometry of N-methylimidazole and possibilities of its determination. *Tonk. Khim. Tekhnol. = Fine Chem. Technol.* 2021;16(6):512–525 (Russ., Eng.). <https://doi.org/10.32362/2410-6593-2021-16-6-512-525>

НАУЧНАЯ СТАТЬЯ

Спектрометрия ионной подвижности N-метилимидазола и возможности его определения

Д.А. Александрова^{1,@}, Т.Б. Меламед¹, Е.П. Баберкина¹, А.А. Фенин¹,
Е.С. Осина¹, А.Е. Коваленко¹, Р.В. Якушин¹, Ю.Р. Шалтаева²,
В.В. Беляков², Д.И. Зыкова³

¹Российский химико-технологический университет им. Д.И. Менделеева, Москва, 125047 Россия

²Национальный исследовательский ядерный университет «МИФИ», Москва, 115230 Россия

³Московский авиационный институт (национальный исследовательский университет), Москва, 125080 Россия

@Автор для переписки, e-mail: dasha-25.2012@yandex.ru

Аннотация

Цели. Определение значений ионной подвижности N-метилимидазола. Установление строения ионов, соответствующих характерным сигналам. Определение предела обнаружения N-метилимидазола на ионно-дрейфовом детекторе Кербер.

Методы. Метод спектрометрии ионной подвижности был использован для исследования процессов ионизации. Энтальпии реакций мономерных и димерных ионов рассчитаны в программе ORCA 4.1.1 методом функционала плотности B3LYP с набором базисных функций 6-31G(d,p).

Результаты. Определены значения времени дрейфа и ионной подвижности N-метилимидазола. Разработана методика математической обработки спектров и программа для ее реализации. Изучены особенности изменения характера спектра ионной подвижности в процессе измерения в данный момент времени. Предложено строение генерируемых ионов в соответствии с интерпретацией сигналов спектра. Определены энтальпии образования ионов.

Выводы. Выявлен характеристический сигнал иона N-метилимидазола, протонированного по атому азота пиридинового типа. Установлено, что два сигнала в спектрах ионной подвижности N-метилимидазола соответствуют наличию мономерной и димерной формы ионов. Определен предел обнаружения N-метилимидазола на ионно-дрейфовом детекторе Кербер, составляющий 3 пг.

Ключевые слова: спектрометрия ионной подвижности, характеристический сигнал, протонирование, гетероциклические соединения азота, пиридин, имидазол, *N*-метилимидазол

Для цитирования: Александрова Д.А., Меламед Т.Б., Баберкина Е.П., Фенин А.А., Осина Е.С., Коваленко А.Е., Якушин Р.В., Шалтаева Ю.Р., Беляков В.В., Зыкова Д.И. Спектрометрия ионной подвижности *N*-метилимидазола и возможности его определения. *Тонкие химические технологии*. 2021;16(6):512–525. <https://doi.org/10.32362/2410-6593-2021-16-6-512-525>

INTRODUCTION

Ion mobility spectrometry is a promising fast modern method for analyzing chemical compounds in the gas phase [1, 2]. The method is promising for solving a wide range of analytical problems because of its speed, high sensitivity, lack of vacuum systems, and portability [3–9]. However, a large number of possible ion-molecular reactions take place in the drift space of an ion mobility spectrometer, as well as an incompletely studied mechanism of ion formation complicate the reliable interpretation of ion mobility spectra. Expanding the capabilities of the method is of great theoretical and practical interest.

Recently, the so-called “designer drugs” have become popular. Small changes in the chemical structure of legally controlled substances (homologs and small newly introduced functional groups) make it possible to circumvent existing bans and sell potentially hazardous substances disguised as legal drugs. Often the consequences of exposure to modified substances on the body cause the rapid development of physical and psychological dependence (addiction) to them, which turns out to be far more dangerous than the original drugs. Such compounds are difficult to detect because they are not included in the major databases of analytical instruments.

As a result, determining the characteristic signal of a whole class of compounds becomes important for detecting synthetic cannabinoids [10, 11].

Earlier, to develop conditions for the detection of synthetic cannabinoids based on imidazole by ion mobility spectrometry, a research on the behavior of imidazole was conducted on the ion-drift detector Kerber, which is already used by the Ministry of Internal Affairs, Federal Security Service, Ministry of Emergency Situations, and Federal Customs Service of the Russian Federation to detect main drugs and explosives [12–15]. It was discovered that the spectrum of the ion mobility of

imidazole always contains two signals with ion mobility of 2.100 cm²/(V·s) and 1.700 cm²/(V·s), corresponding to the monomer and dimer ions, respectively. The effect of concentrations on the characteristics of the spectrum is investigated. An assumption was made about the structure of the dimer, and it was demonstrated that the interconversion of the monomer–dimer forms occurs during measurement, depending on the concentration of the sample.

According to the published data, imidazole can form dimers as well as long chains associated with water [16, 17]. However, in the range of spectrum registration, a multitude of signals of oligomeric chains was not recorded; instead only one signal of the dimer was recorded, therefore, it was assumed that it was this signal that was formed. Its structure was proposed considering the formation of a complex with water [1].

The results of the study of *N*-methylimidazole, which is not prone to the formation of stable dimer forms, are presented in this paper to obtain additional data on the nature of the ion mobility spectra of imidazole derivatives.

The goal of this work is to determine the characteristic signals of *N*-methylimidazole using ion mobility spectrometry, thereby confirming the proposed structure of ions formed during corona discharge ionization.

EXPERIMENTAL

The studies were conducted on an ion-drift detector (IDD) Kerber¹ manufactured by *Yuzhpolimetal-Holding Group of Companies* (Russia). The characteristics of the device are given in Table 1.

Ion mobility spectra were obtained at atmospheric pressure using ambient air as the drift gas. Target

¹ Yuzhpolymetal Holding. Kerber-T portable ion-drift detector. <http://www.analizator.ru/production/ims/kerber-t/>. Accessed September 16, 2021.

Table 1. Specifications of IDD Kerber

Characteristic	IDD Kerber value
Detection range of low-volatile organic substances by 2,4,6-trinitrotoluene (TNT), g	from 1.0×10^{-11} to 2.0×10^{-7}
Low-volatile organic matter detection limit for 2,4,6-trinitrotoluene (TNT) – for solid particles, g – in pairs, g/cm ³	no more 1.0×10^{-11} no more 1.0×10^{-14}
Ionization method	Pulsed corona discharge
Drift tube temperature, °C	100
Time of detection and identification for all detectable substances, s	no more 5
The probability of a false alarm, %	no more 1
Detector cleaning time in case of contamination with target substances within the detection range, s	no more 180

substances were registered using the software IDD Kerber in the “Spectrum” format. The measurement results were text files containing information about the parameters of the system, the detected target substances and the drift time. Ionograms were constructed according to the indicated data.

A sample of *N*-methylimidazole produced by *Acros Organics* (USA) with a purity of 99% was selected for the study.

We used a balance of the brand A&D GR-120 (*AND*, Japan) with a discreteness of 0.0001 g.

A Lempipet Light 1–10 μ L dispenser (*Thermo Scientific*, USA) was used to prepare solutions of the required concentrations and to apply the substance to a sampling napkin. The sampling napkin is an aluminum foil with dimensions of 120×60 mm and a thickness of 11–16 μ m.

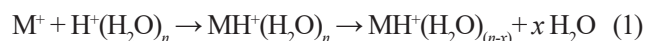
The enthalpies of reactions were calculated using the ORCA 4.1.1 program of the Max Planck Institute for Energy Conversion Chemistry (Germany) by the density functional method B3LYP with a set of basic functions 6-31G (d, p).

POSITIVE ION FORMATION BY CORONA DISCHARGE

The method of ion mobility spectrometry is based on the ionization of the molecules of the investigated substance at atmospheric pressure. First, reactant ions

$H^+(H_2O)_n$ are formed in the discharge chamber, whose concentration significantly exceeds that of the substances to be detected.

Reactant ions transfer charge to molecules of the target substances by the mechanism of chemical ionization presented below:



where M—test compound molecule, $H^+(H_2O)_n$ —reactant ion, $MH^+(H_2O)_n$ —cluster ion, $MH^+(H_2O)_{(n-x)}$ —test compound ion.

In the process, product monomer and dimer ions can be formed, $M_2H^+(H_2O)_n$, as well as other molecular ions. Product ions are associated with water molecules. Depending on the nature of the compound, the number of water molecules in the resulting cluster can vary from one to three [1, 2].

The drift time τ_d (the arrival time of ions to the collector) is determined by the charge, mass, and effective cross-section of the formed ion. The drift time is proportional to the length of the drift chamber L (cm) and inversely proportional to the electric field gradient E :

$$\tau_d = 1/K \times L/E \quad (2)$$

where K —mobility coefficient, $\text{cm}^2/(\text{V}\cdot\text{s})$. Ion mobility depends on temperature and atmospheric pressure. To compare the values of ion mobility, the values of K obtained under different conditions lead to normal conditions and obtain the reduced mobility K_0 (or reduced coefficient of mobility):

$$K_0 = (K \times P) / 101325 \times 273 / T \quad (3)$$

where T —temperature (Kelvin) and P —pressure (Pascal) of the gas atmosphere in which the ions move [2]. This work shows the values of the reduced ion mobility.

The results are presented in the form of a “spectrum” of ion mobility (ionograms).

METHODS

The spectrum of ion mobility of *N*-methylimidazole was obtained while passing through the drift chamber’s ionized molecules. The analyte sample was collected either at room temperature 22°C or after heating the substrate to 100°C for some seconds. The spectrum was captured at a frequency of 1 s. This approach to the analysis of spectra made it possible to determine both the ion mobility of characteristic signals and the redistribution of their intensities, which characterizes the formation and interconversion of ions in the drift chamber of an ion-drift detector.

It was discovered that the ion mobility of *N*-methylimidazole is unaffected by temperature of the analyte sample. As a result, the sampling was carried out by heating to 100°C to obtain a signal with a high value of the ion current.

For mathematical data processing, a program was developed that allows obtaining data and processing a large number of ion mobility spectra for the purpose of their subsequent study and analysis. The interpreted programming language Python 3.3 was used to create the program.

In general, the operation of the program can be described as follows. The program consists of three scripts, each with a specific task. In the first step, the list of source files is sorted alphabetically, as the `os.walk()` function returns filenames in no particular order. This operation is necessary in order to accurately reproduce the order of recording spectra on the Kerber IDD.

The presence of substance signals is considered relative to background signals, since the air always contains a certain amount of ions (impurities), and the spectrum of the background signal may change depending on the current concentrations of impurities in the air. Therefore, it is imperative that a “zero”

or “background” measurement is performed first. Background data is also required when determining the detection limit of a sample.

IDD Kerber of Classic and Next series saves spectra files in .dat and .spe formats, respectively. Depending on the format of the files in the directory, the program calls the corresponding function from the imported local modules `imp_spe` and `imp_dat`. Further processing is carried out by procedures described in the `imp_dat` and `imp_spe` modules. The reduced ion mobility is calculated at each moment of time, considering the conversion factor, which contains the values of temperature and atmospheric pressure during the measurement.

Next, the program requests data to remove noise signals. During the subsequent processing of the spectra, the values of the ion current signals of the ambient air background are subtracted from the values of the ion current signals of the sample, which increases the visibility of the spectrum. Before this operation is performed, the initial signal of the device is stored in adjacent columns; if necessary, it is possible to construct a spectrum with the initial data.

Further investigation of the ionization processes requires the calculation of the peak areas of the sample characteristic signal. In terms of mathematical analysis, all signals on the ionogram are curved trapezoids. Therefore, to obtain additional data on the structure and interconversion of analyte ions, the area of a curved trapezoid was calculated using the method of middle rectangles. The length of the rectangle was taken as 1/2 the sum of the values between the corresponding points along the ion current axis. The spectrum was used to determine the boundaries of the signal of the substance (along the abscissa) and the area of the peak (curvilinear trapezoid) was calculated by summing the corresponding values. The boundaries of the array to be summed for the formula `=SUM(number1; [number2]; ...)` were determined manually or using the formula `=MATCH(search_value; lookup_array; [match_type])`. Further, depending on the tasks of the user and the nature of the investigated substance, one can compare the intensity of signals, their changes, similarities and differences.

As a result of the mathematical processing, an Excel file was created that included all the selected data in both the positive and negative ionization regions.

Figure 1 illustrates the processing of the ion mobility spectrum using the program.

To determine the limit of detection of *N*-methylimidazole on the Kerber IDD, a method of serial dilution of the solution was developed. For this, a solution of *N*-methylimidazole in diethyl ether with a concentration of 0.0003 g/cm^3 was used. One mm^3

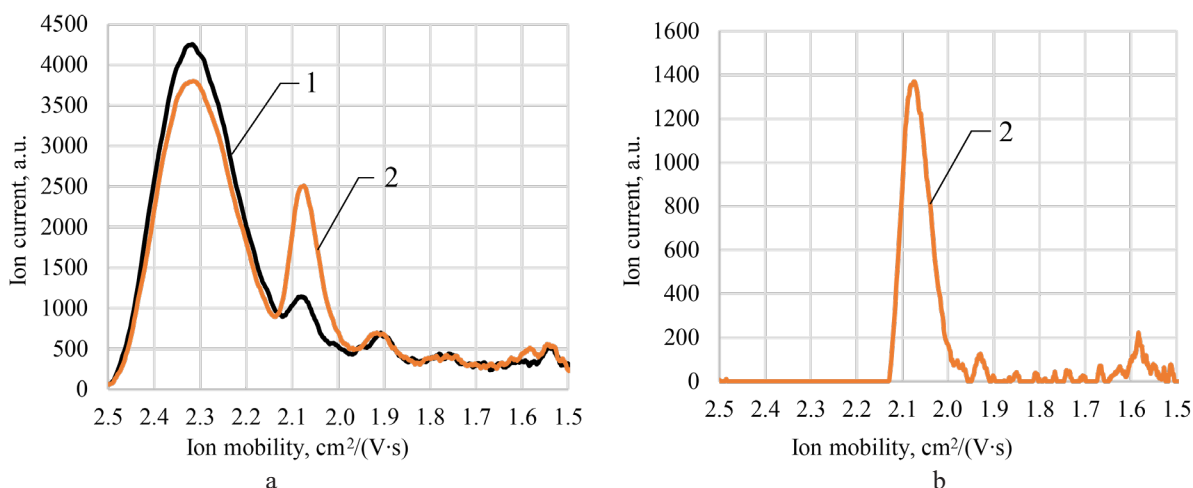


Fig. 1. Ion mobility spectrum of *N*-methylimidazole before (a) and after (b) mathematical processing. (1) Background and (2) *N*-methylimidazole.

of the solution was applied with a dispenser onto a sampling tissue. After evaporation of the solvent, a sample weighing $3 \cdot 10^{-7}$ g was taken with heating for 5 s. As a result, a spectrum was obtained with an amplitude of 5000 analog-to-digital conversion units (a.u.). Then the analyte solution was diluted in order to decrease the concentration of the solution by one order of magnitude by adding a solvent, until a signal of the sample with a mass of 3 pg with an amplitude of 800 a.u. was obtained. The signal of the substance did not exceed the noise values with a decrease in the concentration of the solution by one more order of magnitude.

RESULTS AND DISCUSSION

Heterocyclic nitrogen compounds that have basic properties and an sp²-hybrid nitrogen atom of the pyridine type were selected for the studies. As a result of the research, a series of *N*-methylimidazole,

imidazole, and pyridine spectra were obtained. They were mathematically processed to identify the characteristic signals of ions (Fig. 2).

As seen from Fig. 2, in all spectra of ion mobility, a characteristic signal is observed in the range of 2.1 cm²/(V·s), previously assigned to the protonated form of the monomer at the pyridine nitrogen atom, which is consistent with preliminary studies of other heterocyclic compounds [12, 14, 15]. This signal is the only characteristic in the spectrum of ion mobility of pyridine. The spectra of imidazole and *N*-methylimidazole (Fig. 1) also show stable signals with ion mobility of 1.7 and 1.6 cm²/(V·s), respectively, preliminarily assigned to the protonated forms of their dimers. It should be noted that the nature of the spectra of imidazole and *N*-methylimidazole is identical in the number of signals obtained, which suggests the formation of an *N*-methylimidazole dimer, despite the presence of a methyl substituent on the pyrrole nitrogen atom.

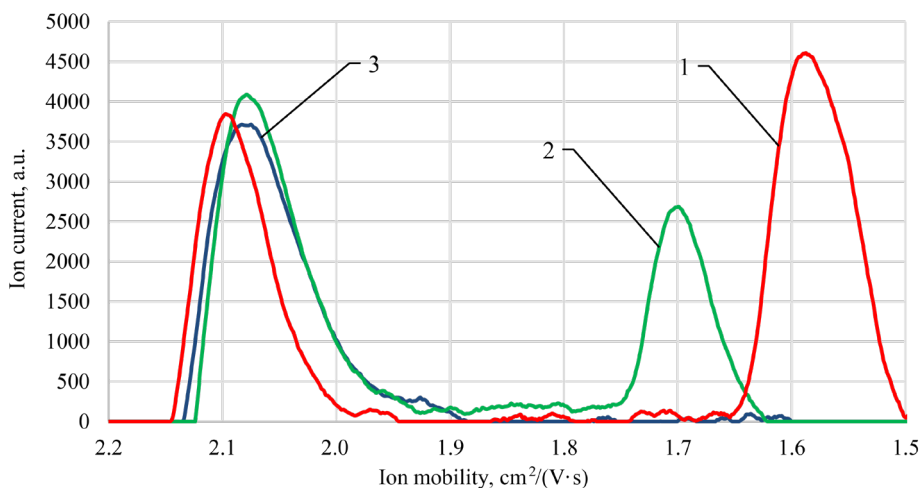


Fig. 2. Ionogram of *N*-methylimidazole (1), imidazole (2), and pyridine (3).

To establish the structure of generated ions, we calculated the enthalpies of specific reactions occurring during the formation of analyte ions (Table 2).

There have been several proposed structures for monomer and dimer analyte ions. The enthalpies of reactions were calculated in the ORCA 4.1.1 program using the B3LYP density functional method with a set of basis functions 6-31G (d, p). Based on the obtained data, the most probable structures of imidazole and

N-methylimidazole ions were proposed. The structure of the monomers of the ions of imidazole No. 2 and *N*-methylimidazole No. 4 coincides, as evidenced by the enthalpies of the reaction processes and close values of the ion mobility. The presence of a water molecule in the structure of an analyte ion is in complete agreement with the data on the formation of ions during a corona discharge in the form of associates with water [1].

Table 2. Monomeric ion reaction enthalpies of imidazole and *N*-methylimidazole

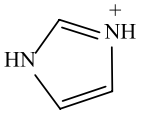
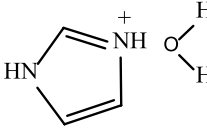
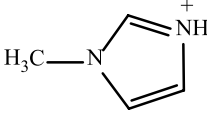
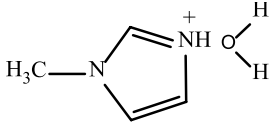
No.	Ion structure	Reaction enthalpy, kJ/mol
1		-247
2		-331
3		-265
4		-346

Table 3. Reaction enthalpies of dimeric and trimeric ions of imidazole and *N*-methylimidazole

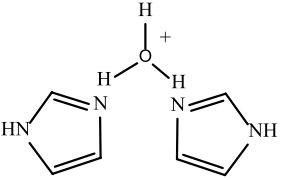
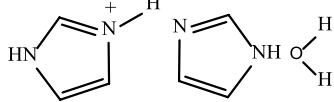
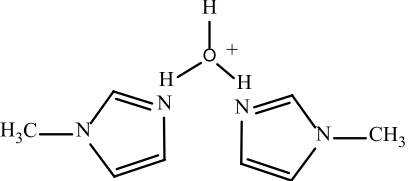
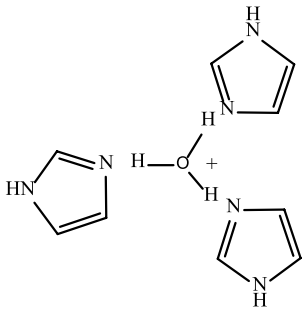
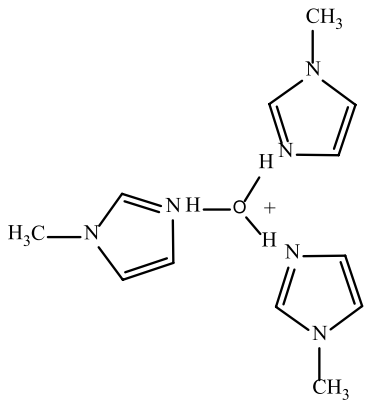
No.	Ion structure	Reaction enthalpy, kJ/mol
1		-96.4
2		-112
3		-97.6

Table 3. Continued

No.	Ion structure	Reaction enthalpy, kJ/mol
4		-85.4
5		-84.1

Various structures were proposed for dimer ions (Table 3).

Since imidazole tends to form chains under normal conditions and the enthalpy of formation of such a dimer is lower, the formation of dimer No. 2 is most likely. For *N*-methylimidazole, such a structure is impossible due to the substituent at the first

atom; therefore, dimer No. 3 is formed. Signals corresponding to oligomer forms of ions were not observed in the spectrum.

To establish the limit of detection of *N*-methylimidazole, the ion mobility spectra were studied at various concentrations. The corresponding ionograms are shown in Figs. 3 and 4.

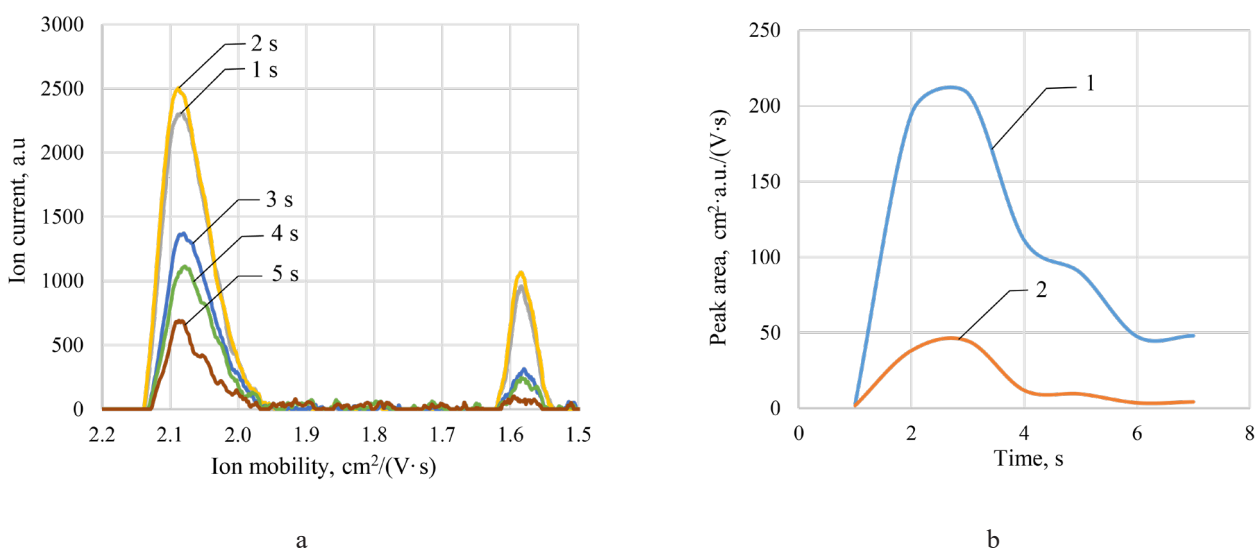


Fig. 3. Ion mobility spectrum of *N*-methylimidazole with a mass of 3 ng and time dependence of the signal intensity: (a) dependence of the ion current on the ion mobility of *N*-methylimidazole (spectra were taken every 1 s after the start of measurement); (b) ion mobility change in the spectrum of *N*-methylimidazole: (1) monomer ion and (2) dimer ion.

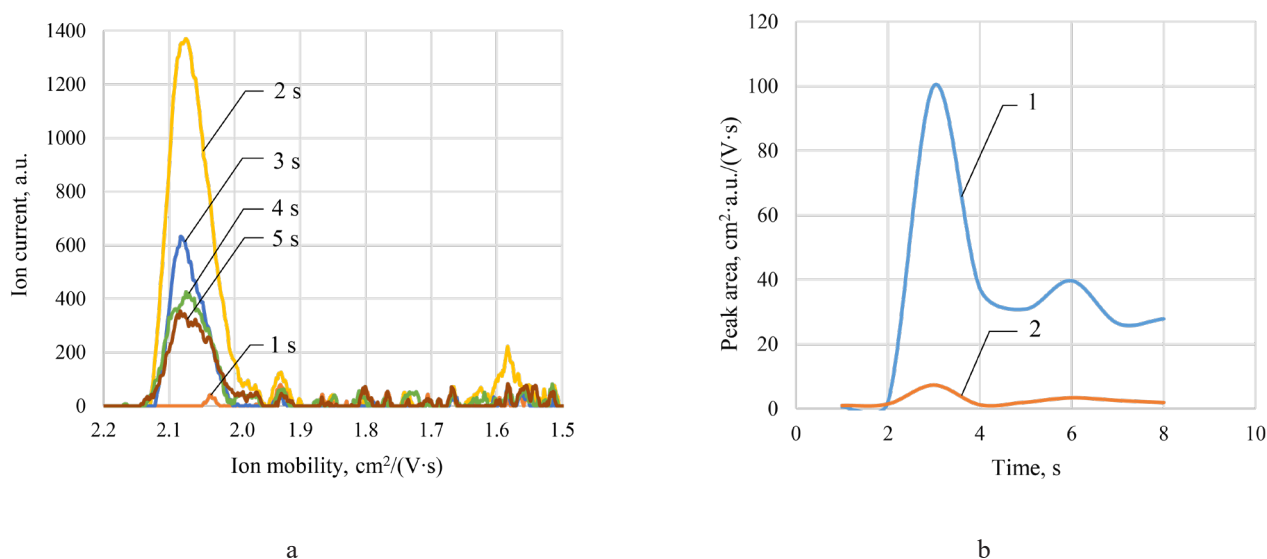


Fig. 4. Ion mobility spectrum of *N*-methylimidazole with a mass of 0.3 ng and time dependence of the signal intensity: (a) dependence of the ion current on the ion mobility of *N*-methylimidazole (spectra were taken every 1 s after the start of measurement); (b) ion mobility change in the spectrum of *N*-methylimidazole: (1) monomer ion and (2) dimer ion.

The change in the peak areas completely correlates with the signal intensity and indicates the simultaneous presence of two ions. A simultaneous increase and then a decrease in the intensity of the signals of both peaks was observed, with the monomer peak having a higher amplitude than the dimer peak (Fig. 3).

With a decrease in the mass of the sample, the following changes occur in the spectrum (Fig. 4).

The ion mobility of the monomer signal corresponds to the mobility of the 3-ng *N*-methylimidazole sample (Fig. 3). And the dimer peak is practically absent. With a decrease in the concentration of *N*-methylimidazole in the sample in the ion mobility spectrometer, the destruction of the dimer begins due to collision with gas molecules in the drift chamber, which is reflected in the ion mobility spectrum.

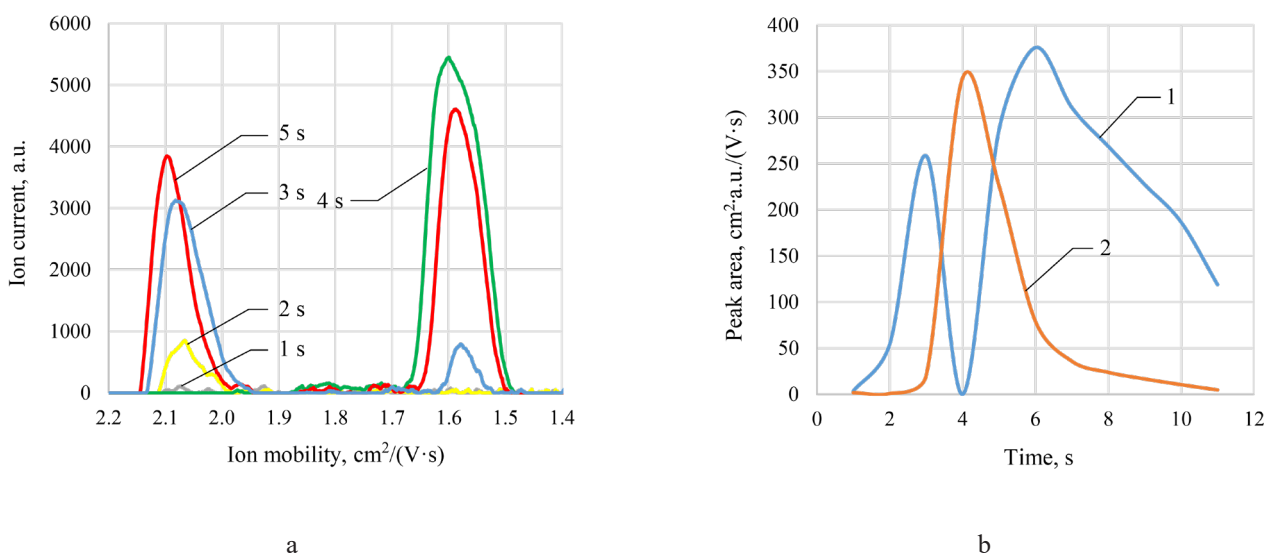


Fig. 5. Ion mobility spectrum of *N*-methylimidazole in water solution and time dependence of the signal intensity: (a) dependence of the ion current on the ion mobility of *N*-methylimidazole (spectra were taken every 1 s after the start of measurement); (b) ion mobility change in the spectrum of *N*-methylimidazole: (1) monomer ion and (2) dimer ion.

The analysis of the ion mobility spectra of *N*-methylimidazole water solution is below. The obtained ionogram and the corresponding dependence of the change in signal intensity on time are shown in Fig. 5.

The dimer ion of *N*-methylimidazole shows non-stability and degrades within 4 s after the start of the measurement, while the monomer concentration decreases gradually. Due to the destruction of the dimer ion, the monomer concentration begins to increase

again. Similar processes were observed for unsubstituted imidazole, which is demonstrated in Fig. 6.

For the limiting detection value of *N*-methylimidazole with a mass of 3 pcg, a decrease in the intensity of the signal with an ion mobility of 2.1 to 800 a.u. and a complete disappearance of the signal with a lower ion mobility attributed to the signal of the dimer ion are observed (Fig. 7). The nature of the ionogram is identical to the spectrum shown

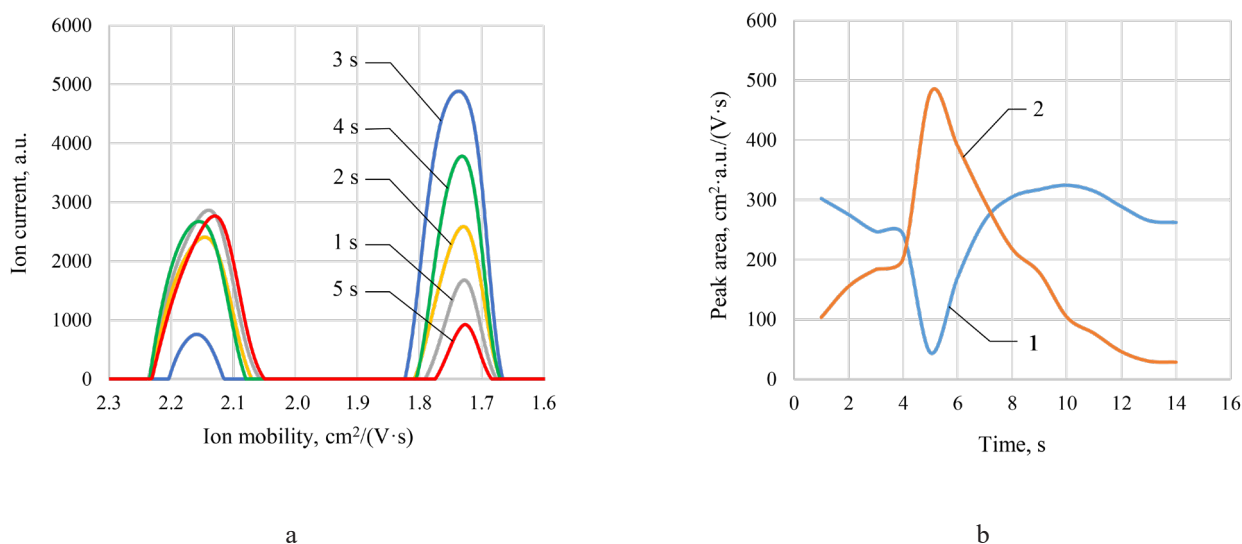


Fig. 6. Ion mobility spectrum of imidazole in water solution and time dependence of the signal intensity: (a) dependence of the ion current on the ion mobility of imidazole (spectra were taken every 1 s after the start of measurement); (b) ion mobility change in the spectrum of imidazole: (1) monomer ion and (2) dimer ion.

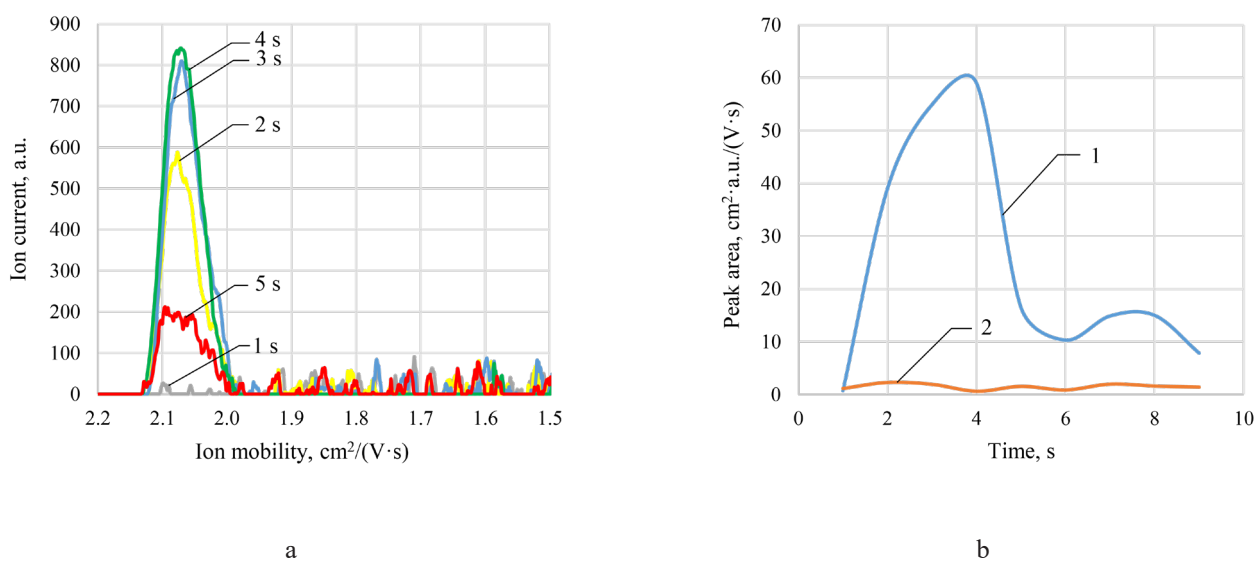


Fig. 7. Ion mobility spectrum of *N*-methylimidazole with a mass of 0.3 pg and time dependence of the signal intensity: (a) dependence of the ion current on the ion mobility of *N*-methylimidazole (spectra were taken every 1 s after the start of measurement); (b) ion mobility change in the spectrum of *N*-methylimidazole: (1) monomer ion and (2) dimer ion.

for a sample weighing 0.3 ng. It is noteworthy that the detection limit for imidazole is 0.3 ng. The difference can be explained by the higher volatility of *N*-methylimidazole.

CONCLUSIONS

It was discovered that the two signals in the ion mobility spectra of *N*-methylimidazole correspond to the presence of protonated monomer and dimer ions. It was also discovered that there was no redistribution of peak intensities as the analyte ions pass through the drift chamber. Nevertheless, the spectrum of the ion mobility of a solution of *N*-methylimidazole in water was characterized by an increase in the monomer concentration due to the decomposition of dimer ions. When the spectra of monomer ions were compared to the spectra of imidazole, it was discovered that the values of the ion mobility of monomer ions appear in a relatively narrow range.

The ion protonated at the pyridine nitrogen atom signal corresponds to ion mobility of $2.1 \pm 0.7\% \text{ cm}^2/(\text{V}\cdot\text{s})$ and can be used to identify the pyridine nitrogen atom in the molecule. Moreover, the stability of dimer ions and the detection limits of compounds differ. The dimer ion is more stable for imidazole. The detection limit of *N*-methylimidazole was determined to be 0.3 pg.

Authors' contributions

D.A. Aleksandrova – methodology development, conducting experiments, analysis of literary sources, writing and editing the text of the article;

T.B. Melamed – methodology development, conducting experiments, processing experimental data, writing and editing the text of the article;

E.P. Baberkina – developing the scientific concept, methodology development, writing and editing the text of the article;

A.A. Fenin – offering consultations on methodology and research, calculations of enthalpies of reactions;

E.S. Osinova – analysis of literary sources, methodology development;

A.E. Kovalenko – offering consultations on methodology and research;

R.V. Yakushin – offering consultations on methodology and research;

Yu.R. Shaltaeva – offering consultations on methodology and research;

V.V. Belyakov – offering consultations on methodology and research;

D.I. Zykova – development of a program for processing ion mobility spectra.

The authors declare no conflicts of interest.

REFERENCES

1. Eiceman G.A., Kapras Z., Hill H.H. *Ion Mobility Spectrometry*: 3rd ed. Boca Raton: CRC; 2013. 444 p. <https://doi.org/10.1201/b16109>
2. Borsdorf H., Eiceman, G.A. Ion mobility spectrometry: Principles and applications. *Appl. Spectrosc. Rev.* 2006;41(3):323–375. <https://doi.org/10.1080/05704920600663469>
3. Marquez-Sillero I., Aguilera-Herrador E., Cardenas S., Valcarcel M. Ion-mobility spectrometry for environmental analysis. *TrAC Trends in Analytical Chemistry.* 2011;30(5):677–690. <https://doi.org/10.1016/j.trac.2010.12.007>
4. Han H.Y., Wang H.M., Jiang H.H., Stano M., Sabo M., Matejcik S., Chu Y.N. Corona discharge ion mobility spectrometry of ten alcohols. *Chinese J. Chem. Phys.* 2009;22(6):605–610. <https://doi.org/10.1088/1674-0068/22/06/605-610>
5. Tabrizchi M., ILbeigi V. Detection of explosives by positive corona discharge ion mobility spectrometry. *J. Hazard. Mater.* 2010;176(1–3):692–696. <https://doi.org/10.1016/j.jhazmat.2009.11.087>
6. Jafari M.T., Khayamian T. Direct determination of ammoniacal nitrogen in water samples using corona discharge ion mobility spectrometry. *Talanta.* 2008;76(5):1189–1193. <https://doi.org/10.1016/j.jhazmat.2009.11.087>

СПИСОК ЛИТЕРАТУРЫ

1. Eiceman G.A., Kapras Z., Hill H.H. *Ion Mobility Spectrometry*: 3rd ed. Boca Raton: CRC; 2013. 444 p. <https://doi.org/10.1201/b16109>
2. Borsdorf H., Eiceman, G.A. Ion mobility spectrometry: Principles and applications. *Appl. Spectrosc. Rev.* 2006;41(3):323–375. <https://doi.org/10.1080/05704920600663469>
3. Marquez-Sillero I., Aguilera-Herrador E., Cardenas S., Valcarcel M. Ion-mobility spectrometry for environmental analysis. *TrAC Trends in Analytical Chemistry.* 2011;30(5):677–690. <https://doi.org/10.1016/j.trac.2010.12.007>
4. Han H.Y., Wang H.M., Jiang H.H., Stano M., Sabo M., Matejcik S., Chu Y.N. Corona discharge ion mobility spectrometry of ten alcohols. *Chinese J. Chem. Phys.* 2009;22(6):605–610. <https://doi.org/10.1088/1674-0068/22/06/605-610>
5. Tabrizchi M., ILbeigi V. Detection of explosives by positive corona discharge ion mobility spectrometry. *J. Hazard. Mater.* 2010;176(1–3):692–696. <https://doi.org/10.1016/j.jhazmat.2009.11.087>
6. Jafari M.T., Khayamian T. Direct determination of ammoniacal nitrogen in water samples using corona discharge ion mobility spectrometry. *Talanta.* 2008;76(5):1189–1193. <https://doi.org/10.1016/j.talanta.2008.05.028>

7. Jafari M.T., Khayamian T., Shaer V., Zarei N. Determination of veterinary drug residues in chicken meat using corona discharge ion mobility spectrometry. *Anal. Chim. Acta.* 2007;581(1):147–153. <https://doi.org/10.1016/j.aca.2006.08.005>
8. Hashemian Z., Mardihallaj A., Khayamian T. Analysis of biogenic amines using corona discharge ion mobility spectrometry. *Talanta.* 2010;81(3):1081–1087. <https://doi.org/10.1016/j.talanta.2010.02.001>
9. Mäkinen M.A., Anttalainen O.A., Sillanpää M.E. Ion mobility spectrometry and its applications in detection of chemical warfare agents. *Anal. Chem.* 2010;82(23):9594–9600. <https://doi.org/10.1021/ac100931n>
10. Aleksandrova D.A., Melamed T.B., Baberkina E.P., Kovalenko A.E., Kuznetsov V.I., Kuznetsov V.V., Fenin A.A., Shaltaeva Yu.R., Belyakov V.V. Ion Mobility Spectrometry of Imidazole and Possibilities of its Determination. *J. Anal. Chem.* 2021;76(11):1282–1289. <https://doi.org/10.1134/S106193482111002>
- [Russian Original Text: Aleksandrova D.A., Melamed T.B., Baberkina E.P., Kovalenko A.E., Kuznetsov V.I., Kuznetsov V.V., Fenin A.A., Shaltaeva Yu.R., Belyakov V.V. Ion Mobility Spectrometry of Imidazole and Possibilities of its Determination. *Zhurnal Analiticheskoi Khimii.* 2021;76(11):989–996 (in Russ.). <https://doi.org/10.31857/S0044450221110025>]
11. Lutz P. Benzimidazole and its derivatives – from fungicides to designer drugs. A new occupational and environmental hazards. *Medycyna Pracy.* 2012;63(4):505–513.
12. Schoeder C., Hess C., Madea B., et al. Pharmacological evaluation of new constituents of “Spice”: synthetic cannabinoids based on indole, indazole, benzimidazole and carbazole scaffolds. *Forensic Toxicol.* 2018;36:385–403. <https://doi.org/10.1007/s11419-018-0415-z>
13. Grishin S.S., Negru K.I., Baberkina E.P., Kovalenko A.E., Gushchina A.A., Aleksandrova D.A., Shutova Y.E., Zharikov A.P., Dorskaya E.V., Shaltaeva Y.R., Belyakov V.V., Golovin A.V., Gromov E.A., Matusko M.A., Khamraev V.F. The influence of chemical structure of nitrogen-containing heterocyclic compounds on the character of ion mobility spectra. *J. Phys.: Conf. Series.* 2019;498(1):012036. <https://doi.org/10.1088/1757-899X/498/1/012036>
14. Aleksandrova D.A., Baberkina E.P., Grishin S.S., Gushchina A.A., Kurbanova D.M., Trefilova V.V., Kovalenko A.E., Shaltaeva Yu.R., Belyakov V.V. Study of the ion mobility spectra of nitrogen-containing heterocycles on the ion-drift detector “Kerber.” In: *Tezisy dokladov XXII Vseross. konf. molodykh uchenykh-khimikov* (Abstracts of XXII All-Russian Conf. of Young Chemists), Nizhnii Novgorod; 2019. p. 277 (in Russ.).
15. Aleksandrova D.A., Baberkina E.P., Dubkina E.A., Kovalenko A.E., Shaltaeva Yu.R., Belyakov V.V. Investigation of the spectra of ionic mobility of aromatic nitrogen-containing heterocyclic compounds on the ion-drift detector “Kerber.” In: *Aktual'nye aspekty khimicheskoi tekhnologii biologicheskii aktivnykh veshchestv: sbornik nauchnykh trudov* (Actual Aspects of Chemical Technology of Biologically Active Substances: Collection of Scientific Papers). Moscow; 2020. P. 34 (in Russ.).
16. Schofield K., Grim-mett M.R., Keene B.R.T. *Heteroaromatic Nitrogen Compounds: The Azoles.* Cambridge: Cambridge University Press; 1976. 437 p.
17. Joule J.A., Mills K. *Heterocyclic Chemistry*, 4th ed. Oxford, U.K.: Blackwell Science; 2000. 608 p.
7. Jafari M.T., Khayamian T., Shaer V., Zarei N. Determination of veterinary drug residues in chicken meat using corona discharge ion mobility spectrometry. *Anal. Chim. Acta.* 2007;581(1):147–153. <https://doi.org/10.1016/j.aca.2006.08.005>
8. Hashemian Z., Mardihallaj A., Khayamian T. Analysis of biogenic amines using corona discharge ion mobility spectrometry. *Talanta.* 2010;81(3):1081–1087. <https://doi.org/10.1016/j.talanta.2010.02.001>
9. Mäkinen M.A., Anttalainen O.A., Sillanpää M.E. Ion mobility spectrometry and its applications in detection of chemical warfare agents. *Anal. Chem.* 2010;82(23):9594–9600. <https://doi.org/10.1021/ac100931n>
10. Александрова Д. А., Меламед Т. Б., Баберкина Е. П., Коваленко А. Е., Кузнецов В. И., Кузнецов В. В., Фенин А. А., Шалтаева Ю. Р., Беляков В. В. Спектрметрия ионной подвижности имидазола и возможности его определения. *Журн. аналит. химии.* 2021;76(11):989–996. <https://doi.org/10.31857/S0044450221110025>
11. Lutz P. Benzimidazole and its derivatives – from fungicides to designer drugs. A new occupational and environmental hazards. *Medycyna Pracy.* 2012;63(4):505–513.
12. Schoeder C., Hess C., Madea B., et al. Pharmacological evaluation of new constituents of “Spice”: synthetic cannabinoids based on indole, indazole, benzimidazole and carbazole scaffolds. *Forensic Toxicol.* 2018;36:385–403. <https://doi.org/10.1007/s11419-018-0415-z>
13. Grishin S.S., Negru K.I., Baberkina E.P., Kovalenko A.E., Gushchina A.A., Aleksandrova D.A., Shutova Y.E., Zharikov A.P., Dorskaya E.V., Shaltaeva Y.R., Belyakov V.V., Golovin A.V., Gromov E.A., Matusko M.A., Khamraev V.F. The influence of chemical structure of nitrogen-containing heterocyclic compounds on the character of ion mobility spectra. *J. Phys.: Conf. Series.* 2019;498(1):012036. <https://doi.org/10.1088/1757-899X/498/1/012036>
14. Александрова Д. А., Баберкина Е. П., Гришин С. С., Гущина А. А., Курбанова Д. М., Трефилова В. В., Коваленко А. Е., Шалтаева Ю. Р., Беляков В. В. Исследование спектров ионной подвижности азотсодержащих гетероциклов на ионно-дрейфовом детекторе «Кербер». *Тезисы докладов XXII Всероссийской конференции молодых ученых-химиков* (с международным участием). Нижний Новгород; 2019. С. 277.
15. Александрова Д. А., Баберкина Е. П., Дубкина Е. А., Коваленко А. Е., Шалтаева Ю. Р., Беляков В. В. Исследование спектров ионной подвижности ароматических азотсодержащих гетероциклических соединений на ионно-дрейфовом детекторе «Кербер». В: *Актуальные аспекты химической технологии биологически активных веществ: сборник научных трудов.* Москва; 2020. С. 34.
16. Schofield K., Grim-mett M.R., Keene B.R.T. *Heteroaromatic Nitrogen Compounds: The Azoles.* Cambridge: Cambridge University Press; 1976. 437 p.
17. Joule J.A., Mills K. *Heterocyclic Chemistry*, 4th ed. Oxford, U.K.: Blackwell Science; 2000. 608 p.

About the authors:

Daria A. Aleksandrova, Postgraduate Student, Department of Expertise in Doping and Drug Control, Mendeleev University of Chemical Technology of Russia (9, Miusskaya pl., Moscow, 1125047, Russia). E-mail: dasha-25.2012@yandex.ru. Scopus Author ID 57208706352, <https://orcid.org/0000-0001-8389-3964>

Tatiana B. Melamed, Master Student, Department of Expertise in Doping and Drug Control, Mendeleev University of Chemical Technology of Russia (9, Miusskaya pl., Moscow, 1125047, Russia). E-mail: melamed.tanya@gmail.com. <https://orcid.org/0000-0002-6457-2417>

Elena P. Baberkina, Cand. Sci. (Chem.), Associate Professor, Department of Expertise in Doping and Drug Control, Mendeleev University of Chemical Technology of Russia (9, Miusskaya pl., Moscow, 1125047, Russia). E-mail: bettycka@mail.ru. Scopus Author ID 56636782900, <https://orcid.org/0000-0002-9226-3478>

Anatolii A. Fenin, Senior Lecturer, Department of High Energy Chemistry and Radioecology, Mendeleev University of Chemical Technology of Russia (9, Miusskaya pl., Moscow, 1125047, Russia). E-mail: fenin@muctr.ru. Scopus Author ID 16202751400, ResearcherID T-9318-2017, <https://orcid.org/0000-0002-5193-33609>

Ekaterina S. Osinova, Postgraduate Student, Department of Expertise in Doping and Drug Control, Mendeleev University of Chemical Technology of Russia (9, Miusskaya pl., Moscow, 1125047, Russia). E-mail: osinova_kat@mail.ru. <https://orcid.org/0000-0003-4088-6822>

Aleksei E. Kovalenko, Cand. Sci. (Eng.), Associate Professor, Department of Expertise in Doping and Drug Control, Mendeleev University of Chemical Technology of Russia (9, Miusskaya pl., Moscow, 1125047, Russia). E-mail: aekov@muctr.ru. Scopus Author ID 57208702823, <https://orcid.org/0000-0002-8412-0311>

Roman V. Yakushin, Cand. Sci. (Eng.), Associate Professor, Department of Organic Chemistry, Dean of the Faculty of Chemical and Pharmaceutical Technologies and Biomedical Products, Mendeleev University of Chemical Technology of Russia (9, Miusskaya pl., Moscow, 1125047, Russia). E-mail: yakushin@muctr.ru. Scopus Author ID 56974245100, ResearcherID A-5116-2014, <https://orcid.org/0000-0003-2923-5471>

Yulia R. Shaltayeva, Senior Lecturer, Division of Nanotechnologies in Electronics, Spintronics and Photonics, Office of Academic Programs (414), Institute of Nanoengineering in Electronics, Spintronics and Photonics, National Research Nuclear University MEPhI (31, Kashirskoe sh., Moscow, 115409, Russia). E-mail: YRShaltayeva@mephi.ru. Scopus Author ID 56018762000, <https://orcid.org/0000-0002-9856-6031>

Vladimir V. Belyakov, Cand. Sci. (Eng.), Associate Professor, Division of Nanotechnologies in Electronics, Spintronics and Photonics, Office of Academic Programs (414), Institute of Nanoengineering in Electronics, Spintronics and Photonics, National Research Nuclear University MEPhI (31, Kashirskoe sh., Moscow, 115409, Russia). E-mail: VVBelyakov@mephi.ru. Scopus Author ID 7103252626, <https://orcid.org/0000-0002-0236-1243>

Daria I. Zykova, Master Student, Department 806 "Computational Mathematics and Programming," Moscow Aviation Institute (National Research University) (4, Volokolamskoe sh., Moscow, 125993, Russia). E-mail: zykova.daria.999@gmail.com. <https://orcid.org/0000-0002-1230-9895>

Об авторах:

Александрова Дарья Алексеевна, аспирант, кафедра экспертизы в допинг- и наркоконтроле, Российский химико-технологический университет им. Д.И. Менделеева (125047, Россия, Москва, Миусская пл., д. 9). E-mail: dasha-25.2012@yandex.ru. Scopus Author ID 57208706352, <https://orcid.org/0000-0001-8389-3964>

Меламед Татьяна Борисовна, магистрант, кафедра экспертизы в допинг- и наркоконтроле, Российский химико-технологический университет им. Д.И. Менделеева (125047, Россия, Москва, Миусская пл., д. 9). E-mail: melamed.tanya@gmail.com. <https://orcid.org/0000-0002-6457-2417>

Баберкина Елена Петровна, к.х.н., доцент, кафедра экспертизы в допинг- и наркоконтроле, Российский химико-технологический университет им. Д.И. Менделеева (125047, Россия, Москва, Миусская пл., д. 9). E-mail: bettycka@mail.ru. Scopus Author ID 56636782900, <https://orcid.org/0000-0002-9226-3478>

Фенин Анатолий Александрович, старший преподаватель, кафедра химии высоких энергий и радиэкологии, Российский химико-технологический университет им. Д.И. Менделеева (125047, Россия, Москва, Миусская пл., д. 9). E-mail: fenin@muctr.ru. Scopus Author ID 16202751400, ResearcherID T-9318-2017, <https://orcid.org/0000-0002-5193-33609>

Осинова Екатерина Сергеевна, аспирант, кафедра экспертизы в допинг- и наркоконтроле, Российский химико-технологический университет им. Д.И. Менделеева (125047, Россия, Москва, Миусская пл., д. 9). E-mail: osinova_kat@mail.ru. <https://orcid.org/0000-0003-4088-6822>

Коваленко Алексей Евгеньевич, к.т.н., доцент, кафедра экспертизы в допинг- и наркоконтроле, Российский химико-технологический университет им. Д.И. Менделеева (125047, Россия, Москва, Миусская пл., д. 9). E-mail: aekov@muctr.ru. Scopus Author ID 57208702823, <https://orcid.org/0000-0002-8412-0311>

Якушин Роман Владимирович, к.т.н., доцент кафедры органической химии, декан факультета химико-фармацевтических технологий и биомедицинских препаратов, Российский химико-технологический университет им. Д.И. Менделеева (125047, Россия, Москва, Миусская пл., д. 9). E-mail: yakushin@muctr.ru. Scopus Author ID 56974245100, ResearcherID A-5116-2014, <https://orcid.org/0000-0003-2923-5471>

Шалтаева Юлия Ринатовна, старший преподаватель, отделение нанотехнологий в электронике, спинтронике и фотонике офиса образовательных программ (414), Институт нанотехнологий в электронике, спинтронике и фотонике, Национальный исследовательский ядерный университет «МИФИ» (115409, Россия, Москва, Каширское ш., д. 31). E-mail: YRShaltayeva@mephi.ru. Scopus Author ID 56018762000, <https://orcid.org/0000-0002-9856-6031>

Беляков Владимир Васильевич, к.т.н., доцент, отделение нанотехнологий в электронике, спинтронике и фотонике офиса образовательных программ (414), Институт нанотехнологий в электронике, спинтронике и фотонике, Национальный исследовательский ядерный университет «МИФИ» (115409, Россия, Москва, Каширское ш., д. 31). E-mail: VVBelyakov@mephi.ru. Scopus Author ID 7103252626, <https://orcid.org/0000-0002-0236-1243>

Зыкова Дарья Ильинична, магистрант, кафедра 806 «Вычислительная математика и программирование», Московский авиационный институт (Национальный исследовательский университет) (125993, Россия, Москва, Волоколамское ш., д. 4). E-mail: zykova.daria.999@gmail.com. <https://orcid.org/0000-0002-1230-9895>

The article was submitted: November 01; approved after reviewing: November 26, 2021; accepted for publication: December 04, 2021.

Translated from Russian into English by H. Moshkov

Edited for English language and spelling by Enago, an editing brand of Crimson Interactive Inc.

**MATHEMATICS METHODS AND INFORMATION
SYSTEMS IN CHEMICAL TECHNOLOGY**

**МАТЕМАТИЧЕСКИЕ МЕТОДЫ И ИНФОРМАЦИОННЫЕ
СИСТЕМЫ В ХИМИЧЕСКОЙ ТЕХНОЛОГИИ**

ISSN 2686-7575 (Online)

<https://doi.org/10.32362/2410-6593-2021-16-6-526-540>

UDC 539.3



RESEARCH ARTICLE

Thermal destruction of polymeric fibers in the theory of temporary dependence of strength

Eduard M. Kartashov

MIREA – Russian Technological University (M.V. Lomonosov Institute of Fine Chemical Technologies),
Moscow, 119571 Russia

@Corresponding author, e-mail: kartashov@mitht.ru

Abstract

Objectives. This study mathematically describes the mutual influence of micro- and macrostages of the process of destruction of polymer materials and determines its main parameters and limiting characteristics. In addition, a relationship is established between molecular constants characterizing the structure of a material and those characterizing its macroscopic characteristics of strength. Finally, theoretical representations of the thermokinetics of the process of thermal destruction of polymer fibers from the standpoint of the kinetic thermofluctuation concept are developed, which makes it possible to predict the thermal durability of a sample under thermal loading.

Methods. The structural–kinetic thermofluctuation theory was used to describe the initial stages of the fracture process and to derive a generalized formula for the rate of crack growth. The mathematical theory of cracks is used to describe the thermally stressed state of a material in the vicinity of an internal circular crack under mechanical and thermal loadings of the sample.

Results. A theoretical formula for the full isotherm of durability in the range of mechanical stresses from safe to critical, as well as a theoretical relationship for the time dependence of the strength of polymer fibers under purely thermal loading in the full range of heat loads from safe to critical and at the stage of nonthermal crack growth, is given. The main parameters and limiting characteristics of durability under thermal loading are also indicated.

Conclusions. A generalized structural-kinetic theory of the fracture of polymer fibers under purely thermal action on cracked specimens is presented. The developed theory combines three independent approaches: structural-kinetic (thermofluctuation theory), mechanical, and thermodynamic. The obtained theoretical relations are of practical interest for the development of methods for localization, intensification, and control of the crack growth kinetics.

Keywords: polymer fibers, time dependence of strength, thermal loads, durability at thermal dest

For citation: Kartashov E.M. Thermal destruction of polymeric fibers in the theory of temporary dependence of strength. *Tonk. Khim. Tekhnol. = Fine Chem. Technol.* 2021;16(6):526–540 (Russ., Eng.). <https://doi.org/10.32362/2410-6593-2021-16-6-526-540>

НАУЧНАЯ СТАТЬЯ

Тепловое разрушение полимерных волокон в теории временной зависимости прочности

Э.М. Карташов

МИРЭА – Российский технологический университет (Институт тонких химических технологий им. М.В. Ломоносова), Москва, 119571 Россия

@ Автор для переписки, e-mail: kartashov@mitht.ru

Аннотация

Цели. Математически описать взаимное влияние микро- и макростадий процесса разрушения полимерных материалов, определить его основные параметры и предельные характеристики, установить связь между молекулярными константами, характеризующими структуру материала с одной стороны и макроскопическими характеристиками прочности с другой. Разработать теоретические представления термокинетики процесса теплового разрушения полимерных волокон с позиций кинетической термофлуктуационной концепции, позволяющей прогнозировать термическую долговечность образца при его тепловом нагружении.

Методы. Использована структурно-кинетическая термофлуктуационная теория для описания элементарного акта процесса разрушения и вывода обобщенной формулы скорости роста трещины и математическая теория трещин для описания термонапряженного состояния материала в окрестности внутренней круговой трещины при механическом и тепловом нагружениях образца.

Результаты. Приводится теоретическая формула полной изотермы долговечности в интервале механических напряжений от безопасного до критического, а также теоретическое соотношение для временной зависимости прочности полимерных волокон при чисто тепловом нагружении в полном интервале тепловых нагрузок от безопасной до критической и на стадии атермического роста трещины. Указаны основные параметры и предельные характеристики долговечности при тепловом нагружении.

Выводы. Представлена обобщенная структурно-кинетическая теория разрушения полимерных волокон при чисто тепловом воздействии на образцы с трещиной. Развитая теория объединяет три самостоятельных подхода: структурно-кинетический (термофлуктуационная теория), механический и термодинамический. Полученные теоретические соотношения представляют практический интерес для разработки способов локализации, интенсификации и управления кинетикой роста трещины.

Ключевые слова: полимерные волокна, временная зависимость прочности, тепловые нагрузки, долговечность при тепловом разрушении

Для цитирования: Карташов Э.М. Тепловое разрушение полимерных волокон в теории временной зависимости прочности. *Тонкие химические технологии*. 2021;16(6):526–540. <https://doi.org/10.32362/2410-6593-2021-16-6-526-540>

One of the fundamental characteristics of polymer materials is their strength. Even in cases where other properties of polymers are directly used (e.g., optical, electrical, thermal, and magnetic), the material must have a certain minimum strength. In this regard, theoretical methods for assessing the strength of polymers without lengthy laboratory tests are of great importance. This problem is one of the most urgent challenges in the physics and mechanics of polymer strength, both in practical and scientific terms. Its solution is complicated by the need to consider the effect of various operational factors on the strength of polymers, especially when they act together. An important step in this direction is the construction of appropriate generalized models that allow describing the behavior of materials in a wide range of external influences. However, the general methodology for constructing such models is still far from complete, primarily to models describing the processes of thermal destruction of materials caused by the interaction of intense heat fluxes with solids. The direction of research is the content of the problem of thermal strength, whose relevance has grown especially in recent decades in connection with the creation of powerful energy emitters and their use in technological operations. New technological methods in various industries are based on intensive heating of materials by plasma flows, laser, or electron beams.

A huge number of publications have been accumulated describing these processes in nuclear power engineering, aircraft and rocket engineering, space technology, turbine engineering, and others [1–6]. The intensive development in these areas, as well as in microelectronics and electrical engineering, required the creation of structural especially polymer materials that are characterized by thermal shock resistance and thermal strength [7–11]. The issues of thermal destruction of materials have become especially relevant in connection with the practical requirements of modern technology [12–14].

Many aspects of this problem have been theoretically and experimentally developed [15–17]. At the same time, the issues of thermokinetics of the process of destruction of materials, especially polymer fibers, under purely thermal loading have not yet been sufficiently developed in the theory of thermal destruction from the standpoint of the kinetic theory within the framework of the time dependence of strength [18]. This article is devoted to the construction of this theory for polymer fibers and continues the research begun in [19] and [20]. The proposed theory combines three independent approaches, namely, structural–kinetic, mechanical, and thermodynamic, within the framework of mathematical modeling for the study of such complex phenomena. Of greatest interest are the cases of the steady-state thermal state $T(x, y, z)$ in solids with a crack. Experimental data in [21] indicate that with a steady-state heat flow in a body with a crack, there is a significant increase in temperature stresses caused by a local increase in the value of the temperature gradient in a small vicinity of the crack fluctuation volume.

It can be assumed that thermoelastic expansion fields, like their mechanical analogs, increase the stress intensity at the crack tip, forcing it to grow. Experiments confirm this assumption [22]. A polymer sample in the form of a bar (final solid cylinder) with an internal disk-shaped axisymmetric crack was exposed to a heat flow along the sample symmetry axis orthogonal to the crack. As the sample was heated, the stress state of the sample changed: the stress concentration increased in the (small) circular vicinity of the crack, and after a while, the sample collapsed. Since the mechanical load remained unchanged during the experiment, the factor determining the fracture was the thermoelastic field. Thus, this case is of particular interest for the theory of thermal destruction from the standpoint of the kinetic thermofluctuation concept: it is necessary to describe the growth of the fracture

crack and calculate the corresponding durability, main parameters, and limiting characteristics of the thermal destruction process, depending on the type of thermal load, physicomaterial, and thermophysical characteristics of the material and its structure. This is important in order to develop methods of localization, intensification, and control of the kinetics of crack growth. It is obvious that knowledge, prevention, and control of this kind of process is an urgent task of materials science.

The corresponding model concepts are based on experimental data [18, 20] obtained on the basis of direct physical methods on the accumulation of violations in loaded samples (i.e., force perturbation and rupture of bonds in polymers), on submicroscopic cracks and their characteristics, on fractographic studies of rupture surface, on the kinetics of the growth of the main crack when the specimen is stretched with a uniform stress $\sigma = \text{const}$, and on temperature–time dependence of durability in the full range of stresses $\sigma_0 \leq \sigma \leq \sigma_{cr}$ from safe to critical.

MAIN APPROACHES IN STUDYING THE STRENGTH OF SOLIDS

To date, studies of the problem of brittle fracture of solids (in particular, polymer materials) are developing in two main directions: mechanical and kinetic approaches. The first direction is associated with calculating the strength of defective bodies by methods of fracture mechanics. It is based on the difference between theoretical and real values of strength, which is interpreted in terms of the classical elastic model of Griffith [23]. The mechanical approach uses the concept of a limiting state as a fracture criterion, upon reaching which fracture occurs. The second direction is associated with the development of the kinetic thermofluctuation concept based on the ideas of Frenkel [24] on thermal motion in solids. In the kinetic approach, main attention is paid to the atomic–molecular process of destruction, and the rupture is considered as the result of the gradual development and accumulation of microdestructions or as the process of development of a microcrack. In this concept, the durability of the body under load is taken as a fundamental quantity that determines the strength and is the basis for the kinetic thermofluctuation theory of fracture, which finds its natural expression in the equations of the time dependence of strength $\tau = (\sigma, T)$ [19]. Both aspects should be included in a complete description of the polymer degradation process in order to construct a generalized theory of strength that considers the structural features of polymer materials. The first results in this direction are presented in an author's survey [21] and in a book [20].

The urgent need for generalized approaches to solve the problem of the strength of solids is now generally recognized. According to the authors [18]: “For further progress in the theory of fracture, it is necessary to develop both physical research and phenomenological, mechanical theories of fracture. The connection between both approaches can be seen primarily in the further development of the concept of damage accumulation at different levels (from the molecular level to the propagation of main cracks). It is necessary to compare the fracture models with the results of direct experiments, where the damage parameters are directly measured.”

Temperature–time dependence of strength

A characteristic feature of the durability depending on $\lg \tau (\sigma, T)$ at different temperatures is the presence of a linear section described by the Zhurkov equation [18]:

$$\tau = \tau_0 \exp\left(\frac{U_0 - \gamma\sigma}{kT}\right), \quad (1)$$

where τ_0 , U_0 , and γ are material constants, which can be considered constant in a certain range of stresses and temperatures, corresponding to a certain mechanism of destruction [20, 25]. Equation (1) has certain limits of applicability. The lower limit of its applicability is the safe stress, and the upper (maximum) limit is the critical stress σ_{cr} . Experiments have confirmed the existence of safe and critical voltages. Thus, in the region of small values of σ for the brittle state, where deformation processes in polymers are weakly expressed, a deviation of the dependence $\lg \tau (\sigma, T)$ from linear is observed and a sharp rise in the life curve occurs. The curve asymptotically approaches the vertical $\sigma = \sigma_0$:

$$\lim_{\sigma \rightarrow \sigma_0} \lg \tau(\sigma, T) = +\infty, \quad (2)$$

corresponding to the safe stress σ_0 . In quasi-brittle fracture, the deflection is smoother, which is associated with the relaxation properties of polymers; however, in this case, condition (2) also holds. According to the authors of [26], there is a certain limit for solids, below which, in the absence of aggressive media, destruction does not occur. In the region of high stress intensity ($\sigma \geq \sigma_{cr}$), a transition to the limiting value τ_{cr} is also experimentally observed, associated with the existence of the maximum growth rate of the fracture crack v_{cr} . Thus, Kerkhoff [27] showed the tendency of the fracture crack velocity in the region of high stresses to the value $v_{cr} = \text{const}$.

Experiments carried out on glass and rosin [28] showed that v_{cr} does not depend on temperature and practically on voltage, indicating that it is a nonthermal value. With a sample width of $L = 3$ mm and a value of $v_{cr} = 700\text{--}800$ m/s characteristic of polymers, the τ_{cr} value is 10^{-6} to 10^{-5} s. The existence of a segment of the curve $\lg\tau_{cr} = \text{const}$ for $\sigma \geq \sigma_{cr}$ was theoretically predicted in [29] and later experimentally confirmed in [30]. On the $\lg\tau(\sigma, T)$ graph, this case corresponds to the bend of the curve toward constant values of durability, which is associated with the transition to the nonthermal mechanism of destruction. Analyzing the state of the matter, the author of [20] comes to the following conclusion: the dependence $\lg\tau(\sigma, T)$ has the form shown in Fig. 1. In the range of stresses (σ_0, σ_{cr}), not too close to the safe and critical, the dependence $\lg\tau(\sigma, T)$ is linear. In the vicinity of σ_0 and σ_{cr} , the indicated curve bends to the vertical and horizontal asymptotes, respectively, based on the fulfillment of the limit relation (2), as well as on the following condition:

$$\lim_{\sigma \rightarrow \sigma_{cr}} \tau(\sigma, T) = \tau_{cr}. \quad (3)$$

Shown in Fig. 1 is the graphical dependence $\lg\tau(\sigma, T)$ in the full range of stresses $[\sigma_0, \sigma_{cr}]$, which is called the complete isotherm of durability. The graph shows four areas of manifestation of the thermofluctuation mechanism of destruction: I ($\sigma \leq \sigma_0$) and IV ($\sigma \geq \sigma_{cr}$) are the boundary areas of the safe and nonthermal mechanisms, II ($\sigma_0 < \sigma < \sigma_{cr}$) is the area of pure thermal fluctuation mechanism, and III ($\sigma_f < \sigma < \sigma_{cr}$) is the transition region, where the nonthermal mechanism begins to appear.

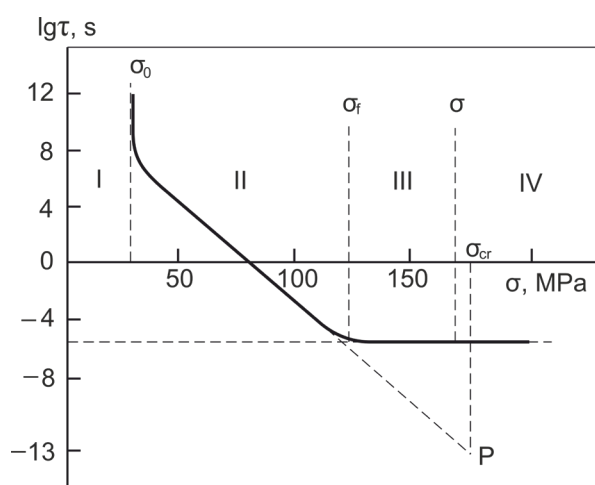


Fig. 1. Temperature–time dependence of strength in the full stress range.

Ideological research scheme

Registration of submicroscopic cracks in real polymer fibers made it possible to establish their disk-like shape, their location within the sample volume perpendicular to the loading axis, and very small sizes of microcracks ($900\text{--}3000$ Å) with a $2R'$ sample diameter of several millimeters. It was also established that the critical crack length R_{cr} is independent of the sample cross-section. Thus, for the characteristics of the crack, there is a very important relation:

$$\lambda \ll R_0 \leq R(t) \leq R_{cr} \leq R^*, 0 \leq t \leq \tau, \quad (4)$$

where R_0 is the initial radius of the crack, $R(t)$ is the current value of the radius, τ is the sample lifetime, and λ is the fluctuation propagation of the crack. A direct study of the kinetics of the fracture process in each specific case of loading a polymer sample (e.g., thermal, mechanical, and electrical) is carried out on the basis of the analytical formula for the rate of crack growth as a function of its current radius $R(t)$, stress field σ' in the defect region V_a (fluctuation volume), temperature T in the circular vicinity of the crack, and molecular constants characterizing the polymer structure, as well as the elementary act of breaking strained bonds:

$$v = v(R, \sigma', T, V_a, U, \dots), \quad (5)$$

where U is the activation energy of the bond-breaking process in the fluctuation volume. The main problem in this case is to obtain a specific expression for (5), taking into account the basic physical laws of the kinetics of the destruction process, which were experimentally revealed for this case, and their influence on the elementary act of destruction in the volume V_a . Local stress in (5) $\sigma' = \varphi(\sigma, \beta, R, \dots)$ is one of the most important strength characteristics. The value of σ' depends on the external stress σ applied to the sample, current radius of the crack $R = R(t)$, geometry of the sample, configuration of the crack and its location in the sample, and stress concentration factor β . The value σ' is calculated by the methods of brittle fracture mechanics based on the solution of boundary value problems of the mathematical theory of cracks. In fact, on the basis of (5), the mutual influence of the macro- and microstages of the fracture process is studied. Using (5), the main parameters and limiting characteristics of the fracture process are determined, a connection is established between the molecular constants characterizing the structure of materials and the macroscopic characteristics of strength, and finally a methodology for calculating the durability of a specimen under various test conditions is being

developed. Thus, within the framework of this research scheme, three approaches are combined: structural-kinetic approach (thermal fluctuation theory for describing the initial stages of the of the destruction process, which is associated with the derivation of (5)), mechanical approach (methods of brittle fracture mechanics for describing local stress at the crack tip under conditions of a certain specimen loading mode), and thermodynamic approach (to calculate the value of the safe voltage).

The durability of the specimen $\tau = \tau(\sigma, T)$ (T is the test temperature, which is generally different from the temperature T_t at the crack tip) is the sum of the times of the rupture process at the first (fluctuation) stage $\tau_f(\sigma, T)$ when the crack grows at a rate (5) from the initial radius R_0 to the critical radius R_{cr} and the second (nonthermal) stage σ_{cr} with the limiting velocity of fracture propagation in a solid $v_{cr} = 0.38\sqrt{E/\rho}$ (Roberts–Wells formula), where E is Young's modulus and ρ is the material density:

$$\tau = \tau_f + \tau_{cr} = \int_{R_0}^{R_{cr}} \frac{dr}{v(r, \sigma, T_t, \dots)} + \frac{R - R_{cr}}{v_{cr}}. \quad (6)$$

STRESS INTENSITY COEFFICIENTS IN THE REGION OF A CIRCULAR CRACK

Calculation of the magnitude of the local stress σ^* is fundamental in the development of this theory of fracture. Based on (4), a fiber-like sample is interpreted as an elastic space (x, y, z) with an internal circular axisymmetric crack $0 \leq r \leq R (r^2 = x^2 + y^2)$ in the plane $z = 0$. Considering that the fracture of brittle polymers is localized in a small vicinity of a crack in the volume (V_a), for the mathematical theory of cracks, it is of interest to study the asymptotic distribution of stresses near the crack front in a homogeneous, elastic, and isotropic continuum. The problem is to find the stress intensity factors $K^{(M)}$ of mechanical and $K^{(T)}$ thermal loads in the asymptotic representation of axial (breaking bond) stress $\sigma_{zz}(r, 0) = K(\sigma, R) / \sqrt{2(r-R)}$, $r > R$ from the basic equations of thermomechanics. It should be noted that the approach proposed below for finding the asymptotic solution of the problem is of independent interest for the mathematical theory of cracks.

In a cylindrical coordinate system (r, φ, z) under the conditions of symmetry about the z axis, as well as symmetry about the plane $z = 0$, the formulated problem is reduced to solving a thermoelastic axisymmetric problem for a half-space $z \geq 0$, consisting of the equilibrium (7), geometrical (8), and physical (9) equations:

$$\left. \begin{aligned} \frac{\partial \sigma_{rr}}{\partial r} + \frac{\partial \sigma_{rz}}{\partial z} + \frac{\sigma_{rr} - \sigma_{\varphi\varphi}}{r} &= 0 \\ \frac{\partial \sigma_{rz}}{\partial r} + \frac{\partial \sigma_{zz}}{\partial z} + \frac{\sigma_{rz}}{r} &= 0 \end{aligned} \right\}, \quad z > 0, \quad r > 0 \quad (7)$$

$$\left. \begin{aligned} \varepsilon_{rr} &= \frac{\partial U}{\partial r}; \varepsilon_{\varphi\varphi} = \frac{U}{r}; \varepsilon_{zz} = \frac{\partial W}{\partial z} \\ \varepsilon_{rz} &= \frac{1}{2} \left(\frac{\partial U}{\partial z} + \frac{\partial W}{\partial r} \right) \end{aligned} \right\} \quad (8)$$

$$\left. \begin{aligned} \sigma_{rr} &= 2G \left[\varepsilon_{rr} + \frac{\nu}{(1-2\nu)} e^{-\frac{1+\nu}{(1-2\nu)} \alpha_T T} \right] \\ \sigma_{\varphi\varphi} &= 2G \left[\varepsilon_{\varphi\varphi} + \frac{\nu}{(1-2\nu)} e^{-\frac{1+\nu}{(1-2\nu)} \alpha_T T} \right] \\ \sigma_{zz} &= 2G \left[\varepsilon_{zz} + \frac{\nu}{(1-2\nu)} e^{-\frac{1+\nu}{(1-2\nu)} \alpha_T T} \right] \\ \sigma_{rz} &= 2G \varepsilon_{rz}. \end{aligned} \right\} \quad (9)$$

Here, $\sigma_{ij} = \sigma_{ij}(r, z)$, $\varepsilon_{ij} = \varepsilon_{ij}(r, z)$ are the components of the stress tensor and strain tensor ($i, j = r, \varphi, z$), respectively; $U = U(r, z)$ and $W = W(r, z)$ are the components of the displacement vector in the radial and axial directions; $T = T(r, z)$ is the temperature function, ν is Poisson's ratio, G is the shear modulus, α_T is the coefficient of linear thermal expansion, and e is the volumetric deformation:

$$e(r, z) = \frac{\partial U}{\partial r} + \frac{U}{r} + \frac{\partial W}{\partial z}. \quad (10)$$

The boundary conditions for the problem posed are as follows:

$$\sigma_{zz}(r, z) \Big|_{z=0} = -\sigma, \quad (11)$$

$$\sigma_{rz}(r, z) \Big|_{z=0} = 0, \quad r \geq 0, \quad (12)$$

$$W(r, z) \Big|_{z=0} = 0, \quad r > R, \quad (13)$$

$$\left| \sigma_{ij}(r, z), W(r, z), U(r, z), \varepsilon_{ij}(r, z) \right| < \infty, \quad r \geq 0, \quad z \geq 0. \quad (14)$$

The temperature function included in (5) is a solution to the heat problem:

$$\frac{\partial^2 T}{\partial r^2} + \frac{1}{r} \frac{\partial T}{\partial r} + \frac{\partial^2 T}{\partial z^2} = 0, \quad z > 0, r > 0, \quad (15)$$

$$\left. \frac{\partial T(r, z)}{\partial z} \right|_{z=0} = \frac{1}{\lambda_T} q_T, \quad 0 \leq r < R, \quad (16)$$

$$T(r, z) \Big|_{z=0} = 0, \quad r > R, \quad (17)$$

$$\left. \frac{\partial T(r, z)}{\partial z} \right|_{z=\infty} = 0, \quad r > 0, \quad (18)$$

where λ_T is the thermal conductivity of the material and q_T is the value of the heat flux entering the sample through a unit of area per unit of time. In (15)–(18), for the convenience of the solution, which does not affect the final result, the heat problem is written with respect to the reduced function $T(r, z) = T(r, z)^* + (q_T / \lambda_T)z$, where $T^*(r, z)$ is the temperature function, corresponding to the initial experiment when the heat flow enters the sample through its end $(\partial T^* / \partial z) \Big|_{z=\infty} = -(q_T / \lambda_T)$. Furthermore, it is assumed that the flow does not go $(\partial T^* / \partial z) \Big|_{z=0} = 0, 0 \leq r < R$, and the transfer of heat by radiation through the crack can be neglected, which is true for not too high temperatures.

A similar problem in the presence of only mechanical loads and only surface temperature of the crack was studied by Sneddon and by Sheil, respectively. Borodachev considered both cases in the original setting, generalizing at the same time the dependences reported by Goodyear and Florence as well as those of Sneddon and Lovengrub [20, 31, 32]. Below is a different approach to solve the problem that is more rational from the point of view of the generality of the results obtained.

Let us introduce the thermoelastic potential of displacements $\Phi(r, z)$ by the following relations [33]:

$$U = \frac{\partial \Phi}{\partial r}; W = \frac{\partial \Phi}{\partial z} \quad (e(r, z) = \Delta \Phi(r, z)). \quad (19)$$

If we substitute (9) in (7) and then (8) into the obtained relation, then equalities (7)–(9) can be written in displacements:

$$\left. \begin{aligned} \Delta U - \frac{1}{r^2} U + \frac{1}{1-2\nu} \frac{\partial e}{\partial r} - \frac{2(1+\nu)}{1-2\nu} \alpha_T \frac{\partial T}{\partial r} = 0 \\ \Delta W + \frac{1}{1-2\nu} \frac{\partial e}{\partial z} - \frac{2(1+\nu)}{1-2\nu} \alpha_T \frac{\partial T}{\partial z} = 0 \end{aligned} \right\} \quad (20)$$

Substituting relation (19) into (20) and integrating the first of them over r and the second over z , we find the following equation:

$$\Delta \Phi(r, z) = \frac{(1+\nu)\alpha_T}{1-\nu} T(r, z). \quad (21)$$

If any particular solution of (21) is found, then strains and stresses can be calculated based on this solution as follows:

$$\bar{\varepsilon}_{rr} = \frac{\partial^2 \Phi}{\partial r^2}; \bar{\varepsilon}_{\varphi\varphi} = \frac{1}{r} \frac{\partial \Phi}{\partial r}; \bar{\varepsilon}_{zz} = \frac{\partial^2 \Phi}{\partial z^2}; \bar{\varepsilon}_{rz} = \frac{\partial^2 \Phi}{\partial r \partial z}; \quad (22)$$

$$\left. \begin{aligned} \bar{\sigma}_{rr} = 2G \left(\frac{\partial^2 \Phi}{\partial r^2} - \Delta \Phi \right); \bar{\sigma}_{\varphi\varphi} = 2G \left(\frac{1}{r} \frac{\partial \Phi}{\partial r} - \Delta \Phi \right) \\ \bar{\sigma}_{zz} = 2G \left(\frac{\partial^2 \Phi}{\partial z^2} - \Delta \Phi \right); \bar{\sigma}_{rz} = 2G \frac{\partial^2 \Phi}{\partial r \partial z} \end{aligned} \right\} \quad (23)$$

In the Hankel expression

$$\begin{aligned} \bar{\Phi}(\xi, z) &= \int_0^\infty r J_0(\xi r) \Phi(r, z) dr, \\ \bar{T}(\xi, z) &= \int_0^\infty r J_0(\xi r) T(r, z) dr \end{aligned} \quad (24)$$

the general solutions of (15) and (21) have the following forms, respectively:

$$\bar{T}(\xi, z) = \bar{T}(\xi, 0) \exp(-\xi z), \quad (25)$$

$$\begin{aligned} \bar{\Phi}(\xi, z) = \\ = \left[\frac{1}{2G\xi^2} \bar{\sigma}_{zz}(\xi, 0) - \frac{z(1+\nu)}{2\xi(1-\nu)} \alpha_T \bar{T}(\xi, 0) \right] \exp(-\xi z). \end{aligned} \quad (26)$$

The unknown functions of ξ entering into (26) are found from boundary conditions (11) and (13) and from relations (19) for $\bar{W}(\xi, z) = d\bar{T}(\xi, z) / dz$. This leads to a dual integral equation

$$\left. \begin{aligned} \int_0^\infty \xi \bar{f}(\xi) J_0(\xi r) d\xi = h(r), \quad 0 \leq r < R, \\ \int_0^\infty \bar{f}(\xi) J_0(\xi r) d\xi = 0, \quad r > R \end{aligned} \right\} \quad (27)$$

where the following labels are made:

$$\left. \begin{aligned} \bar{f}(\xi) &= \frac{1-\nu}{G} \bar{\sigma}_{zz}(\xi, 0) + (1+\nu)\alpha_T \bar{T}(\xi, 0) \\ h(r) &= -\frac{1-\nu}{G} \sigma + (1+\nu)\alpha_T T_0(r), \quad 0 \leq r < R \end{aligned} \right\} \quad (28)$$

here, $T_0(r) = T(r, 0)$. The author of this article has previously developed extensive tables of dual integral equations and paired summation series [34]. We find from the tables the solution of the dual integral (27):

$$\bar{f}(\xi) = \frac{2}{\pi} \int_0^R \sin \eta \xi d\eta \int_0^\eta \frac{yh(y)dy}{\sqrt{\eta^2 - y^2}}, \quad (29)$$

where from (28), we find in the space of originals

$$\bar{\sigma}_{zz}(r, 0) = -\frac{2G}{\pi(1-\nu)} \int_0^R \frac{\eta d\eta}{(r^2 - \eta^2)^{3/2}} \int_0^\eta \frac{yh(y)dy}{\sqrt{\eta^2 - y^2}} - \frac{(1+\nu)\alpha_T G}{(1-\nu)} T(r, 0). \quad (30)$$

Relation (30) refers to the case when either the temperature (then at $r > R$, the value is $\partial T / \partial z|_{z=0} = 0$), or heat flow is set.

According to Irwin [18], the asymptotic behavior of the voltage $\bar{\sigma}_{zz}$ in the region of the circular crack is expressed as

$$\left[\bar{\sigma}_{zz}(r, 0) \right]_{\max} = \frac{K(\sigma, R)}{\sqrt{2(r-R)}}, \quad r > R, \quad (31)$$

where $K(\sigma, R)$ is the stress intensity factor, i.e., parameter reflecting the redistribution of stresses in the body due to the presence of a crack:

$$K(\sigma, R) = \lim_{r \rightarrow R+0} \sqrt{2(r-R)} \left[\bar{\sigma}_{zz}(r, 0) \right]. \quad (32)$$

In (30), we sequentially consider the cases of only mechanical loading at a constant test temperature ($T_0(r) = 0$) and only thermal loading in the absence of mechanical stress. From (32) in the first case, we have $K^{(M)} = (2/\pi)\sigma\sqrt{R}$, and from relation (31), the maximum tensile stress in the vicinity of a circular crack, attained in the plane of the crack, is expressed as follows:

$$\left[\bar{\sigma}_{zz}^{(M)}(r, 0) \right]_{\max} = \frac{\sigma\sqrt{2R}}{\pi\sqrt{r-R}}. \quad (33)$$

Direct experiments by IR spectroscopy to measure stresses on individual chemical bonds for

solid polymers [18] showed that as the crack front approaches the maximum stress bonds, the load increases up to a certain value, after which it remains constant and exceeds the average stress on bonds in sample volume by several orders of magnitude. Such bonds are highly deformed and break in the first place. Their rupture is due to the stress applied to the bond, which is spaced from the crack tip at the distance of its fluctuation advance. Thus, the sought local stress in the vicinity of a circular crack can be written as $\sigma_{(M)}^* = (\sqrt{2/\pi})\sigma\sqrt{R/\lambda}$, but in the final form, it is expressed as follows:

$$\sigma_{(M)}^* = \sigma\beta(R_0)\sqrt{R/R_0}, \quad (34)$$

where $R = R(t)$ is the variable radius of the growing crack, $2R_0$ is the diameter of the initial (in the sample) circular microcrack, and $\beta(R_0)$ is the stress concentration factor for an internal circular crack defined as

$$\beta(R_0) = 0.5\sqrt{R_0/\lambda}. \quad (35)$$

In experiments on creep ($\sigma = \text{const}$) [18], it was shown that the coefficient β practically does not change during the lifetime of the sample and is determined only by the initial dimensions of the defect in the sample. From (35), we find an estimate of the diameter of the initial microcrack in polymer fibers:

$$R_0 = 4\lambda\beta^2. \quad (36)$$

According to [18], for oriented fibers (e.g., polyethylene, polypropylene, and polycapromide) $\lambda = 4 \text{ \AA}$, $\beta = 4-7$, the value from (36) is the radius of the initial microcrack $R_0 = (10^{-8}-10^{-7}) \text{ m}$, which is experimentally confirmed.

Let us further find the local stress with only thermal loading in the modes (15)–(18), for which it is necessary to find the value $T(r, 0)$. In the Hankel expression (24), the solution of (15) with boundary conditions (16)–(18) is reduced to a dual integral equation:

$$\left. \begin{aligned} \int_0^\infty \xi^2 J_0(\xi r) \bar{T}(\xi, 0) d\xi &= -(\lambda_T/q_T), \quad 0 \leq r < R \\ \int_0^\infty \xi J_0(\xi r) \bar{T}(\xi, 0) d\xi &= 0, \quad r > R \end{aligned} \right\} \quad (37)$$

where, according to the tables in [34], we find the equation $\xi \bar{T}(\xi, 0) = -(2q_T / \pi \lambda_T) \int_0^R \eta \sin \eta \xi d\eta$, as well as the original

$$T(r, 0) = -(2q_T / \pi \lambda_T) \sqrt{R^2 - y^2}, \quad 0 \leq r < R. \quad (38)$$

As a result, from (30)

$$\left[\sigma_{zz}^{(T)}(r, 0) \right]_{\max} = A \left[\frac{H(R)}{\sqrt{r^2 - R^2}} - \int_0^R \frac{H'(\eta) d\eta}{\sqrt{r^2 - \eta^2}} \right], \quad r > R, \quad (39)$$

$$H(\eta) = \int_0^\eta \frac{y \sqrt{R^2 - y^2}}{\sqrt{\eta^2 - y^2}} dy, \quad A = \frac{2E\alpha_T q_T}{\pi^2 (1-\nu) \lambda_T}. \quad (40)$$

From (32) and (39)–(40), we find $K^{(T)} = (A/2)R^{3/2}$ and, at the same time, the desired local stress in the vicinity of a circular crack under thermal loading of the sample in the framework of the thermal problems (15)–(18):

$$\sigma_{(T)}^* = \sigma_T \beta(R_0) (R/R_0)^{3/2}, \quad (41)$$

$$\sigma_T = \frac{0.3\alpha_T q_T E R_0}{(1-\nu) \lambda_T}; \quad \beta(R_0) = 0.5 \sqrt{R_0 / \lambda}. \quad (42)$$

The resulting ratio for σ_T in (42) is a fundamental result for the theory of thermal destruction of polymer fibers: σ_T is a mechanical analog of thermal loading and connects the thermophysical, elastic, and structural characteristics of polymers, which makes it possible to trace the influence of each factor on the thermal reaction of a polymer material from the initial circular microcrack. As the temperature T_t included in (5), we take the average integral temperature in the ring $R \leq r < R + \lambda$ with a fluctuation increase in the radius of the circular crack by λ . This gives the following estimate for the value of T_t :

$$T_t = \frac{2q_T \lambda \beta(R_0)}{\lambda_T}. \quad (43)$$

Here, as well as in (42), the relationship between the macro- and microparameters and their influence on the thermal state of the polymer material in the vicinity of the circular crack is traced.

Thus, all quantities included in (5) and (6) have been calculated, which makes it possible to describe the thermokinetics of the growth of a circular crack in polymer fibers and calculate the corresponding durability, both under mechanical and thermal loads.

To complete the solution of the thermoelastic problems (7)–(18), it is necessary to return to boundary condition (12). Since the stresses $\sigma_{rz}(r, z)$ determined in (23) using the thermoelastic potential may not satisfy condition (12), then solution of (20) should be imposed on the resulting solution at $T=0$ so that condition (12) is satisfied. To do this, we use the Love movement function $L(r, z)$ as follows [1]:

$$\begin{aligned} \bar{U} &= -\frac{1}{(1-2\nu)} \frac{\partial^2 L}{\partial r \partial z}; \quad \bar{W} = \\ &= \frac{1}{(1-2\nu)} \left[2(1-\nu) \Delta L - \frac{\partial^2 L}{\partial z^2} \right]; \quad \bar{e} = \Delta L_z, \quad (L_z = \partial L / \partial z) \end{aligned} \quad (44)$$

$$\left. \begin{aligned} \bar{\sigma}_{rr} &= \frac{2G}{(1-2\nu)} \frac{\partial}{\partial z} \left(\nu \Delta L - \frac{\partial^2 L}{\partial r^2} \right) \\ \bar{\sigma}_{\varphi\varphi} &= \frac{2G}{(1-2\nu)} \frac{\partial}{\partial z} \left(\nu \Delta L - \frac{1}{r} \frac{\partial L}{\partial r} \right) \\ \bar{\sigma}_{zz} &= \frac{2G}{(1-2\nu)} \frac{\partial}{\partial z} \left((2-\nu) \Delta L - \frac{\partial^2 L}{\partial z^2} \right) \\ \bar{\sigma}_{rz} &= \frac{2G}{(1-2\nu)} \frac{\partial}{\partial r} \left((1-\nu) \Delta L - \frac{\partial^2 L}{\partial z^2} \right) \end{aligned} \right\} \quad (45)$$

Moreover, the function $L(r, z)$ is in accordance with the biharmonic equation as follows:

$$\Delta^2 L(r, z) = 0, \quad r > 0, \quad z > 0. \quad (46)$$

If the function $L(r, z)$ is defined, then the total stresses amount to the following equation:

$$\sigma_{ij}(r, z) = \bar{\sigma}_{ij}(r, z) + \bar{\sigma}(r, z), \quad (i, j = r, \varphi, z). \quad (47)$$

In this case, the movements are always unambiguous. Using the above relations, let us calculate $\sigma_{rz}(r, 0)$:

$$\bar{\sigma}_{rz}(r, 0) = \int_0^\infty \left[\frac{2G\xi}{\pi(1-\nu)} \int_0^R \varphi(\eta) \sin \eta \xi d\eta \right] J_1(r\xi) d\xi, \quad (48)$$

where

$$\left. \begin{aligned} \varphi(\eta) &= \int_0^\eta \frac{yh(y) dy}{\sqrt{\eta^2 - y^2}}, \\ h(r) &= -\frac{(1-\nu)}{G} \sigma + (1+\nu) \alpha_T T(r, 0). \end{aligned} \right\} \quad (49)$$

If the following condition is required

$$\bar{\sigma}_{rz}(r, z) \Big|_{z=0} = -\bar{\sigma}_{rz}(r, 0), \quad r \geq 0, \quad (50)$$

$$\bar{\sigma}_{zz}(r, z) \Big|_{z=0} = 0, \quad r \geq 0, \quad (51)$$

then all boundary conditions (11)–(14) will be satisfied.

In the Hankel expression, the bounded solution to (44) has the following form:

$$\bar{L}(\xi, z) = [\bar{A}(\xi) + \bar{B}(\xi)z] \exp(-\xi z). \quad (52)$$

To determine the constants in (52) from boundary conditions (50)–(51), we write the following equations using (45) and (52):

$$\begin{aligned} \bar{\sigma}_{rz}(r, z) = \\ = \frac{2G}{(1-2\nu)} \int_0^\infty \xi^2 J_1(r\xi) \left[\nu \frac{d^2 \bar{L}(\xi, z)}{dz^2} + (1-\nu)\xi^2 \bar{L}(\xi, z) \right] d\xi; \end{aligned} \quad (53)$$

$$\begin{aligned} \bar{\sigma}_{zz}(r, z) = \\ = \frac{2G}{(1-2\nu)} \int_0^\infty \xi J_0(r\xi) \left[(1-\nu) \frac{d^3 \bar{L}(\xi, z)}{dz^3} - (2-\nu) \frac{d \bar{L}(\xi, z)}{dz} \right] d\xi. \end{aligned} \quad (54)$$

Equations (51), (52), and (54) give

$$\bar{A}(\xi) = -\frac{(1-2\nu)}{\xi} \bar{B}(\xi). \quad (55)$$

Equations (49), (50), (52), and (53) give:

$$\bar{B}(\xi) = \frac{(1-2\nu)}{\pi(1-\nu)\xi^2} \int_0^R \varphi(\eta) \sin \eta \xi d\eta, \quad (56)$$

which concludes in finding the desired solution for (7)–(18).

MAIN PARAMETERS, LIMITING CHARACTERISTICS AND DURABILITY UNDER THERMAL STRESS

Thermofluctuation processes of destruction at the atomic–molecular level are described using the model of weakly coupled harmonic oscillators, where the elementary act of destruction is interpreted as a classical transition through a potential barrier. At the atomic–molecular model, taking into account the frequencies of rupture and restoration of chemical bonds at the crack tip, the average rate of crack growth is described by the following expression [1]:

$$v(l, \sigma^*, T_t, \dots) = 2\lambda\nu_0 \exp\left[-\frac{U - V_a \sigma_0^*}{kT_t(l, t)} (\sigma^* - \sigma_0^*)\right], \quad (57)$$

where λ is the fluctuation crack propagation upon breaking one or a group of bonds; ν_0 is the frequency of thermal vibrations of the kinetic units involved in breaking and restoring bonds ($\nu_0 \sim 10^{13} \text{ s}^{-1}$); k is Boltzmann's constant; $U = U_0 - qT_t$ is the activation energy of the destruction process, which linearly decreases with increasing temperature; U_0 is the fracture activation energy extrapolated to absolute zero; q is the coefficient of temperature dependence of activation energy (for polymer (organic) glasses $q \sim 15\text{--}20 \text{ J}/(\text{mol}\cdot\text{K})$); and σ_0 is the thermal fluctuation fracture threshold (safe overvoltage at the crack tip). For stresses σ that are not too close to and do not exceed the safe critical intensities ($\sigma_0 < \sigma < \sigma_{cr}$), respectively, the probability of bond recovery at the crack tip is negligible compared to the probability of their breaking. If we neglect the bond recombination process in the vicinity of the crack tip, the rate of its growth will take on a simpler form:

$$v(l, \sigma^*, T_t) = \lambda\nu_0 \exp\left[-\frac{U - V_a \sigma_0^*}{kT_t(l, t)}\right]. \quad (58)$$

In our case, we have

$$v(R, \sigma_{(T)}^*, T_t) = \lambda\nu_0 \exp\left(-\frac{U - V_a \sigma_{(T)}^*}{kT_t}\right), \quad (59)$$

where all basic values are calculated. Calculating integral (6), we obtain the desired expression for the durability $\tau = \tau_f + \tau_{cr}$ under purely thermal loading of a specimen with an internal circular crack within the thermal models (15)–(18):

$$\begin{aligned} \tau = \frac{2R_0 \exp(-q/k)}{3\lambda\nu_0 \alpha \sigma_T} \exp\left(\frac{U_0 - V_a \beta \sigma_T}{kT_t}\right) + \\ + 2.63R^* \sqrt{\rho/E} (1 - 4\lambda\beta^2/R^*), \end{aligned} \quad (60)$$

where $\alpha = V_a \beta / kT_t$. Several important parameters and limiting characteristics of the fracture process should also be added to these ratios. The characteristic of σ_0 corresponds to the voltage at which a sharp rise in the life isotherm curve is experimentally observed to the region of arbitrarily long-time values. In the kinetic theory, this quantity is introduced by the following relation:

$$\sigma_0 = \alpha_s / (\beta \lambda_m), \tag{61}$$

where α_s is the free surface energy of material (in a vacuum) and λ_m is the pre-breaking bond lengthening. The value from (61) is the safe voltage. It should be emphasized that the question of the existence of a safe stress has been controversial for many decades. Only recently when investigating the true meaning of the Griffith energy criterion for brittle polymers, this article has shown [35] that the value σ_0 coincides with the Griffith (safe) fracture threshold for a disk-shaped crack:

$$\sigma_0 = \sigma_G = \sqrt{\frac{2E\alpha_s}{2R_0(1-\nu^2)}}. \tag{62}$$

Critical stress is expressed as follows:

$$\sigma_{cr} = \frac{U_0 - qT}{V_a \beta}. \tag{63}$$

The main external factor causing the growth of a crack at a rate (59) is the heat load with power q_T , which is one of the stress components in (42). Relationships (61) and (62) (at $T = T_l$) determine the range of stresses from safe $\sigma_r^{(0)}$ to critical $\sigma_r^{(cr)}$, which makes it possible to identify the corresponding values of external thermal stress from safe (64) to critical (65):

$$q_T^{(0)} = \frac{36.3\lambda_T}{\alpha_T} \sqrt{\frac{(1-\nu)\alpha_s}{(1+\nu)E}} R_0^{-3/2}; \tag{64}$$

$$q_T^{(cr)} = \frac{12(1-\nu)\lambda_T \sqrt{\lambda}(U_0 - qT)}{\alpha_T E V_a} R_0^{-3/2}. \tag{65}$$

Thus, the reduced interval of external thermal loading ($q_T^{(0)}, q_T^{(cr)}$) determines the time dependence of strength (60). For values $q_T \geq q_T^{(cr)}$ ($\sigma_T \geq \sigma_r^{(cr)}$) the time dependence (60) ceases to be fulfilled, and the crack grows with a maximum speed v_{cr} . The latter means that the dependence ($\lg \tau, \sigma_T$) or ($\lg \tau, q_T$) is parallel to the stress axis σ_T or the heat load axis q_T .

Figure 2 shows the curve of durability for a sample in the form of a monofilament made of organic glass, which was calculated from the following obtained ratios: $\alpha_s = 39 \cdot 10^{-3} \text{ J/m}^2$, $\alpha_T = 8 \cdot 10^5 \text{ grad}^{-1}$, $\lambda_T = 0.197 \text{ W/(m}\cdot\text{K)}$, $v_0 = 10^{-13} \text{ s}^{-1}$, $\lambda = 12 \cdot 10^{-4} \text{ }\mu\text{m}$, $q_T^{(0)} = 210 \text{ W/mm}^2$,

$q_T^{(cr)} = 1700 \text{ W/mm}^2$, $R_0 = 10^{-7} \text{ m}$, $U_0 = 133 \text{ kJ/mol}$, $\beta = 9$, $q = 8.2 \text{ J/(mol}\cdot\text{K)}$, $V_a = 1.4 \cdot 10^{-28} \text{ m}^3$, $R^* = 10^{-3} \text{ m}$, $v_{cr} = 800 \text{ m/s}$, $E = 3.93 \cdot 10^9 \text{ N/m}^2$, $\rho = 1.2 \cdot 10^3 \text{ kg/m}^3$, $\sigma_0 = 21 \text{ MPa}$, and $\sigma_{cr} = 168 \text{ MPa}$.

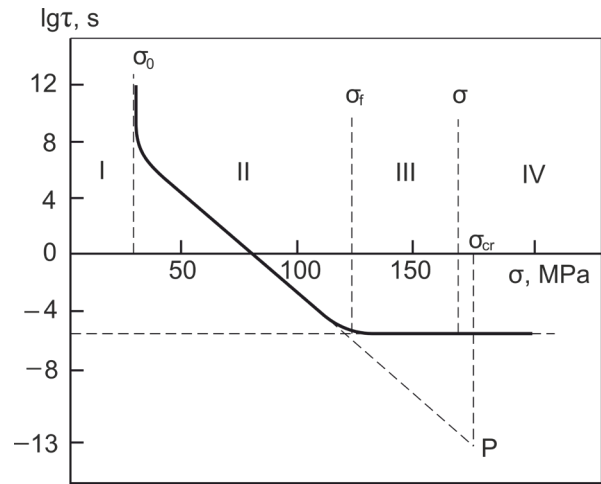


Fig. 2. Life curve for the plexiglass monofilament sample.

The resulting curve gives a clear idea of the possibility of predicting the time dependence of the “thermal” durability of a sample under its thermal loading within the framework of the above thermal model. The calculated relations of dependence (60) contain a complex of physicomaterial, thermophysical, and structural characteristics of a material with a crack, which makes it possible to evaluate their individual influence on the thermokinetics of crack growth and possible control of the process of thermal destruction. Similarly, one can consider other cases of thermal loading of a polymer sample with an internal circular crack, as well as more general ones, when thermal fields are simultaneously coupled with fields of different physical nature, including relaxation processes at the initial stages of heat propagation [36].

CONCLUSIONS

Modern structural and functional polymer materials, which are a set of micro- or nanostructures, have unique mechanical and thermophysical properties that allow them to be used in structures subject to various external influences. An important stage in the creation and use of these materials is the development of appropriate mathematical models to describe their behavior in a wide range of changes in the presence of external operating factors. First, this refers to models describing the thermokinetics of the process of destruction of polymer

materials (in particular, polymer fibers) caused by the interaction of intense heat fluxes with solids: heating of materials by plasma flows, laser, or electron beams.

The mutual influence of micro- and macrostages of the process of destruction of polymer materials is mathematically described, its main parameters and limiting characteristics are determined, and a relationship is established between molecular constants characterizing the structure of a material and those characterizing macroscopic characteristics of strength. A generalized structural–kinetic theory of the destruction of polymer fibers under purely thermal action on cracked specimens is presented. The developed theoretical concepts of the thermokinetics of the process of thermal destruction of polymer fibers from the standpoint of

the kinetic thermofluctuation concept make it possible to predict the thermal durability of a sample under its thermal loading. The obtained theoretical relations are of practical interest for the development of methods for localization, intensification, and control of the kinetics of crack growth in polymer materials.

Author's contribution

E.M. Kartashov – developing the theory for thermokinetics of the polymer fiber thermal destruction process from the standpoint of the kinetic thermofluctuation concept, research and derivation of formulas, and writing the text of the article.

The author declares no conflicts of interests.

REFERENCES

1. Kartashov E.M., Kudinov V.A. *Analiticheskie metody teorii teploprovodnosti i ee prilozhenii (Analytical methods of the theory of heat conduction and its applications)*. Moscow: URSS; 2012. 1080 p. (in Russ.). ISBN 978-5-9710-4994-4
2. Lee H., Lim C.H.J., Low M.J., Tham N., Murukeshan V.M., Kim Y.-J. Lasers in Additive Manufacturing: A Review. *Int. J. of Precis. Eng. Manuf.-Green Tech.* 2017;4(3):307–322. <https://doi.org/10.1007/s40684-017-0037-7>
3. Negi S., Nambolan A.A., Kapil S., Joshi P.S., Manivannan R., Karunakaran K.P., *et al.* Review on electron beam based additive manufacturing. *Rapid Prototyping Journal.* 2020;26(3):485–498. <https://doi.org/10.1108/RPJ-07-2019-0182>
4. Bijanzad A., Munir T., Abdulhamid F. Heat-assisted machining of superalloys: a review. *Int. J. Adv. Manuf. Technol.* 2021. <https://doi.org/10.1007/s00170-021-08059-2>
5. Nasim H., Jamil Y. Diode lasers: From laboratory to industry. *Optics & Laser Technology.* 2014;56:211–222. <https://doi.org/10.1016/j.optlastec.2013.08.012>
6. Nemani S.K., Annavarapu R.K., Mohammadian B., Raiyan A., Heil J., Haque Md.A., *et al.* Surface Modification of Polymers: Methods and Applications. *Adv. Mater. Interfaces.* 2018;5(24):1801247. <https://doi.org/10.1002/admi.201801247>

СПИСОК ЛИТЕРАТУРЫ

1. Карташов Э.М., Кудинов В.А. *Аналитические методы теории теплопроводности и ее приложений*. М.: URSS; 2012. 1080 с. ISBN 978-5-9710-4994-4
2. Lee H., Lim C.H.J., Low M.J., Tham N., Murukeshan V.M., Kim Y.-J. Lasers in Additive Manufacturing: A Review. *Int. J. of Precis. Eng. Manuf.-Green Tech.* 2017;4(3):307–322. <https://doi.org/10.1007/s40684-017-0037-7>
3. Negi S., Nambolan A.A., Kapil S., Joshi P.S., Manivannan R., Karunakaran K.P., *et al.* Review on electron beam based additive manufacturing. *Rapid Prototyping Journal.* 2020;26(3):485–498. <https://doi.org/10.1108/RPJ-07-2019-0182>
4. Bijanzad A., Munir T., Abdulhamid F. Heat-assisted machining of superalloys: a review. *Int. J. Adv. Manuf. Technol.* 2021. <https://doi.org/10.1007/s00170-021-08059-2>
5. Nasim H., Jamil Y. Diode lasers: From laboratory to industry. *Optics & Laser Technology.* 2014;56:211–222. <https://doi.org/10.1016/j.optlastec.2013.08.012>
6. Nemani S.K., Annavarapu R.K., Mohammadian B., Raiyan A., Heil J., Haque Md.A., *et al.* Surface Modification of Polymers: Methods and Applications. *Adv. Mater. Interfaces.* 2018;5(24):1801247. <https://doi.org/10.1002/admi.201801247>

7. Zhang C. Progress in semicrystalline heat-resistant polyamides. *e-Polymers*. 2018;18(5):373–408. <https://doi.org/10.1515/epoly-2018-0094>
8. Fu M.-C., Higashihara T., Ueda M. Recent progress in thermally stable and photosensitive polymers. *Polym J*. 2018;50(1):57–76. <https://doi.org/10.1038/pj.2017.46>
9. Peelman N., Ragaert P., Ragaert K., De Meulenaer B., Devlieghere F., Cardon L. Heat resistance of new biobased polymeric materials, focusing on starch, cellulose, PLA, and PHA. *Journal of Applied Polymer Science*. 2015;132(48):42305. <https://doi.org/10.1002/app.42305>
10. Rezakazemi M., Sadrzadeh M., Matsuura T. Thermally stable polymers for advanced high-performance gas separation membranes. *Progress in Energy and Combustion Science*. 2018;66:1–41. <https://doi.org/10.1016/j.peccs.2017.11.002>
11. Tant M.R., Connell J.W., McManus H.L.N. *High-Temperature Properties and Applications of Polymeric Materials*. Washington, DC: American Chemical Society; 1995. 264 p. ISBN 978-0-12-801981-8
12. Bilibin A.Y., Zorin I.M. Polymer degradation and its role in nature and modern medical technologies. *Russ. Chem. Rev.* 2006;75(2):133–145. <https://doi.org/10.1070/RC2006v075n02ABEH001213>
13. Brinson H.F., Brinson L.C. Characteristics, Applications and Properties of Polymers. In: Brinson H.F., Brinson L.C. (eds.) *Polymer Engineering Science and Viscoelasticity: An Introduction*. Boston, MA: Springer US; 2008. p. 55–97. https://doi.org/10.1007/978-0-387-73861-1_3
14. Witkowski A., Stec A.A., Hull T.R. Thermal Decomposition of Polymeric Materials. In: Hurley M.J., Gottuk D., Hall J.R., Harada K., Kuligowski E., Puchovsky M., et al. (eds.) *Handbook of Fire Protection Engineering*. New York, NY: Springer New York; 2016. p. 167–254. https://doi.org/10.1007/978-1-4939-2565-0_7
15. Bogdanov V.L., Guz A.N., Nazarenko V.M. Spatial Problems of the Fracture of Materials Loaded Along Cracks (Review). *Int. Appl. Mech.* 2015;51(5):489–560. <https://doi.org/10.1007/s10778-015-0710-x>
16. Sicsic P., Marigo J.-J., Maurini C. Initiation of a periodic array of cracks in the thermal shock problem: A gradient damage modeling. *Journal of the Mechanics and Physics of Solids*. 2014;63:256–284. <https://doi.org/10.1016/j.jmps.2013.09.003>
17. Tang S.B., Zhang H., Tang C.A., Liu H.Y. Numerical model for the cracking behavior of heterogeneous brittle solids subjected to thermal shock. *International Journal of Solids and Structures*. 2016;80:520–531. <https://doi.org/10.1016/j.ijsolstr.2015.10.012>
18. Regel' V.R., Slutsker A.I., Tomashevskii E.E. *Kineticheskaya priroda prochnosti tverdykh tel (Kinetic nature of the strength of solids)*. Moscow: Nauka; 1974. 560 p. (in Russ.).
19. Kartashov E.M., Anisimova T.V. Model ideas of thermal fracture on the basis of the theory of strength. *Matem. Mod.* 2007;19(11):11–22 (in Russ.).
20. Kartashov E.M. Modern concepts of the kinetic thermofluctuation theory of polymer strength. *Itogi nauki i tekhniki. Seriya Khimiya i tekhnologiya vysokomolekulyarnykh soedinenii*. 1991. V. 27. 112 p. (in Russ.).
21. Kartashov E.M., Tsoi B., Shevelev V.V. *Razrushenie plenok i volokon. Strukturno-statisticheskie aspekty (Destruction of films and fibers. Structural and statistical aspects)*. Moscow: URSS; 2015. 779 p. (in Russ.). ISBN 978-5-9710-0944-3
7. Zhang C. Progress in semicrystalline heat-resistant polyamides. *e-Polymers*. 2018;18(5):373–408. <https://doi.org/10.1515/epoly-2018-0094>
8. Fu M.-C., Higashihara T., Ueda M. Recent progress in thermally stable and photosensitive polymers. *Polym J*. 2018;50(1):57–76. <https://doi.org/10.1038/pj.2017.46>
9. Peelman N., Ragaert P., Ragaert K., De Meulenaer B., Devlieghere F., Cardon L. Heat resistance of new biobased polymeric materials, focusing on starch, cellulose, PLA, and PHA. *Journal of Applied Polymer Science*. 2015;132(48):42305. <https://doi.org/10.1002/app.42305>
10. Rezakazemi M., Sadrzadeh M., Matsuura T. Thermally stable polymers for advanced high-performance gas separation membranes. *Progress in Energy and Combustion Science*. 2018;66:1–41. <https://doi.org/10.1016/j.peccs.2017.11.002>
11. Tant M.R., Connell J.W., McManus H.L.N. *High-Temperature Properties and Applications of Polymeric Materials*. Washington, DC: American Chemical Society; 1995. 264 p. ISBN 978-0-12-801981-8
12. Билибин А.Ю., Зорин И.М. Деструкция полимеров, ее роль в природе и современных медицинских технологиях. *Успехи химии*. 2006;75(2):151–165. <https://doi.org/10.1070/RC2006v075n02ABEH001213>
13. Brinson H.F., Brinson L.C. Characteristics, Applications and Properties of Polymers. In: Brinson H.F., Brinson L.C. (eds.) *Polymer Engineering Science and Viscoelasticity: An Introduction*. Boston, MA: Springer US; 2008. p. 55–97. https://doi.org/10.1007/978-0-387-73861-1_3
14. Witkowski A., Stec A.A., Hull T.R. Thermal Decomposition of Polymeric Materials. In: Hurley M.J., Gottuk D., Hall J.R., Harada K., Kuligowski E., Puchovsky M., et al. (eds.) *Handbook of Fire Protection Engineering*. New York, NY: Springer New York; 2016. p. 167–254. https://doi.org/10.1007/978-1-4939-2565-0_7
15. Bogdanov V.L., Guz A.N., Nazarenko V.M. Spatial Problems of the Fracture of Materials Loaded Along Cracks (Review). *Int. Appl. Mech.* 2015;51(5):489–560. <https://doi.org/10.1007/s10778-015-0710-x>
16. Sicsic P., Marigo J.-J., Maurini C. Initiation of a periodic array of cracks in the thermal shock problem: A gradient damage modeling. *Journal of the Mechanics and Physics of Solids*. 2014;63:256–284. <https://doi.org/10.1016/j.jmps.2013.09.003>
17. Tang S.B., Zhang H., Tang C.A., Liu H.Y. Numerical model for the cracking behavior of heterogeneous brittle solids subjected to thermal shock. *International Journal of Solids and Structures*. 2016;80:520–531. <https://doi.org/10.1016/j.ijsolstr.2015.10.012>
18. Регель В.Р., Слуцкер А.И., Томашевский Э.Е. *Кинетическая природа прочности твердых тел*. М.: Наука; 1974. 560 с.
19. Карташов Э.М., Анисимова Т.В. Модельные представления теплового разрушения на основе кинетической теории прочности. *Математическое моделирование*. 2007;19(11):11–22.
20. Карташов Э.М. Современные представления кинетической термофлуктуационной теории прочности полимеров. *Итоги науки и техники. Серия Химия и технология высокомолекулярных соединений*. 1991. Т. 27. 112 с.
21. Карташов Э.М., Цой Б., Шевелев В.В. *Разрушение пленок и волокон. Структурно-статистические аспекты*. М.: URSS; 2015. 779 с. ISBN 978-5-9710-0944-3

22. Finkel' V.M. *Fizicheskie osnovy tormozheniya razrusheniya (The physical basis of inhibition of destruction)*. Moscow: Metallurgiya; 1977. 360 p. (in Russ.).
23. Sun C.T., Jin Z.-H. Griffith Theory of Fracture. In: Sun C.T., Jin Z.-H. (eds.) *Fracture Mechanics*. Boston: Academic Press; 2012. p. 11–24. <https://doi.org/10.1016/B978-0-12-385001-0.00002-X>
24. Frenkel' Ya.I. *Kineticheskaya teoriya zhidkosti (Kinetic theory of liquids)*. Leningrad: USSR RAS Publishing House; 1945. 424 p. (in Russ.).
25. Bartenev G.M. *Prochnost' i mekhanizmy razrusheniya polimerov (Strength and degradation mechanisms of polymers)*. Moscow: Khimiya; 1984. 280p. (in Russ.).
26. Gubanov A.I., Chevychelov A.D. On the theory of tensile strength of polymers. *Fizika tverdogo tela*. 1962;4(4):928–933 (in Russ.).
27. Kerkhof F. *Bruchvorqänge in Gläsern*. Frankfurt/Main: Verlag Deutsch Gesellschaft; 1970. 340 p.
28. Kuz'min E.A., Pukh V.P. *Nekotorye problemy prochnosti tverdogo tela (Some problems of solid strength)*. Moscow, Leningrad: Izd. Akad. Nauk SSSR; 1959. 386 p. (in Russ.).
29. Bartenev G.M., Razumovskaya I.V., Rebinde P.A. On the theory of spontaneous dispersion of solids. *Kolloidnyi zhurnal = Colloid J*. 1958;20(5):654–664 (in Russ.).
30. Zlatin N.A., Mochalov S.N., Pugachev G.S., Bragov A.M. Temporary patterns of destruction of metals under intense loads. *Fizika tverdogo tela*. 1974;16(6):1752–1755 (in Russ.).
31. Borodachev N.M. The thermoelastic problem for an infinite axisymmetrically cracked body. *Soviet Applied Mechanics*. 1966;2(2):54–58. <https://doi.org/10.1007/BF00895610>
32. Borodachev N.M. The sinking of a die into the end face of a semi-infinite elastic cylinder. *Soviet Applied Mechanics*. 1967;3(9):55–58. <https://doi.org/10.1007/BF00886390>
33. Melan E., Parkus G. Melan E., Parkus G. *Temperaturnye napryazheniya, vyzyvayemye stacionarnymi temperaturnymi polyami (Temperature stresses caused by stationary temperature fields)*. Transl. from German. Moscow: Fizmatgiz; 1958. 167 p. (in Russ.).
[Melan E., Parkus H. *Wärmespannungen: Infolge Stationärer Temperaturfelder*. Wein: Springer Verl.; 1953. 154 p.]
34. Kartashov E.M. *Analiticheskie metody v teorii teploprovodnosti tverdykh tel (Analytical methods in the theory of thermal conductivity of solids)*. Moscow: Vysshaya shkola; 2001. 540 p. (in Russ.). ISBN 5-06-004091-7
35. Kartashov E.M. The Griffith energy problem for brittle polymers. *J. Eng. Phys. Thermophys.* 2007;80(1):166–175. <https://doi.org/10.1007/s10891-007-0023-y>
36. Kartashov E.M. Analytical solutions of hyperbolic models of non-stationary thermal conduction. *Tonk. Khim. Tekhnol. = Fine Chem. Technol.* 2018;13(2):81–90 (in Russ.). <https://doi.org/10.32362/2410-6593-2018-13-2-81-90>
22. Финкель В.М. *Физические основы торможения разрушения*. М.: Metallurgiya; 1977. 360 с.
23. Sun C.T., Jin Z.-H. Griffith Theory of Fracture. In: Sun C.T., Jin Z.-H. (eds.) *Fracture Mechanics*. Boston: Academic Press; 2012. p. 11–24. <https://doi.org/10.1016/B978-0-12-385001-0.00002-X>
24. Френкель Я.И. *Кинетическая теория жидкостей*. Л.: Изд-во АН СССР; 1945. 424 с.
25. Бартнев Г.М. *Прочность и механизмы разрушения полимеров*. М.: Химия; 1984. 280 с.
26. Губанов А.И., Chevychelov A.D. К теории разрывной прочности полимеров. *Физика твердого тела*. 1962;4(4):928–933.
27. Kerkhof F. *Bruchvorqänge in Gläsern*. Frankfurt/Main: Verlag Deutsch Gesellschaft; 1970. 340 p.
28. Кузьмин Е.А., Пух В.П. *Некоторые проблемы прочности твердого тела*. М.-Л.: Изд-во АН СССР; 1959. 386 с.
29. Бартнев Г.М., Разумовская И.В., Ребиндер П.А. К теории самопроизвольного диспергирования твердых тел. *Коллоидный журнал*. 1958;20(5):654–664.
30. Златин Н.А., Мочалов С.Н., Пугачев Г.С., Брагов А.М. Временные закономерности разрушения металлов при интенсивных нагрузках. *Физика твердого тела*. 1974;16(6):1752–1755.
31. Бородачев Н.М. Термоупругая задача для бесконечного с осесимметричной трещиной. *Прикл. Механика*. 1966;2(2):93–99.
32. Бородачев Н.М. О вдавливании штампа в торец полубесконечного упругого цилиндра. *Прикл. Механика*. 1967;3(9):83–89.
33. Мелан Э., Паркус Г. *Температурные напряжения, вызываемые стационарными температурными полями: пер. с нем.* М.: Физматгиз; 1958. 167 с.
34. Карташов Э.М. *Аналитические методы в теории теплопроводности твердых тел*. М.: Высшая школа; 2001. 540 с. ISBN 5-06-004091-7
35. Карташов Э.М. Энергетическая проблема Гриффита для хрупких полимеров. *Инженерно-физ. журн.* 2007;80(1):156–165.
36. Карташов Э.М. Аналитические решения гиперболических моделей нестационарной теплопроводности. *Тонкие химические технологии*. 2018;13(2):81–90. <https://doi.org/10.32362/2410-6593-2018-13-2-81-90>

About the authors:

Eduard M. Kartashov, Dr. Sci. (Phys.-Math.), Professor, Department of Higher and Applied Mathematics, M.V. Lomonosov Institute of Fine Chemical Technologies, MIREA – Russian Technological University (86, Vernadskogo pr., Moscow, 119571, Russia). E-mail: kartashov@mitht.ru. Scopus Author ID 7004134344, ResearcherID Q-9572-2016, <https://orcid.org/0000-0002-7808-4246>.

Об авторах:

Карташов Эдуард Михайлович, д.ф.-м.н., профессор кафедры высшей и прикладной математики Института тонких химических технологий им. М.В. Ломоносова ФГБОУ ВО «МИРЭА – Российский технологический университет» (119571, Россия, Москва, пр-т Вернадского, д. 86). E-mail: kartashov@mitht.ru. Scopus Author ID 7004134344, ResearcherID Q-9572-2016, <https://orcid.org/0000-0002-7808-4246>

The article was submitted: September 25, 2020; approved after reviewing: November 24, 2020; accepted for publication: December 02, 2021.

Translated from Russian into English by H. Moshkov

Edited for English language and spelling by Enago, an editing brand of Crimson Interactive Inc.

MIREA – Russian Technological University
78, Vernadskogo pr., Moscow, 119454, Russian Federation.

Publication date *December 30, 2021.*

Not for sale

МИРЭА – Российский технологический университет
119454, РФ, Москва, пр-кт Вернадского, д. 78.

Дата опубликования *30.12.2021.*

Не для продажи

